SYNTHESIS, CHARACTERIZATION AND CATALYTIC PROPERTIES OF METALLOSILICATE MOLECULAR SIEVES WITH MFI TOPOLOGY

A THESIS
SUBMITTED TO THE
UNIVERSITY OF PUNE
FOR THE DEGREE OF
DOCTOR OF PHILOSOPHY
(IN CHEMISTRY)

by

T. SELVAM

TH-1056

CATALYSIS DIVISION
NATIONAL CHEMICAL LABORATORY
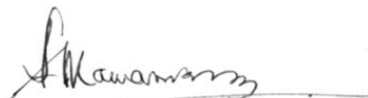PUNE-411 008 (INDIA)

SEPTEMBER 1996

.... TO MY LOVING SISTERS DIVYA & MALLIGA

TH-1056

CERTIFICATE

Certified that the work incorporated in the thesis entitled "**Synthesis, Characterization and Catalytic Properties of Metallosilicate Molecular Sieves with MFI Topology**" submitted by Mr. T. Selvam, for the degree of Doctor of Philosophy, was carried out by the candidate under my supervision in the National Chemical Laboratory, Pune. Such material as has been obtained from other sources has been duly acknowledged in the thesis.

Dr. A. V. Ramaswamy

(Research Guide)

ACKNOWLEDGEMENTS

I express my deep sense of gratitude to Dr. A. V. Ramaswamy, Deputy Director, National Chemical Laboratory, Pune for his valuable guidance throughout the course of my research work.

I am equally indebted to Drs. S. Sivasanker, B. S. Rao and A. P. Singh for their unique help during the study. More important, they "have been there" when I needed them.

I thank Drs. R. Vetrivel, K. Vijayamohanan and scientific staffs of catalysis division for their whole hearted help rendered during the study.

Mere words are insufficient to express my feelings to my Parents and Brothers for their utmost tolerance, immeasurable support and above all faith in education.

It is a great pleasure to give my special thanks to Gnana Ravi for his cheerful and constructive criticisms.

I am indebted to my friends Puyam, Sashi, Vinod, Debu, Rajib, Dinesh, Trusar, Santhosh, Radha, Prasad, Venki, Sekhar and Sunny who made my stay at NCL a pleasant and memorable one.

The encouraging assistance rendered by my seniors Drs. Anuja and Ramesh during the initial stages of my research work cannot be summed up by mere words.

I would be remiss if I forget to mention Dr. S. Kannan and Balu who have helped at crucial stages of my research work.

I thank my childhood friends Charles, Siva, Suku, Kumar, Mano, Saravana, Johnson, Amutha and Geetha for their best wishes which inspired me in many ways.

I also thank my juniors Nawal, Selvaraj, Suhas, Ahedi, Bhavana, Sahida and Sushma for their goodwill.

I am thankful to the Director, National Chemical Laboratory, for allowing me to submit this work in the form of thesis.

(T. SELVAM)

CONTENTS

CHAPTER 5
OXIDATION OF ANILINE TO AZOXYBENZENE OVER METALLOSILICATE (Ti, V and Cr) MOLECULAR SIEVES WITH MFI STRUCTURE

CHAPTER 6
SUMMARY AND CONCLUSIONS

CHAPTER 1

GENERAL INTRODUCTION

1.1 INTRODUCTION

One of the important landmarks in the area of heterogeneous catalysis was the introduction of zeolite catalysts. Zeolites have found widespread interest because of their high acidity, extreme regularity in pore size and shape. Zeolites offer unusual opportunities for carrying out catalytic studies. Their well-defined crystalline structure and their regular pore distribution permit a better description of the surface than that offered by alumina-silca gel catalysts. The two most important areas where zeolite catalysts are extensively used are in the petroleum refining/petrochemical industry and in organic fine chemical synthesis. The advantages of the zeolite catalysts are increased selectivity of the desired product, easy work-up, regeneration and most importantly they are environmentally acceptable.

1.2 ZEOLITES

Zeolites are hydrated, crystalline aluminosilicates, having a rigid three dimensional infinite framework structure, with cavities and channels of molecular dimensions. These highly porous crystals are constructed from tetrahedral building units of $[SiO_4]^{4-}$ and $[AlO_4]^{5-}$, which are arranged into various framework structures by sharing of oxygen atoms. The composition of zeolites can be expressed by the empirical formula:

$$M_{x/n} [(AlO_2)_x (SiO_2)_y] . z H_2O$$
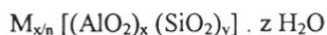
where 'n' is the valence of M cation. The net negative charge of the framework equals the number of constituent aluminium atoms and is balanced by exchangeable cations, typically Na^+, NH_4^+ or H^+. When M is a proton the Brönsted acidity is generated in the zeolites. Thus, the Si/Al molar ratio decides the number of acid sites in the zeolites. Si/Al ratio is always greater than or equal to one, because Al^{3+} does not occupy adjacent tetrahedral sites, according to Loewenstein rule[1].

1.3 CLASSIFICATION AND NOMENCLATURE OF ZEOLITES

Classification of zeolites has been made on the basis of their variations in pore shape (circular, elliptical, etc), dimensionality of the pore system (1-D, 2-D, 3-D), presence or absence of cages and framework composition[2]. Zeolites have traditionally been classified as small, medium and large pore types, based on the ring size of the largest pore that limits access to the pore system. Small pore zeolites are limited by 8-rings, medium pore by 10-rings and large pore by 12-rings. Recently, a very large pore aluminophosphate molecular sieve (VPI-5)[3], containing 18-membered rings and a gallophosphate molecular sieve with 20-membered rings have been discovered[4].

Following the rules set up by IUPAC Commission on Zeolite Nomenclature[5], designations consisting of three capital letters have been used to identify structure types. These mnemonic codes are generally derived from the names of the type of materials and do not include numbers and characters other than capital Roman letters. A large body of structure related literature exists on these zeolite materials including excellent reviews on the topochemistry of zeolites by Smith[6] and zeolite crystallography by McCusker[7]. An invaluable reference for the study of zeolite frameworks and materials is Meier and Olson's Atlas of Zeolite Structure Types[8]. A comprehensive handbook of zeolite nomenclature, synthesis and characterization data, with extensive references to the journals and patent literature has recently been compiled by Szostak[9].

1.4 ZEOLITE SYNTHESIS

1.4.1 ALKALINE MEDIUM

Since the first known zeolites were completely inorganic materials, it is not surprising that the early work on zeolite synthesis involved the use of only inorganic reagents. The most extensive early studies on synthesis of zeolites were conducted by Barrer[10]. The synthesis method comprises the hydrothermal crystallization of reactive metal aluminosilicate gels at

relatively low temperatures under autogeneous pressure. The gels were typically prepared by mixing alkali hydroxides, reactive forms of silica and alumina, and water. The use of organic cations[11] is an important step in hydrothermal synthesis of silicon-rich types of zeolites, whose characteristic features are high acidity, high resistance to water and acids, and high thermal stability. The nature of the product is controlled by kinetic factors and even small changes in the conditions can alter the products[9]. For example, variation of the inorganic base can result in a different range of products. Amongst the large number of organic components, known as templates, which control the crystallization of new zeolite structures, the organic amines have a dominating position. Synthesis of zeolites in alcohols[12] and ethers[13] are also known. Many aspects of zeolite crystallization have been discussed in great detail[14].

The role of organic and inorganic agents is therefore multifarious but can be summarized as follows:

- Supplying OH⁻

- Influencing the gel chemistry, such as the kinetics of gel dissolution by the mineralizing agents, and generating "precursors", like silicate oligomers in the case of zeolites.

- Templating action by organizing around the agent all the elements of the molecular sieve crystals.

- Stabilizing some structures

1.4.2 FLUORIDE MEDIUM

Zeolites are obtained usually by hydrothermal crystallization from an alkaline medium. In such conditions hydroxide ions appear to ensure dissolution of silica and alumina to form the soluble species for zeolite crystallization. A new route to prepare pentasil zeolites was developed by Guth et al.[15] in the presence of fluoride ions. The synthesis of zeolites in the presence of fluoride ions is particularly interesting. Fluoride ions play a mineralizing role as do

OH⁻ ions in alkaline synthesis condition. Generally, HF and NH₄F are used as fluoride sources. Zeolites, in particular the MFI type, obtained in fluoride media are B-, Al-, Si-, Fe-, Ga-, Ge-, and Ti-MFI[16-22].

The advantages of zeolite synthesis in presence of fluoride ions are as follows:

- Obtaining large crystals size of the known zeolites.

- Incorporation of elements, for instance, Co^{2+} ions which are sparingly soluble in alkaline medium.

- Incorporation of elements, for instance, Cr^{3+} ions which are not stable in alkaline medium.

1.5 METALLOSILICATE MOLECULAR SIEVES

With the growth of interest in the utilization of zeolites as catalysts, more attention has been devoted to the introduction of various elements as substitute for lattice Si^{4+} or Al^{3+} to yield molecular sieves normally called metallosilicates. Isomorphous substitution can be performed either during the synthesis or by post-synthesis methods. The substituted element may be strongly or weakly bound to the framework i.e may remain stable or may give rise to well dispersed metallic oxide particles entrapped in the zeolites. In particular, isomorphous substitution of titanium and vanadium into the molecular sieves during hydrothermal synthesis has been studied extensively.

1.5.1 TITANIUM SILICATE MOLECULAR SIEVES

The isomorphous substitution of silicon by titanium has been achieved by direct synthesis for MFI, MEL, BEA and ZSM-48[23-26]. The synthesis of first titanium silicalite (TS-1) with MFI structure was claimed by Taramasso et al.[23] in 1983. The catalytic activity of TS-1, never observed before with other Ti-containing materials, opened up new and very interesting perspectives for industrial application of shape selective catalysis. In the recent years, several papers dealing with the synthesis, characterization and catalytic properties of the

4

TS-1 have been published. In 1990, Reddy et al.[24] reported that a new titanium silicate with MEL structure (TS-2), could be obtained from a gel containing tetrabutylammonium hydroxide as templating molecule. Recently, titanium has also been introduced by direct synthesis into the structure of MCM-41[27].

1.5.2 VANADIUM SILICATE MOLECULAR SIEVES

Vanadium silicate molecular sieves are a new class of catalysts with remarkable catalytic properties in the selective oxidation of various organic molecules. Molecular sieves with vanadium in the framework positions of MFI, MEL, ZSM-48, NCL-1, MTW, BEA and EU-1 structures have been reported recently[28-34]. The activity of vanadium-containing molecular sieves depend substantially on the oxidation state and redox property of the vanadium ions. More recently, mesoporous vanadium silicate molecular sieves, V-MCM-41 has also been synthesized[35].

1.6 PHYSICO-CHEMICAL CHARACTERIZATION

1.6.1 X-RAY DIFFRACTION

X-ray diffraction (XRD) is the primary diagnostic tool for the identification of zeolite structure. XRD is based on the fact that every crystalline material has its own characteristic X-ray diffraction pattern. The intensity of the diffraction peaks can be used to determine the crystallinity of the sample. Additionally, the average size of the crystallite can be determined from the width of the diffraction peaks[36]. X-ray diffraction thus can be employed to give information about identification of the structure, crystallinity, unit cell parameters and average particle size of the sample. Recently, there have been numerous reports of structure determination of zeolites using single crystal XRD[37]. Furthermore, atomic coordinates of the zeolite structure can be optimized using distance least-squares (DLS) program[38]. Progresses in powder pattern analysis, especially by the Reitveld refinement procedure[39], have greatly

5

improved the characterization since it allows detailed analysis and accuracy in crystallographic structural parameter values.

1.6.2 INFRARED SPECTROSCOPY

Infrared spectroscopy has been routinely used to confirm the isomorphous substitution and acidic nature of the zeolite samples. A typical infrared spectrum of lattice is in the range of 400-1300 cm^{-1} (vibrational mode region) and in the range of 3500-3750 cm^{-1} (hydroxyl group region). It has been reported that the infrared vibrations can be divided into two types namely structure insensitive and structure sensitive vibrations[40]. Apart from XRD, the degree of crystallinity can also be estimated from the 550 : 450 cm^{-1} band ratios since the 550 cm^{-1} band is typical of pentasil vibrations while the 450 cm^{-1} band as observed for SiO_2 is common to all silicates and zeolites[41]. A prominent band at 960 cm^{-1} is often attributed to the framework substitution of hetero atoms[42]. It is also possible to study the Brönsted as well as Lewis-acid sites in zeolites by adsorption of probe molecules such as pyridine[43] and CO[44]. Position of the IR-band corresponding with the acidic OH-groups for a series of zeolites with varying Si/Al ratio has been reported by Barthomeuf[45]. Recently Aronson et al.[46] examined the adsorption of a series of simple alcohols on H-ZSM-5 using infrared spectroscopy.

1.6.3 NUCLEAR MAGNETIC RESONANCE SPECTROSCOPY

'Magic-angle-spinning' Nuclear Magnetic Resonance(MAS NMR) spectroscopy yields valuable information on the atomic environment of the elements in zeolites[47-52]. This technique is based on the appropriate averaging of the various solid-state interactions, by spinning the sample at a certain angle to the applied magnetic field. Fyfe et al.[47] reported the ^{29}Si spectrum of a sample of silicalite with low Al concentration. The chemical shifts of all the peaks are characteristic of Si (4Si) groupings in highly siliceous materials. The observed multiplicity arises from crystallographically inequivalent tetrahedral environments of the Si(4Si) sites. The Si/Al ratio in the aluminosilicate framework can also be calculated from the ^{29}Si MAS

6

NMR spectra[48]. In zeolites, tetrahedral framework aluminium can be distinguished from non-tetrahedral extra-framework species by means of ^{27}Al MAS NMR[49]. High-resolution ^{1}H MAS NMR is also a powerful tool for the measurement of zeolitic acidity[50]. Scholle et al. used ^{1}H MAS NMR to study the acidity of the hydroxyl groups in zeolite H-ZSM-5 and its boron analog[51]. ^{13}C NMR has been used to study the organic template enclathrated in the course of synthesis[52].

1.6.4 ELECTRON SPIN RESONANCE SPECTROSCOPY

Electron spin resonance (ESR) spectroscopy is applicable only to compounds containing a transition metal atom with an odd number of electrons in the d or f orbitals. Numerous articles have been devoted to identify the state of the cations in the zeolites, especially in the case of zeolites containing transition-metal ions (Ti, V and Cr). Titanium-containing silicalite have been prepared and studied by ESR spectroscopy[53]. The incorporation of vanadium into the MFI structure during hydrothermal synthesis has been characterized in detail by using ESR spectroscopy[54]. Vogt et al.[55] studied Cr-Na-Y zeolites with different chromium content loading by ESR spectroscopy. Treatment of the zeolite in a stream of dry air at 626 K causes oxidation of the Cr^{3+} ions to the Cr^{5+} and Cr^{6+} states. The parameters of the ESR spectra of Cr^{5+} ion in calcined Cr-containing Y zeolite is consistent with the formation of chromyl ions (CrO^{3+}) in an octahedral configuration. The nature of the environment of chromium in chromium silicate molecular sieves with MFI structure has recently been reported by Kucherov et al[56].

1.6.5 CYCLIC VOLTAMMETRY

Cyclic voltammetry offers a powerful survey of the electrochemical response of a system and provides qualitative insight into the electrochemical and chemical reversibility of an electron-transfer species that reside in the zeolites[57]. In cyclic voltammetry, the current at the working electrode is measured, as the potential (versus a reference electrode) is varied linearly

in time to a chosen potential (E_{sw}, the switching potential) and then reversed with the entire waveform repeated as desired. This cycling of the potential in time permits both the forward and reverse electron-transfer steps to be observed. The speed at which the potential is swept (scan rate) can be varied to study the chemical stability of the metal ions of interest. Cyclic voltammetry has recently emerged as a useful technique to characterize the transition metal ions titanium in TS-1[58] and vanadium in VS-1[59].

1.7 ACTIVE SITES IN ZEOLITES

The term active sites are often used to describe an ensemble of sites at which a catalytic reaction takes place[60]. Zeolites possess Lewis acid at Al^{3+} sites and Brönsted acids due to ion exchanged H^+ ions. The high performance of zeolite catalyst in reactions such as aromatization, alkylation, cracking and isomerization has been attributed to its high acidity and microcrystalline nature of the zeolites[61]. Brönsted acidity of the zeolite can be controlled by the substitution of the Al^{3+} with other trivalent (Fe^{3+}, Ga^{3+} and B^{3+}) , tetravalent (Ti^{4+}) and petavalent (V^{5+}) cations. In contrast to most other zeolites, silicalites, the silica polymorphs which are isostructural with say MFI[62] or MEL[63], do not have acidity. Although, a neutral framework is obtained by the incorporation of Ti^{4+} in the silicalite framework, it has been found to be a remarkable catalyst for the oxidation of various organic substrates with H_2O_2[64]. Vanadium ions (V^{4+}/V^{5+}) can also be inserted into the silicalite framework, which, in this case, possess medium Lewis and weak Brönsted acidity[42]. Vanadium silicates are also shown to have some interesting catalytic properties[65]. The titanium and vanadium ions which are in the framework are believed to be the active sites for these oxidation reactions.

1.8 ZEOLITE ACIDITY AND BASICITY

1.8.1 ACIDITY OF ZEOLITE

The total acidity of zeolites is mainly caused by the presence of Brönsted acidity by means of adsorbed H^+ ions. The Brönsted acidity of zeolite is a function of the equilibrium

established between the Si-OH silanol group and its associated aluminium site. The proton is rendered acidic through the interaction between the unshared pair of electrons on the oxygen atom and the unoccupied orbital of the aluminium atom which weakens the bond between the oxygen atom and the proton coordinated to it so that the proton has donor acidity. Lewis acidity arises at the defect sites where trigonal aluminium is present in the framework. Although there are several techniques, which are normally used to characterize the acidity of the zeolites, pyridine adsorption at 423 K followed by infrared spectroscopy is generally used as a quantitative measurement of both the Brönsted and Lewis acid site concentration[66,67].

1.8.2 BASICITY OF ZEOLITE

In principle, two types of basicity may be considered in zeolite catalysts. The Brönsted basic sites (terminal OH groups), which should exhibit a considerable proton affinity and the Lewis basic sites which are the framework oxygen atoms. The extent of charge on the oxygen determines their basic strength. The basic property of the zeolites are enhanced by exchange with alkali ions. Among alkali ions, Cs^+ is the most effective for enhancing the basicity. The basic sites of the alkali-exchanged zeolites promote a number of base-catalyzed reactions[68, 69].

1.9 MOLECULAR SHAPE SELECTIVITY

Shape selectivity of zeolites[70,71] arises from the fact that the probabilities of forming various products in the narrow intracrystalline cavities and channels are largely determined by molecular dimension and configuration. Four kinds of shape selectivity have been envisaged in the classic review article reported by Csicsery[72].

Reactant shape selectivity occurs when access to intracrystalline catalytic sites is afforded to one class of reactant molecules and denied to another, based on molecular shape and dimensions. Reactant selectivity was demonstrated by the selective cracking of n-hexane in the presence of 3-methylpentane[73].

When, in the cavities of a pore system, a mixture of products occurs not all of which can pass through the ports linking these cavities, product shape selectivity is observed.

Restricted-transition-state selectivity takes place when certain reactions can not proceed at all because they would involve transition states requiring more space than is available in the intracrystalline space. This type of selectivity was first proposed by Csicsery[74] when he observed the absence of symmetrical trialkylbenzenes in the product from the disproportionation of a dialkyl benzene over H-mordenite.

Molecular traffic control may occur in zeolites with more than one type of pore systems. This concept was first proposed by Derouane and Gabelica who termed it the molecular traffic control effect[75]. According to this concept, the smaller molecules enter the sinusoidal channels while the larger product molecules exit from the elliptical channels.

1.10 COMMERCIAL APPLICATIONS OF ZEOLITES

The traditional catalytic applications of zeolites have been in a variety of processes of the petroleum industry and organic fine chemical synthesis. Modified zeolites play an important role in many commercial applications as heterogeneous catalysts.

1.10.1 PETROLEUM AND PETROCHEMICAL PROCESSES

Microporous materials, notably zeolites, occupy a prominent place as catalysts in the hydrocarbon processing industry. In more traditional oil refining, zeolite catalysis is involved in the processing of almost every fraction of the crude oil. In the emerging industry of synfuels manufacture, zeolites catalysts have already found a place and will become more important as this industry assumes a greater role in the future. Some major commercial processes in the oil refining and synfuels industries are listed below[76].

- Catalytic cracking

- Hydrocracking

10

- Isomerization of light paraffins

- Reformate upgrading

- Distillate and lube oil dewaxing

- Gasoline and light olefins from methanol

- Gasoline and middle distillates from light olefins

- Deep hydrogenation of diesel fuel

- Isobutene production from normal butenes

1.10.2 ORGANIC FINE CHEMICAL SYNTHESIS

The potential of zeolites as catalysts for a large variety of organic reactions was reviewed about 28 years ago[77]. Since then, studies on the application of zeolite catalysts have been centered on a number of organic fine chemicals of industrial significance. Zeolites catalyze several types of reaction involving organic molecules. The most important are aromatic substitution[78], isomerization[79], condensation[80], rearrangement[81] and cyclization reactions[82].

A number of excellent review papers have dealt with the application of zeolite catalysts for a wide variety of organic synthesis[83-85]. Most importantly, the discovery of transition metallosilicates, especially the titanium and the vanadium silicate molecular sieves opened up new area in the selective oxidation of organic compounds using aqueous H_2O_2 as the oxidant[86]. Titanium and vanadium silicates have been reported to catalyze a number of organic transformations[65,87,88] like (i) oxyfunctionalization of alkanes, (ii) hydroxylation of aromatics, (iii) oxidation of amines and (iv) oxidation of thioethers.

1.11 STRUCTURAL FEATURES OF ZSM-5 (MFI)

Zeolite ZSM-5 is known for its unusually high silica/alumina ratio, depending on the synthesis conditions[62,89]. The properties which make ZSM-5 suitable and important for industrial applications are its exceptionally high degree of thermal stability and high selectivity

11

in certain conversions[90]. The framework structure and structural features of ZSM-5 have been described by Kokotailo et al[91]. The crystals have an idealized orthorhombic symmetry with the cell constants being, a = 20.1 Å, b = 19.9 Å, and c = 13.4 Å; however it shows a reversible phase transition[92] at about 330 K. ZSM-5 has an effective three-dimensional channel defined by 10-membered ring openings. Straight channels parallel to [010] have openings defined by 10-rings of size 5.4 x 5.6 Å based on oxygen radii of 1.35 Å. Intersecting this channel at right angles is a sinusoidal channel along [100] with openings of 5.1 x 5.4 Å.

The secondary building unit (SBU) of the framework is most adequately considered to comprise 12 "T" atoms and is shown in Fig. 1.1a. These SBUs can be linked to form chains as shown in Fig. 1.1b. Such a chain can simply can be generated by applying the operations of a 2-fold screw axis to a SBU. Fig. 1.1c illustrates the joining of the resulting chains to give layers. In ZSM-5 the neighboring layers are connected so that they are related by an inversion (i) operator.

1.12 CHROMIUM OXIDE CATALYSTS

The catalytic properties of chromium compounds and especially of its oxides are well known[93]. They are mainly due to their ability of facile change in oxidation state of chromium. Many reports have been concerned with the use of homogeneous chromium catalysts[94]. Chromium-containing materials are interesting catalysts for the dehydrogenation of alcohols and alkanes, and the oligomerization and polymerization of olefins[95]. Chromium catalysts are commonly supported on silica or alumina[96]. Recently, efforts were undertaken to prepare self-supporting porous chromium catalysts, that is zeolitic materials containing either occluded chromium and /or chromium incorporated into the framework.

1.13 CHROMIUM ALUMINOPHOSPHATE MOLECULAR SIEVES

Several papers report the synthesis of chromium-containing aluminophosphate molecular sieves[97-105]. Helliwell et al.[97] concluded from a single crystal study of a chromium-
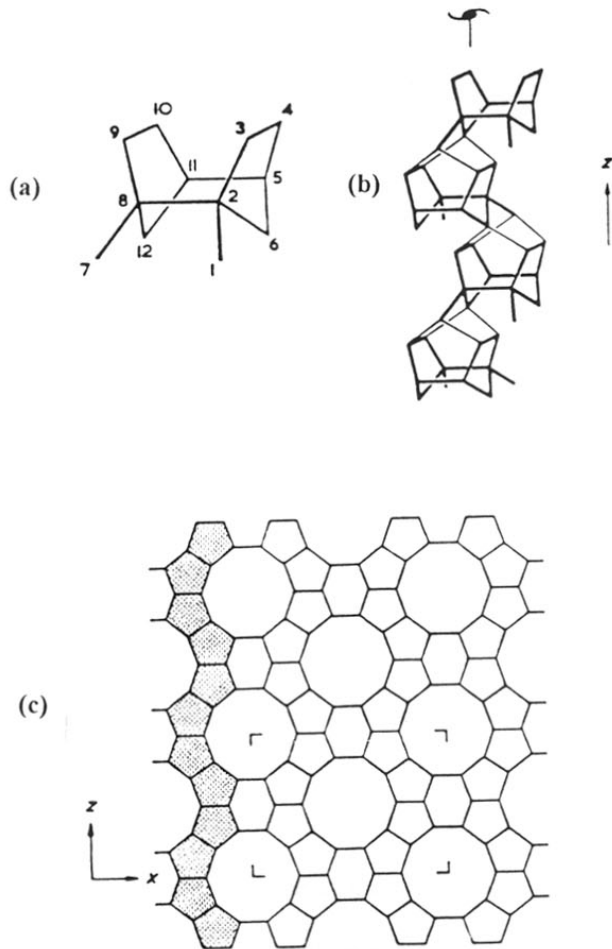
Fig. 1.1 (a) Secondary building unit,   (b) Linkage of SBUs to form   chains and
(c) Linkage of chains to generate layers in ZSM-5 structure.

13

containing aluminophosphate with a GAPO-14 structure that chromium was occupying 6 % of the octahedral framework sites. Diffuse reflectance UV-Visible spectra seem to indicate that octahedral Cr^{3+} is present in as-synthesized CrAPO-5 which is oxidized to tetrahedral Cr^{6+} upon calcination[98] . Chromium aluminophosphate molecular sieves (CrAPO-5) were hydrothermally synthesized by Weckhuysen and Schoonheydt[99]. They revealed that no structural chromium is found in CrAPO-5 molecular sieves. Later Chen et al.[100] claimed isomorphous substitution of aluminium by chromium in the AlPO$_4$-5 framework and useful for the oxidation of various hydrocarbons using molecular oxygen as the oxidant[101]. Very recently, Chen et al. reported chromium-containing AlPO$_4$-5 to be an active and selective catalyst in the decomposition of cyclohexyl[102] and cyclohexenyl[103] hydroperoxide towards ketones. Chromium substituted AlPO$_4$-11 (CrAPO-11) has also been shown to catalyze the oxidations of alkylaromatics with t-butyl hydroperoxide[104]. Incorporation of chromium into the chabazite-type aluminophosphate lattice (SAPO-34) has also been reported[105].

1.14 CHROMIUM SILICATE MOLECULAR SIEVES

Because of the importance of supported chromium oxides as selective oxidation catalysts, several attempts have been made with the aim of inserting chromium in the zeolite framework[106-109]. For example, Naccache and Ben Taarit[106], Atanasova et al.[107] and Pearce et al.[108] have investigated the chromium species mainly in zeolites A , X and Y, whereas Hemidy et al.[109] reported the results of chromium in zeolite mordenite (MOR).

In 1981, Klotz[110] patented the synthesis of chromium-containing molecular sieves. Although isomorphous substitution of chromium has been claimed by Pastore et al.[111] and Borade and Rao[112,113], no evidence was given for the isomorphous substitution of chromium in the MFI lattice. Cr^{3+} ions are relatively unstable in tetrahedral coordination[114]. Cornaro et al. have shown by IR spectroscopy that predominant part of Cr^{3+} ions in silicalite is present in cationic positions and no chromium is inserted in the framework[115]. Sugimoto et al.[116] found

that in the chromium silicate, chromium atoms exist in highly dispersed state and a part of the Cr^{5+} cations might substitute for silicon atoms in the silicate framework. It was recently shown that both Cr^{3+} and Cr^{5+} ions can be incorporated in the cationic positions of zeolites of the ZSM-5 type[117]. Chapus et al.[118] revealed that a part of the chromium ions are present in substitutional sites. Mambrim et al.[119] identified at least three different chromium species in chromium silicalite-1. Puil et al.[120] also reported the synthesis of chromium silicalite-1 by using tetrapropyl ammonium bromide as organic template. Recently, Kucherov et al.[56] reported that the Cr^{3+} ions substitute isomorphically for Si^{4+} in the lattice of as-synthesized samples and after calcination some part of the chromium is stabilized inside the zeolitic structure as isolated low-coordinated Cr^{5+} ions in two discrete modes of coordination. The synthesis of chromium silicalite, CrS-2 which has an MEL structure, has recently been reported[121].

The chromium-containing zeolite catalysts described in the literature are mainly characterized on the basis of XRD and catalytic activity, while little information is available on the thermal stability of chromium and its transformation upon thermal treatments.

1.15 MOTIVATION OF THE PRESENT WORK

The papers and patents dealing with transition metal containing molecular sieves are not only interesting for their applications in organic fine chemical synthesis but are also beautiful examples for the scientific preparation of catalysts. In this regard, chromium is a potential candidate for such incorporation because of its different accessible oxidation states. Although chromium-containing molecular sieves with MFI structure and their characterization have been reported earlier in the literature, their stability is questionable because almost all the chromium incorporated into the molecular sieves can be leached out by ammonium (acetate) exchange[115] or by treating with acetic acid[118]. One of the main reasons is that Cr^{3+} ions are not stable in basic medium, normally used in the synthesis of molecular sieves[122]. Therefore, an

alternative synthetic procedure must be used to synthesize thermally stable chromium in the MFI structure.

In our laboratory, an intensive research programme is pursued on the synthesis of various transition metallosilicates, mainly concentrating on the physicochemical characterization and catalytic properties of the resultant materials. In particular, the motivation of the present work is to synthesize thermally stable chromium silicate that can efficiently catalyze in liquid phase oxidation reactions. The present investigation has the following objectives:

1. To synthesize aluminium-free, thermally stable chromium silicate, CrS-1 (MFI) in fluoride medium and also to study the influence of various synthesis parameters (chromium source, Si/Cr, Si/TPAOH and H_2O/Si ratios) on the kinetics of crystallization of CrS-1.

2. To study the nature of chromium present in the chromium silicate using various physico-chemical characterization techniques such as XRD, UV, IR, NMR, ESR, Cyclic Voltammetry and XPS.

3. To study the intrinsic catalytic activity of CrS-1, in the oxidation of activated and unactivated hydrocarbons with various reaction parameters using t-butyl hydroperoxide (TBHP) as the oxidant.

4. To study the catalytic activity of metallosilicates viz., TS-1, VS-1 and CrS-1 on the selective oxidation of aniline to azoxybenzene under different reaction conditions.

1.16 REFERENCES

1. W. Loewenstein, Am. Mineral., 39, 92 (1954).

2. D. W. Breck, "Zeolite Molecular Sieves. Structure, Chemistry, and Use"; Wiley-Interscience: New York, (1974).

3. M. E. Davis, C. Saldarriaga, C. Montes, J. Garces and C. Crowder, Nature, 331, 698 (1988).

4. M. Estermann, L. B. McCusker, C. Baerlocher, A. Merrouche and H. Kessler, Nature, 352, 320 (1991).

5. R. M. Barrer, "Chemical Nomenclature and Formulation of Compositions of Synthetic and Natural Zeolites", Pure and Appl. Chem., 51, 1091 (1979).

6. J. V. Smith, Chem. Rev., 88, 149 (1988).

7. L. B. McCusker, Acta Cryst., A47, 297 (1991).

8. W. M. Meier and D. H. Olson, Zeolites, 12, 449 (1992).

9. R. Szostak, "Handbook of Molecular Sieves", van Nostrand-Reinhold, New York, 1992.

10. R. M. Barrer, J. Chem. Soc., 2158 (1948).

11. B. M. Lok, T. R. Cannan and C. A. Messina, Zeolites, 3, 282 (1983).

12. W. Hölderich, W. D. Mross and M. Schwarzmann, Eur. Pat. 77946 (1983). BASF AG.

13. W. Hölderich, L. Marosi, W. D. Mross and M. Schwarzmann, Eur. Pat. 51741 (1982). BASF AG.

14. L. B. Sand, Pure and Appl. Chem., 52, 2105 (1980).

15. J. L. Guth, H. Kessler and R. Wey, Proc. 7 th Int. Conf. on Zeolite, Tokyo, p 121 (1986).

16. Q. Shilun, P. Wenqin and Y. Shangqing, Stud. Surf. Sci. Catal., 49A, 133, (1989).

17. J. Patarin, J. L. Guth, H. Kessler, G. Coudurier and F. Raatz, Fr. Pat., Appl. No. 86/17711 (1986).

18. R. Mostowicz, F. Crea and J. B-Nagy, Zeolites, 13, 678 (1993).

19. J. Patarin, H. Kessler and J. L. Guth, Zeolites, 10, 674 (1990).

20. A. Seive, J. L. Guth, F. Raatz and L. Petit, Fr. Pat., Appl. No. 88/06509 (1988).

21. M. H. Tuilier, A. Lopez, J. L. Guth and H. Kessler, Zeolites, 11, 662 (1991).

22. H. Kessler, J. Patarin and C. Schott-Darie, Stud. Surf. Sci. Catal., 85, 75 (1994).

23. M. Taramasso, G. Perego and B. Notari, US. Pat. 4 4100 501 (1983).

24. J. S. Reddy, R. Kumar and P. Ratnasamy, Appl. Catal., 58, L1 (1990).

TH-1056

25. M. A. Camblor, A. Corma and J. Perez-Pariente, Zeolites 13, 82 (1993).

26. M. E. Davis, Acc. Chem. Res., 26, 111 (1993).

27. A. Corma, M. T. Navarro, J. Perez-Pariente and F. Sanchez, Stud. Surf. Sci. Catal., 84, 69 (1994).

28. M. S. Rigutto and H. van Bekkum, Appl. Catal., 68, L1 (1991).

29. P. R. H. P. Rao, A. V. Ramaswamy and P. Ratnasamy, J. Catal., 137, 225 (1992).

30. A. Tuel and Y. Ben Taarit, Appl. Catal., 102, 201 (1993).

31. K. R. Reddy, A. V. Ramaswamy and P. Ratnasamy, J. Catal., 143, 275 (1993).

32. K. M. Reddy, I. Moudrakovski and A. Sayari, J. Chem. Soc. Chem. Commun., 1491 (1994).

33. T. Sen, M. Chatterjee and S. Sivasanker, J. Chem. Soc. Chem. Commun.,207 (1995).

34. M. Chatterjee, D. Bhattacharya, N. Venkatathri and S. Sivasanker, Catal. Lett., 35, 313 (1995).

35. K. M. Reddy, I. Moudrakovski and A. Sayari, J. Chem. Soc. Chem. Commun., 1059, (1994).

36. B. D. Cuillity, in "Elements of X-ray Diffraction", Addison-Wesley Reading, Massachusetts, p. 294 (1987).

37. H. Lermer, M. Draeger, J. Steffen and K. K. Unger, Zeolites 5, 131 (1985).

38. W. M. Meier and H. Villiger, Z. Kristollogr., 129, 411 (1969).

39. Ch. Baerlocher, Zeolites, 6, 325 (1986).

40. E. M. Flanigen, "Zeolite Chemistry and Catalysis", (Ed. J. A. Rabo), ACS Monograph 171, 80 (1976).

41. J. C. Vedrine, Stud. Surf. Sci. Catal., 69, 25 (1991).

42. P. Ratnasamy and R. Kumar, Catal. Lett., 22, 227 (1993).

43. G. Poncelet and M. L. Dubru, J. Catal., 52, 321 (1978).

44. A. Zecchina, S. Bordiga, G. Spoto, L. Marchese, G. Petrini, G. Leofanti and M. Padovan, J. Phys. Chem., 96, 4991 (1992).

45. D. Barthomeuf, in "Catalysis by Zeolites" Elsevier, 5, 55 (1980).

46. M. T. Aronson, R. J. Gorte and W. E. Farneth, J. Catal., 105, 455 (1987).

47. C. A. Fyfe, G. C. Gobbi, J. Klinowski, J. M. Thomas and S. Ramdas; Nature, 296, 530 (1982).

48. J. M. Thomas , C. A. Fyfe , S. Ramdas, J. Klinowski and G. C. Gobbi, J. Phys. Chem., 86, 3061 (1982).

49. C. A. Fyfe, G. C. Gobbi, J. S. Hartman, J. Klinowski and J. M. Thomas, J. Phys. Chem., 86, 1247 (1982).

50. K. F. M. G. J. Scholle, W. S. Veeman, J. G. Post and J. H. C. van Hooff, Zeolites, 3, 214 (1983).

51. K. F. M. G. J. Scholle, A. P. M. Kentgens, W. S. Veeman, P. Frenken and G. P. M. van der Velden, J. Phys. Chem., 88, 5 (1984).

52. G. Boxhoorn, R. A. van Santen, W. A. van Erp, G. R. Hays, R. Huis and D. Clague, J. Chem. Soc. Chem. Commun., 264 (1982).

53. A. Tuel, J. Diab, P. Gelin, M. Dufaux, J-F. Dutel and Y. Ben Taarit, J. Mol. Catal., 63, 95 (1990).

54.. G. Centi, S. Perathoner, F. Trifiro, A. Aboukais, C. F. Aissi and M. Guelton, J. Phys. Chem., 96, 2617 (1992).

55. F. Vogt, H. Bremer, A. M. Rubinstein, M. J. Daschevskii, A. A. Slinkin and A. L. Klaischko, Z. Anirg. Chem., 423, 155 (1976).

56. A. V. Kucherov, A. A. Slinkin, G. K. Beyer and G. Borbely, Zeolites, 15, 431 (1995).

57. D. R. Rolison, Chem. Rev., 90, 867 (1990).

58. S. de Castro-Martins, A. Tuel and Y. Ben Taarit, Zeolites, 14, 130 (1994).

59. N. Venkatathri, M. P. Vinod, K. Vijayamohanan and S. Sivasanker, J. Chem. Soc. Faraday Trans., 92, 473 (1996).

60. H. S. Taylor, Proc. Roy. Soc., A108, 105 (1925).

61. N. Y. Chen and W. E. Garwood, Catal. Rev. -Sci. Eng., 28, 185 (1986).

62. E. M. Flanigen, J. M. Bennett, R. W. Grose, J. P. Cohen, R. L. Patton, R. M. Kirchner and J. V. Smith, Nature, 271, 512 (1978).

63. D. M. Bibby, N. B. Milestone and L. P. Aldridge, Nature, 280, 664 (1979).

64. B. Notari, Stud. Surf. Sci. Catal. 60, 343 (1991).

65. A. V. Ramaswamy and S. Sivasanker, Catal. Lett., 22, 239 (1993).

66. M. R. Basila, Appl. Spectrosc. Rev., 1, 289 (1968).

67. J. W. Ward, Adv. Chem. Ser., 101, 381 (1971).

68. A. Corma, V. Fornes, R. M. Martin-Aranda, H. Garcia and J. Primo, Appl. Catal., 59, 237 (1990).

69. A. Corma and R. M. Martin-Aranda, J. Catal., 130, 130 (1991).

70. P. B. Weisz and V. J. Frilette, J. Phys.Chem., 64, 382 (1960).

71. N. Y. Chen, W. W. Kaeding and F. G. Dwyer, J. Am. Chem. Soc., 101, 6783 (1979).

72. S. M. Csicsery, Zeolites, 4, 202 (1984).

73. J. N. Miale, N. Y. Chen and P. B. Weisz, J. Catal., 6, 278 (1966).

74. S. M. Csicsery, J. Catal., 23, 124 (1971).

75. E. G. Derouane and Z. Gabelica, J. Catal., 65, 486 (1980).

76. S. T. Sie, Stud. Surf. Sci. Catal. 85, 587 (1994).

77. P. B. Venuto and P. S. Landis, Adv. Catal., 18, 346 (1968).

78. C. Gauthier, B. Chiche, A. Finiels and P. Geneste, J. Mol. Catal., 50, 219 (1989).

79. C. D. Chang and P. D. Perkins, Zeolites, 3, 298 (1983).

80. M. J. Climent, A. Corma, H. Garcia and J. Primo, J. Catal., 130, 138 (1991).

81. A. Aucejo, M. C. Burguet, A. Corma and V. Fornes, Appl. Catal., 22, 187 (1986).

82. I. E. Maxwell, R. S. Downing and S. A. J. van Langen, J. Catal., 61, 485 (1980).

83. W. Hölderich, M. Hesse and F. Naumann, Angew. Chem., Int. Ed. Engl., 27, 226 (1988).

84. G. Perot and M. Guisnet, J. Mol. Catal., 61, 173 (1990).

85. C. B. Dartt and M. E. Davis, Catal. Today, 19, 151 (1994).

86. G. Bellussi and M. S. Rigutto, Stud. Surf. Sci. Catal., 85, 177 (1994).

87. R. A. Sheldon and J. Dakka, Catal. Today, 19, 215 (1994).

88. P. Ratnasamy and R. Kumar, Stud. Surf. Sci. Catal., 97, 367 (1995).

89. R. J. Argauer and G. R. Landolt, US. Pat. 3, 702,886 (1972).

90. Y. Ono, Catal. Rev.- Sci. Eng., 34, 179 (1992).

91. G. T. Kokotailo, S. L. Lawton, D. H. Olson and W. M. Meier, Nature, 272, 437 (1978).

92. D. G. Hay and H. Jaeger, J. Chem. Soc. Chem. Commun., 1433 (1984).

93. R. A. Sheldon and J. K. Kochi, "Metal-Catalyzed Oxidations of Organic Compounds", Acad. Press: New York, 1981.

94. J. Muzart, Chem. Rev., 92, 113 (1992).

95. M. P. McDaniel and M. B. Welch, J. Catal., 82, 98 (1983).

96. C. Groeneveld, P. P. M. M. Wittgen, A. M. van Kersbergen, P. L. M. Mestrom, C. E. Nuijten and G. C. A. Schuit, J. Catal., 59, 153 (1979).

97. M. Helliwell, V. Kaucic, G. M. T. Cheetham, M. M. Harding, B. M. Kariuki and P. J. Rizkallah, Extended Abstracts of the 9 th Int. Zeolite. Conf., Montreal, 1992, abstract No. RP203.

98. B. Z. Wan, K. Huang, T. C. Yang and C. T. Tai, J. Chin. Indt. Chem. Eng., 22, 17 (1991).

99. B. M. Weckhuysen and R. A. Schoonheydt, Zeolites, 14, 360 (1994).

100. J. D. Chen and R. A. Sheldon, J. Catal., 153, 1 (1995).

101. J. D. Chen, J. Dakka, E. Neeleman and R. A. Sheldon, J. Chem. Soc. Chem. Commun., 1379 (1993).

102. J. D. Chen, J. Dakka and R. A. Sheldon, Appl. Catal., 108, L1 (1994).

103. H. E. B. Lempers, J. D. Chen and R. A. Sheldon, Stud. Surf. Sci. Catal., 94, 705 (1995).

104. J. D. Chen, M. J. Haanepen, J. H. C. van Hooff and R. A. Sheldon, Stud. Surf. Sci. Catal., 84, 973 (1994).

105. N. Rajic, D. Stojakovic, S. Hocevar and V. Kaucic, Zeolites, 13, 384 (1993).

106. C. Naccache and Y. Ben Taarit, J. Chem. Soc. Faraday Trans.I, 69, 1475 (1973).

107. V. D. Atanasova, V. A. Shvets and V. B. Kazanski, Kinet. Katal., 18, 1033 (1977).

108. J. R. Pearce, D. E. Sherwood, M. B. Hall and J. H. Lunsford, J. Phys. Chem., 84, 3215 (1980).

109. J. F. Hemidy, J. M. Goupil and D. Cornet, J. Chim. Phys., 74, 74 (1977).

110. M. R. Klotz, US. Pat. 4 299 808 (1981); US. Pat. 4 363 718 (1982); US. Pat. 4 405 502 (1983); US. Pat. 4 431 748 (1984).

111. H. O. Pastore, E. Stein, C. U. Davanzo, E. J. S. Vichi, O. Nakamura, M. Baesso, E. Silva and H. Vargas, J. Chem. Soc. Chem. Commun., 772 (1990).

112. T. S. R. Prasada Rao and R. B. Borade, Chem. Exp., 1, 709 (1986).

113. R. B. Borade, A. B. Halgeri and T. S. R. Prasada Rao, Stud. Surf. Sci. Catal., 28, 851 (1986).

114. K. G. Ione, L. A. Vostrikova and V. M. Mastikhin, J. Mol. Catal., 31, 355 (1985).

115. U. Cornaro, P. Jiru, Z. Tvaruzkova and K. Habersberger, Stud. Surf. Sci. Catal., 69, 165 (1991).

116. M. Sugimoto, H. Katsuno, K. Takatsu and N. Kawata, Appl. Catal., 80, 13 (1992).

117. A. V. Kucherov and A. A. Slinkin, Zeolites, 7, 38 (1987).

118. T. Chapus, A. Tuel, Y. Ben Taarit and C. Naccache, Zeolites, 14, 349 (1994).

119. J. S. Mambrim, H. O. Pastore, C. U. Davanzo, E. J. S. Vichi, O. Nakamura and H. Vargas, Chem. Mater., 5, 166 (1993).

120. N. van der Puil, Widyawati, J. C. Jansen and H. van Bekkum, Stud. Surf. Sci. Catal., 84, 211 (1994).

121. R. Joseph, M. Sasidharan, R. Kumar, A. Sudalai and T. Ravindranathan, J. Chem. Soc. Chem. Commun., 1341 (1995).

122. J. D. Lee, "A New Concise Inorganic Chemistry", 3rd ed., p. 324 (1989).

HYDROTHERMAL SYNTHESIS OF CHROMIUM SILICATE, CrS-1

2.1 INTRODUCTION

In recent years, since the disclosure of the synthesis of various heteroatoms substituted zeolites, the interest in these new materials has grown steadily[1-8]. The substitution of a heteroatom in the framework of a zeolite alters the chemical properties of the zeolite without affecting the molecular sieving capabilities. They, indeed, seem to offer a wide application in the field of organic fine chemical synthesis[9-12].

Among the heteroatoms, transition metal substituted molecular sieves continue to be regarded as promising materials for both scientific and technical purposes and therefore are still being investigated intensively[13,14]. In particular, numerous papers[15] have appeared which deal with the synthesis of chromium silicate molecular sieves. However, most of the reports emphasize on the characterization of these materials without considering the stability of chromium ions in the molecular sieves. In an attempt to unveil the problem regarding the chromium ion stability, we have modified the synthetic procedure for the preparation of chromium silicalite-1 in the presence of fluoride ions[16]. However, there are still unsolved problems in synthesizing molecular sieves with high surface area and smaller particle size, essential parameters for good catalytic activity[17]. These shortcomings can better be solved by gaining a deeper insight into kinetics of crystallization. One of the most important factors in the synthesis of molecular sieves is the chemical composition of the gel from which molecular sieves will be harvested.

This chapter delineates the synthesis conditions for the crystallization of chromium silicate molecular sieves with MFI structure in the presence of fluoride ions. The influence of various parameters such as different chromium sources, Si/Cr, Si/TPAOH and H_2O/Si (molar ratios) on crystallization kinetics is studied in detail.

2.2 EXPERIMENTAL

2.2.1 HYDROTHERMAL SYNTHESIS OF CrS-1

The synthesis was carried out in Teflon flask placed into stainless-steel autoclave with a capacity of ~ 250 mL. After each experiment, the autoclave was cleaned with diluted hydrofluoric acid (HF) to avoid seeding effects by residual crystallization products. Reagents and the outline of the synthetic procedures used in the synthesis of CrS-1 are given in Table 2.1 and Fig. 2.1, respectively.

The hydrothermal synthesis of CrS-1 proceeded from gels with a formal molar composition:

$$SiO_2 : x \ Cr_2O_3 : 0.5 \ TPAOH : 0.16 \ Na_2O : 0.5 \ HF : 60 \ H_2O$$

where x = 0.0125, 0.0083 and 0.0062. A typical synthesis of CrS-1 is described below: 20 g tetraethyl orthosilicate (TEOS) was transferred slowly under vigorous stirring into a Teflon beaker containing 26 g of distilled water and 0.96 g of $Cr(NO_3)_3 .9 \ H_2O$. The stirring was continued for 30 minutes. This was added drop by drop to a solution containing 2.4 g of HF (40% aqueous), 35 g of distilled water, 0.32 g of NaOH and 48.6 g of tetrapropylammonium hydroxide (TPAOH, 20% aqueous). The temperature of the Teflon beaker was maintained at 273 K. The final mixture was stirred for 2 h before autoclaving and the pH of the resultant gel was 5.3. The crystallization was conducted in an oven under static conditions at 443 K under autogeneous pressure for 4 days. After the crystallization was completed, the autoclave was cooled and the solid material was recovered by filtration, washed thoroughly with distilled water, dried at 393 K for 6 h, and calcined at 773 K in air for 12 h.

The pure-silica polymorph with MFI (silicalite-1) structure was also synthesized using the same procedure, without adding chromium salt.

Table 2.1

Specification of reagents used in the synthesis of chromium silicate molecular sieves (CrS-1).

S. No	Reagent	Supplier	Formula	Purity
1.	Tetraethyl orthosilicate	E. Merck	$Si(OC_2H_5)_4$	99%
2.	Tetrapropylammonium hydroxide (aqueous)	Aldrich	$(CH_3CH_2CH_2)_4N\text{-}OH$	20%
3.	Chromium(III) nitrate nonahydrate	Loba	$Cr(NO_3)_3.\ 9H_2O$	99%
4.	Chromium(III) chloride hexahydrate	Loba	$CrCl_3.\ 6H_2O$	99%
5.	Chromium(III) sulfate	E. Merck	$Cr_2(SO_4)_3$	97%
6.	Chromium(VI) oxide	Loba	CrO_3	99%
7.	Sodium hydroxide	Loba	$NaOH$	97%
8.	Hydrofluoric acid (aqueous)	Loba	HF	40%

```
┌─────────────────────────┐              ┌──────────────────────────────┐
│  TPAOH + H₂O + NaOH     │              │           TEOS               │
└─────────────────────────┘              └──────────────────────────────┘
            │                                          │
    ┌───────────────┐                    ┌──────────────────────────────┐
    │      HF       │                    │  Cr(NO₃)₃. 9H₂O + H₂O       │
    └───────────────┘                    └──────────────────────────────┘
            │                                  Stirring for 30
            │                                  minutes, 273 K.
    ┌─────────────────────────┐          ┌──────────────────────────────┐
    │    Clear solution       │          │     Green colour solution    │
    └─────────────────────────┘          └──────────────────────────────┘
    Stirring for 15
    minutes, 273 K            drop by drop addition for 1 h

                    Stirring for 2 h, 273 K

            ┌─────────────────────────────────┐
            │        Green colour gel         │
            └─────────────────────────────────┘
                            │
            ┌─────────────────────────────────┐
            │    Crystallization, static      │
            │   conditions,  443 K, 4 days    │
            └─────────────────────────────────┘
                            │
            ┌─────────────────────────────────┐
            │   Washing and  drying at 393 K  │
            │             for 6 h             │
            └─────────────────────────────────┘
                            │
            ┌─────────────────────────────────┐
            │  Calcination in air at 773 K for│
            │             12 h                │
            └─────────────────────────────────┘
                            │
            ┌─────────────────────────────────┐
            │  Ammonium (acetate) exchange    │
            │    (1 M) at 353 K for 5 h       │
            └─────────────────────────────────┘
                            │
            ┌─────────────────────────────────┐
            │  Recalcination in air at 773 K  │
            │           for 12 h              │
            └─────────────────────────────────┘
                            │
            ┌─────────────────────────────────┐
            │             CrS-1               │
            └─────────────────────────────────┘
```
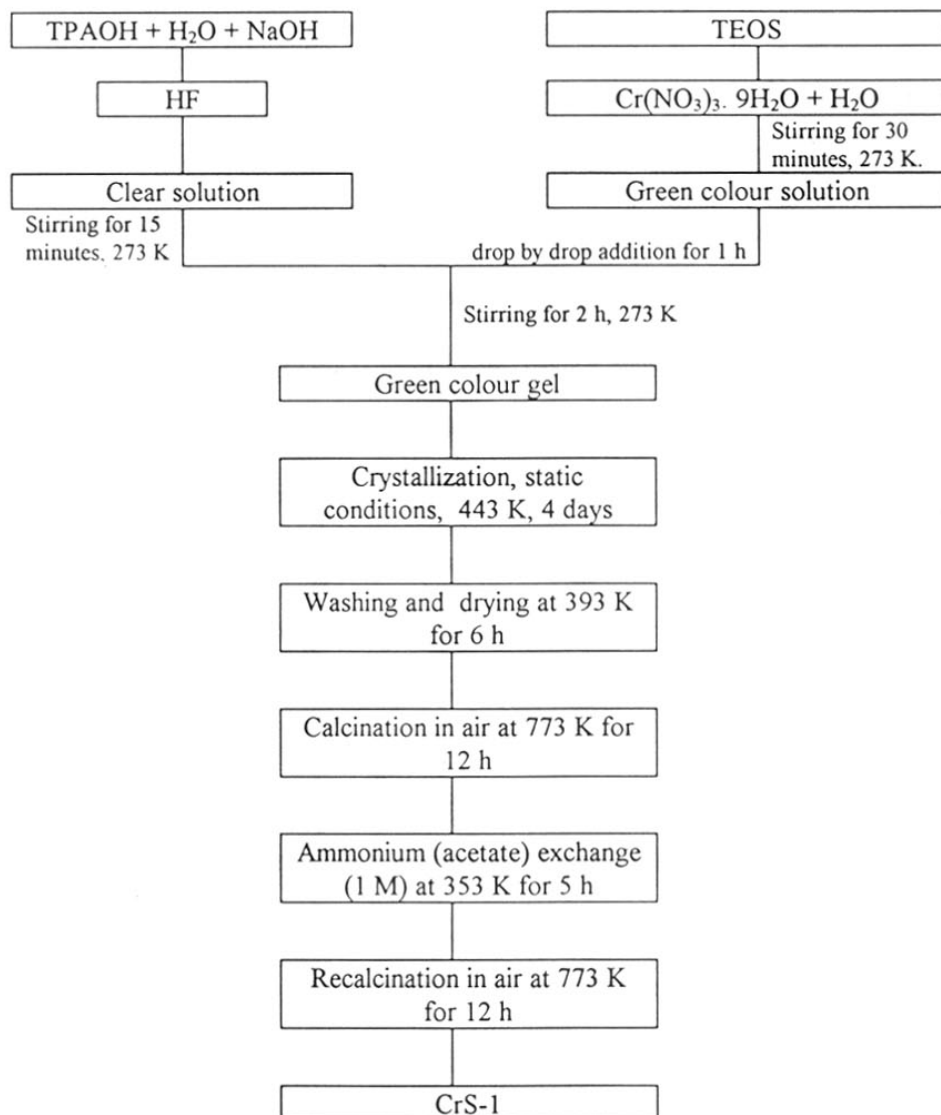
Fig. 2.1   Outline of the synthetic procedure used to synthesize CrS-1

2.2.2 CHARACTERIZATION

2.2.2.1 X-RAY DIFFRACTION

To analyze the crystallinity and phase purity of the crystallization products, X-ray diffraction (XRD) patterns were collected at room temperature using an X-ray diffractometer (Rigaku, model D-Max III VC, Japan) with Ni filtered monochromatic Cu-Kα radiation (λ = 1.5404 Å). All the samples were scanned in the 2θ range 5° to 50° at a scan rate of 2° min^{-1}. The crystallinity of the samples was studied with reference to a standard (highly crystallized sample) obtained previously, which was considered to have 100% crystallinity. The area under the peaks were calculated from the collected data, using a semi-quantitative software provided with the instrument. The relative crystallinity of the sample was determined from the sum of the areas of the peaks between 2θ = 22.5° and 25°. The degree of crystallinity (DC) of the sample was obtained from the following equation:

$$DC = \frac{\text{Peak area between } 2\theta = 22.5° \text{ and } 25° \text{ of the product}}{\text{Peak area between } 2\theta = 22.5° \text{ and } 25° \text{ of the standard sample}} \times 100$$

The phase purity of all the synthesized samples was checked by comparing the X-ray data available in the literature for silica polymorph with MFI structure (silicalite-1)[18].

2.2.2.2 SCANNING ELECTRON MICROSCOPY

The morphology of the crystalline products as well as the crystallite size was determined using a Leica Stereoscan 440 scanning electron microscope. The samples, ground, suspended in ethanol were dispersed on alumina pegs and coated with a thin layer of gold. Scanning electron photomicrographs were taken at identical magnification.

2.2.2.3 THERMAL ANALYSIS

In order to investigate the decomposition of the occluded organic template and to find suitable calcination temperature of the as-synthesized samples, thermogravimetric (TG) and differential thermal analyses (DTA) were carried out in a TG-DTA-92-model (Setaram,

27

France) instrument. The measurements were made in flowing air (30 ml min^{-1}) with a heating rate of 10 K min^{-1} from room temperature to 1273 K. The sample weight of about 25 mg was placed in a platinum crucible and α-alumina was used as a reference.

2.2.2.4 SURFACE AREA MEASUREMENT

The BET surface area and micropore volume were determined by nitrogen adsorption using an Omnisorb 100 CX (Coulter Corporation, USA) instrument. The samples were outgassed at 673 K for 3 h prior to adsorption. High purity nitrogen (99.99 %) was used as adsorbate at liquid nitrogen temperature, 77 K. The adsorption measurements were carried out at relative pressure p/p_o = 0 to 0.9 where p is the adsorption pressure and p_o is the saturated vapour pressure of N_2 at 77 K.

2.2.2.5 CHEMICAL ANALYSIS

The elemental analysis of these samples were determined using Inductively Coupled Plasma Emission analysis (ICP, JOBIN YVON-JY-38 VHR) by dissolving 100 mg of molecular sieves in minimum amount of dilute hydrofluoric acid (HF, 40%). A calibration graph was drawn between concentration (in ppm) and emission intensity using solutions of known concentration. The unknown concentration in the sample was determined from its emission intensity.

2.3 RESULTS AND DISCUSSION

2.3.1 X-RAY DIFFRACTION

The course of crystallization of CrS-1 was followed by XRD; Fig. 2.2 shows X-ray diffraction patterns of product samples withdrawn at different times of crystallization. The curve 'a" in Fig. 2.2 corresponds to the XRD pattern of the sample collected after one day which is amorphous; thereafter as the synthesis time increases the amorphous phase starts to transform into the crystalline phase. Characteristic peaks correspond to the silicalite-1 start appearing after two days and the curve 'd' in Fig. 2.2 corresponds to the highly crystalline
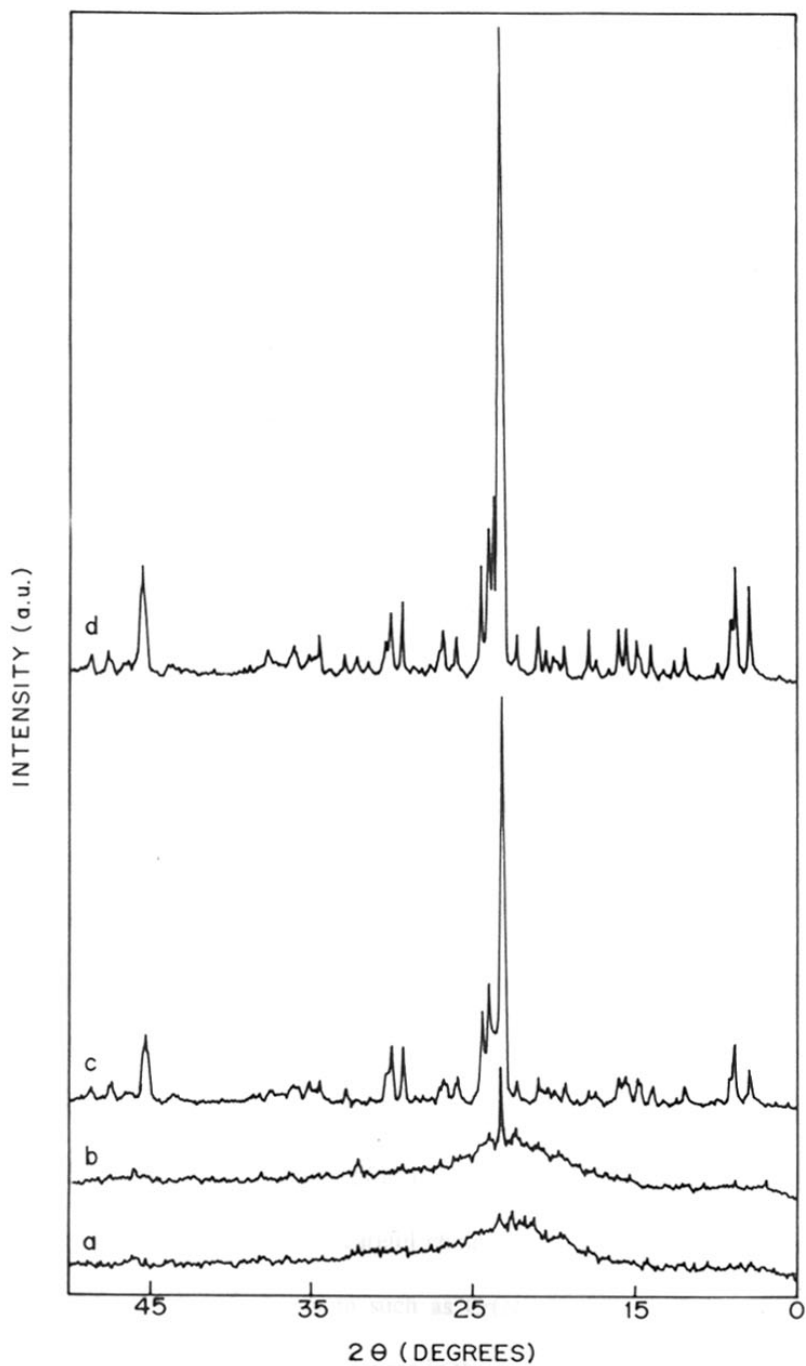
28

Fig. 2.2   Crystallization of CrS-1 at 443 K as followed by X-ray powder diffraction (a) 1 day, (b) 2 days, (c) 3 days and (d) 4 days [SiO_2 : 0.0125 Cr_2O_3 : 0.5 TPAOH : 0.16 Na_2O : 0.5 HF : 60 H_2O].

material obtained at 443 K after 4 days. The crystallinity of CrS-1 improves with increasing time of crystallization. The degree of crystallinity of the samples with drawn at different intervals of time are 3 (1 day), 16 (2 days), 76 (3 days) and 100 % (4 days) respectively. Furthermore, CrS-1 is stable in its reaction mixture for additional four days at 443 K. However, prolonged crystallization time has resulted 5 % decrease in crystallinity, caused by the redissolution of the CrS-1 in the highly acidic medium employed.

2.3.2 SCANNING ELECTRON MICROSCOPY (SEM)

The course of changes in the size and morphology during the synthesis of CrS-1 is also followed by scanning electron microscopy. Fig. 2.3 shows scanning electron photomicrographs of samples withdrawn at different times of crystallization. Scanning electron photomicrograph of the sample collected after 1 day shows that there is no crystallite formation. However, as the crystallization time increases, it can be seen from the Fig. 2.3 that the transformation of amorphous gel into a well-defined lath shaped, twinned crystals. A crystal size of about (5 x 25 μm) is obtained after 4 days at 443 K.

2.3.3 INFLUENCE OF SYNTHESIS PARAMETERS

2.3.3.1 INFLUENCE OF CHROMIUM SOURCE

In zeolite synthesis, the choice of raw materials plays a crucial role by affecting the phase purity and crystallinity. A recent paper on the synthesis of vanadium silicate reveals that change in the source of transition metal salt affected the morphology and size of the crystallites[19]. It also affects the amount of incorporation, surface area and catalytic activity of the samples synthesized. Therefore, a careful choice of the chromium source is needed. In view of this, various salts of chromium such as $Cr(NO_3)_3$. $9H_2O$, $CrCl_3$. $6H_2O$, CrO_3 and $Cr_2(SO_4)_3$ have been used as chromium source in the synthesis of chromium silicate molecular sieves. The ratio of Si/Cr (40) in the starting gel is similar in all the experiments. Since $Cr_2(SO_4)_3$ is not freely soluble in water few drops of sulphuric acid was added to dissolve the
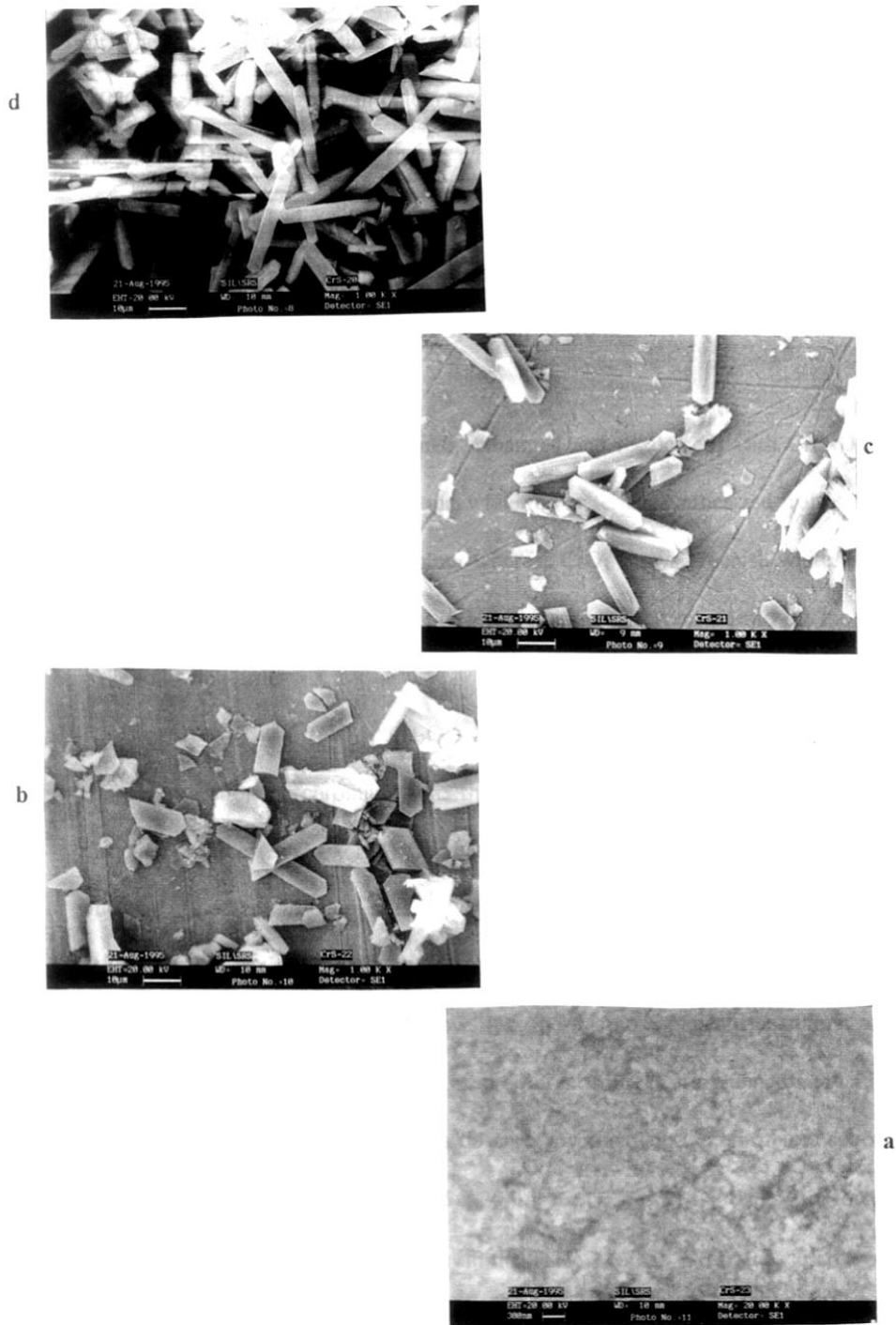
Fig. 2.3 Crystallization of CrS-1 as followed by scanning electron microscopy (a) 1 day, (b) 2 days, (c) 3 days and (d) 4 days [SiO$_2$: 0.0125 Cr$_2$O$_3$: 0.5 TPAOH : 0.16 Na$_2$O : 0.5 HF : 60 H$_2$O].

31

salt. The following observations were made during the gel preparation. The gels prepared with $Cr(NO_3)_3 . 9H_2O$ was green in colour and homogeneous. The gels prepared with $Cr_2(SO_4)_3$ and $CrCl_3 . 6H_2O$ as chromium source were not homogeneous, while that with CrO_3, the gel was homogeneous and yellow in colour. Among the chromium sources tested, $Cr(NO_3)_3 . 9H_2O$ is found to be the best source for homogeneous gel preparation. The physico-chemical properties of the chromium silicates synthesized from different kind of chromium source is given in   Table 2.2.

The sample prepared (calcined, exhanged and recalcined) with $Cr(NO_3)_3 . 9H_2O$ as a chromium source imparts green colour, while the materials synthesized from $CrCl_3 . 6H_2O$ and $Cr_2(SO_4)_3$; show very light green colour whereas CrO_3 shows greenish white. ICP analysis of these samples shows that the amount of incorporation of chromium into the molecular sieves is in the following order:

$$Cr(NO_3)_3 . 9H_2O > CrCl_3 . 6H_2O > Cr_2(SO_4)_3 > CrO_3$$
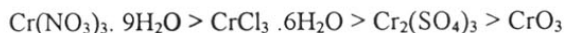
The incorporation of chromium into the molecular sieves is poor when we use CrO_3 as chromium source (Si/Cr = 184) whereas considerable amount of chromium is incorporated when we use other chromium salts.

Fig. 2.4 shows the morphology of the CrS-1 crystals obtained from different sources of chromium. These micrographs shows that there is no significant change in morphology of the crystals. All the crystals obtained from different sources are twinned and lath shaped. But notable change in size of the crystal is observed by changing the chromium source. The sizes are 5 x 25 μm for $Cr(NO_3)_3 . 9H_2O$, 5 x 20 μm for $CrCl_3 . 6H_2O$, 4 x 15 μm for $Cr_2(SO_4)_3$ and 4 x 10 μm for CrO_3. It can be seen from the Table 2.2 that BET surface area of the samples prepared from $Cr(NO_3)_3 . 9H_2O$ is substantially higher (335.7 m^2g^{-1}), in comparison with others namely $CrCl_3 . 6H_2O$ (272.2 m^2g^{-1}), $Cr_2(SO_4)_3$ (183.9 m^2g^{-1}) and CrO_3 (255.9 m^2g^{-1}). Although the size of the crystals synthesized from $Cr(NO_3)_3 . 9H_2O$ is higher than the others, the high

Table 2.2

Physico-chemical properties of CrS-1 prepared from different chromium sources.

| Chromium source	Si/Cr ratio		Yield %	Colour of the sample			Crystal size (μm)	BET surface area (m^2g^{-1})
	Gel	Product[a]		gel	as-synthesized	CrS-1[a]		
$Cr(NO_3)_3. 9H_2O$	40	58	95	Dark green	Dark green	Green	5 x 25	335.7
$CrCl_3 .6H_2O$	40	89	80	Dark green	Light green	Very light green	5 x 20	272.2
$Cr_2(SO_4)_3$	40	108	70	Green	Light green	Very light green	4 x 15	183.9
CrO_3	40	184	80	Yellow	Light green	Greenish white	4 x 10	255.9

[a]Calcined, exchanged and recalcined
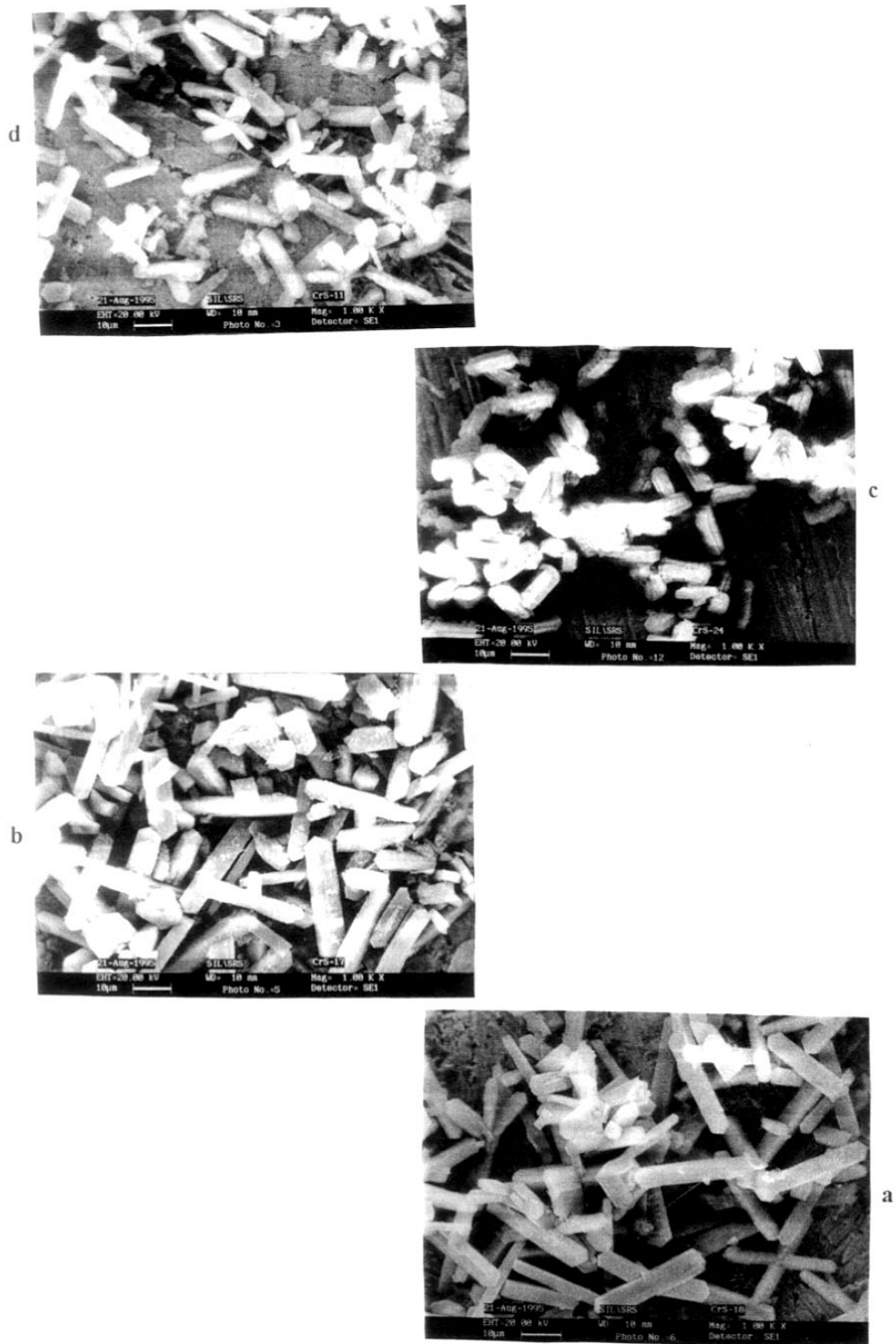
Fig. 2.4 Scanning electron photomicrographs of CrS-1 samples synthesized by using various chromium salts: (a) $Cr(NO_3)_3 \cdot 9H_2O$, (b) $CrCl_3 \cdot 6H_2O$, (c) CrO_3 and (d) $Cr_2(SO_4)_3$.

34

BET surface area can be attributed to the homogenity and crystallinity (100 %) of the sample prepared. Scanning electron photomicrograph also confirms the absence of amorphous material outside the crystals. It is seen from the scanning electron photomicrograph of the sample synthesized from $Cr_2(SO_4)_3$ that this sample possesses considerable amount of macroscopic impurities. Since the sample prepared with $Cr(NO_3)_3$. $9H_2O$ possesses high crystallinity and surface area, we have decided to use $Cr(NO_3)_3$. $9H_2O$ as chromium source for further studies.

2.3.3.2 INFLUENCE OF Si/Cr RATIO

Physico-chemical properties of chromium silicate with different chromium contents are given in Table 2.3. As the chromium content in the gel decreases, the rate of nucleation increased and the crystallization becomes faster[20]. The crystallization of silicalite-1 (chromium-free) is completed within two days. Similar observations have also been made in the synthesis of other metallosilicate molecular sieves[20,21]. As in the synthesis of samples in alkaline medium[22, 23], in this system (fluoride medium) also significant change in the pH of the gel is noticed during the crystallization.

In order to find the influence of chromium content in morphology and size of the crystals, scanning electron photomicrographs were taken for all the samples. The general morphology of the silicalite-1 (chromium-free) (a); and chromium silicalite-1, CrS-1 (Si/Cr = 58) (b); synthesized under similar conditions are displayed in Fig. 2.5. SEM reveals that the crystals of silicalite-1 are uniform, lath shaped, twinned and no amorphous or other crystalline impurities are present in the sample. Almost all the crystals have similar size (6 x 30 μm) and shape (lath shaped). In the literature, it is described that the incorporation of transition metal atom into the MFI structure changes their crystallite size significantly. For examples, for VS-1, the higher the vanadium content, the smaller the

35

Table. 2.3

Physico-chemical properties of chromium silicate with different chromium content.

Gel	Si/Cr ratio		pH		Yield (wt %)	Colour of the sample			Crystallization time (days)	Crystall-inity %
	as-synthesized	CrS-1[b]	Initial	Final		gel	as-synthesized	CrS-1[b]		
40	43 (20)[a]	58 (127)[a]	5.3	5.8	95	Dark green	Dark green	Light green	4	100
60	68 (26)[a]	85 (142)[a]	5.5	6.0	90	Dark green	Green	Very light green	3.5	93
80	94 (29)[a]	122 (160)[a]	5.6	6.0	85	Green	Light green	Very light green	3	89
∞	∞ (90)[a]	∞ (240)[a]	5.9	6.1	85	Colourless	White	White	2	95

[a] In parenthesis are the Si/Na ratio of the corresponding sample.
[b] Calcined, exchanged and recalcined.
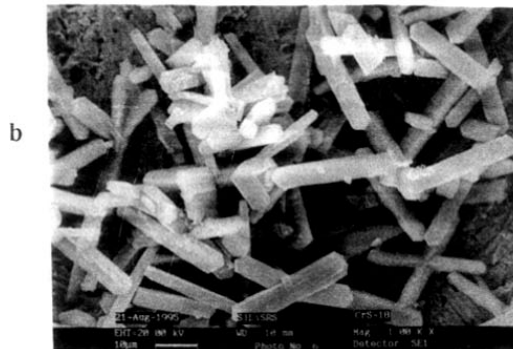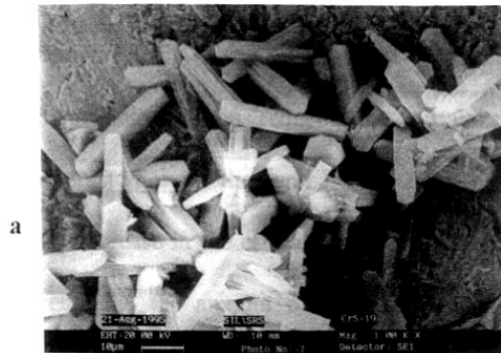
a

b

Fig. 2.5   Scanning electron photomicrographs of: (a) silicalite-1 and   (b) CrS-1
          (Si/Cr = 58).

crystallites obtained[20]. However, in this case of chromium silicate molecular sieves, CrS-1, there is no significant change in morphology and the size (5 x 25 μm) upon incorporation of chromium which is slightly less than that of silicalite-1 (6 x 30 μm).

2.3.3.3 INFLUENCE OF ORGANIC TEMPLATE

The influence of the TPAOH content in the synthesis of CrS-1 from the gels having the molar composition: SiO_2 : 0.0125 Cr_2O_3 : x TPAOH : 0.16 Na_2O : 60 H_2O (where x = 0.5, 0.66 and 1) is shown in Fig. 2.6. As expected, increasing the alkalinity results in a rapid acceleration of crystallinity and thus reducing the crystallization time from 4 days to 24 h. It is known from earlier studies on the synthesis of ZSM-5 that an increase of the content of TPAOH lead to a decrease in the crystal size as a result of an enhanced rate of formation of nuclei[24, 25]. Eventually, the amount of chromium incorporated into the molecular sieves decreases as the TPAOH content is increased. The Si/Cr ratios are 58 (x = 0.5), 93 (x = 0.66) and 178 (x = 1). This trend is attributed to the instability of Cr^{3+} ions in the alkaline medium employed during the synthesis. The availability of Cr^{3+} ions in the gel for the incorporation into the molecular sieves is limited because Cr^{3+} ions are easily oxidized to Cr^{6+} ions at high alkalinity[26]. Moreover, with decrease in the amount of TPAOH (Si/TPAOH = from 2 to 3), there was no increase in the amount of chromium incorporated into the molecular sieves. In all subsequent experiments the Si/TPAOH ratio was kept at a constant value of 2.

2.3.3.4 INFLUENCE OF WATER

The influence of water content in the synthesis mixture is shown in Fig. 2.7. It can be seen from the Fig. 2.7 that the crystallization is faster in a concentrated system (H_2O/Si = 60). The influence of water content on the morphology of the crystal is also followed by SEM. Same morphology of the crystal is found from the synthesis mixture having H_2O/Si = 60, 70 and 80 but the formation of relatively large crystals in the diluted systems is attributed to the slower rate of nucleation.
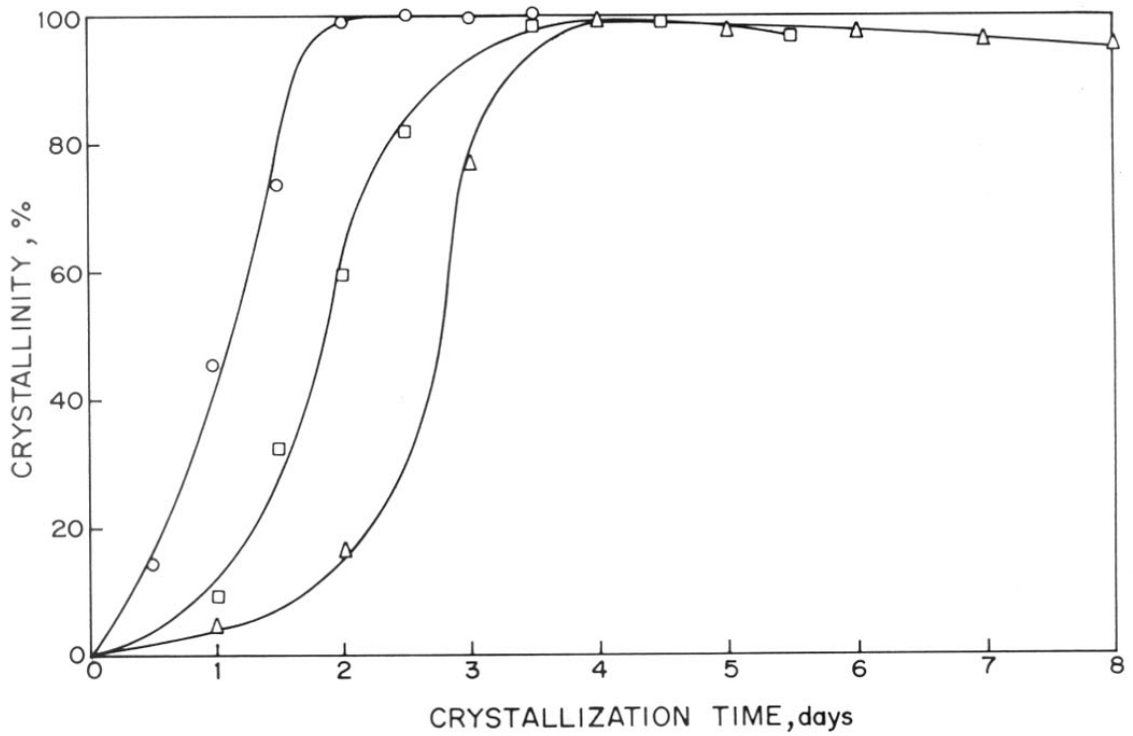
Fig. 2.6   Influence of the TPAOH content on the crystallization of CrS-1 [SiO_2 : 0.0125 Cr_2O_3 : x TPAOH : 0.16 Na_2O : 60 H_2O (where x = 0.5 (△),   0.66 (□) and 1.0 (o)].
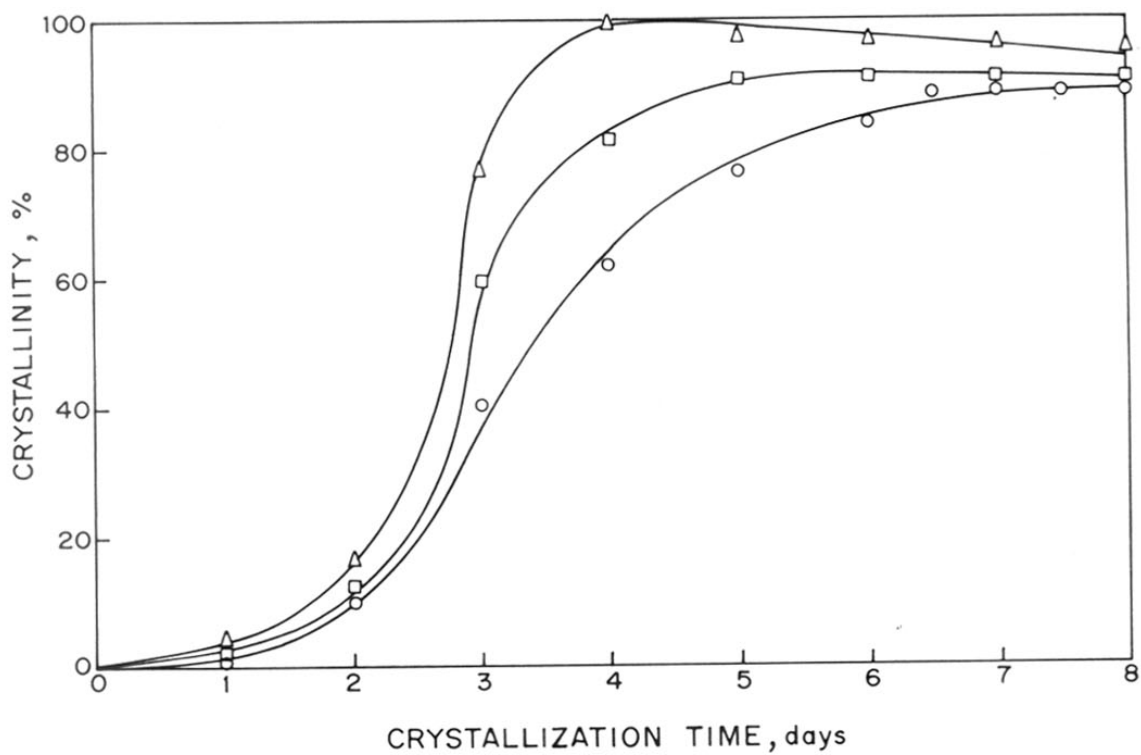
Fig. 2.7 Influence of water content on the crystallization of CrS-1 [SiO_2 : 0.0125 Cr_2O_3 : 0.5 TPAOH : 0.16 Na_2O : x H_2O where x = 60 (△), 70 (□) and 80 (o)].

2.3.3.5 INFLUENCE OF STIRRING

It is well known that the catalytic activity strongly depends on the crystal/particle size of the catalyst synthesized[17]. Catalysts with smaller particle size are more active in the hydroxylation of phenol than the larger ones. Hence, in order to achieve smaller particle size, as well as to compare with static synthesis conditions, crystallization was carried out in a stirred autoclave (60 rpm) using similar molar gel compositions. Fig 2.8 shows the scanning electron photomicrographs of CrS-1 synthesized under static (a) and stirred (b) conditions. As expected, the samples prepared under stirred conditions have crystal size (5 x 20 μm) slightly less than that of the sample prepared under static conditions (5 x 25 μm) and there is no marked change in the morphology of the crystals.

2.3.4 THERMAL ANALYSIS

All the as-synthesized samples were subjected to TG-DTA analyses. TG-DTA patterns of as-synthesized samples are shown in Fig. 2.9. TG measurements showed two distinct weight loss stages from the as-synthesized CrS-1 samples; the first between 373-473 K which is ascribed primarily to the desorption of physically adsorbed water. The second sharp weight loss occurs between 693-753 K which is due to the decomposition of the occluded organic template from the channels of the molecular sieves. The DTA signals in the temperature range 673-773 K showed that the decomposition of the organic template from the CrS-1 occurs in two distinct steps. The organic template occluded in the molecular sieves can be removed completely at 753 K. The following peak assignments are based on the results observed by Crea et al. who have studied the thermal decomposition of TPA$^+$ ions from ZSM-5[27,28]. The first exothermic peak located at 693-703 K is probably due to the inner strained TPA$^+$ ions which neutralize the defect Si-O$^-$ groups. The second exothermic peak located at 693-743 K is due to the removal of the more symmetrical TPA$^+$ ions from the channels of the molecular
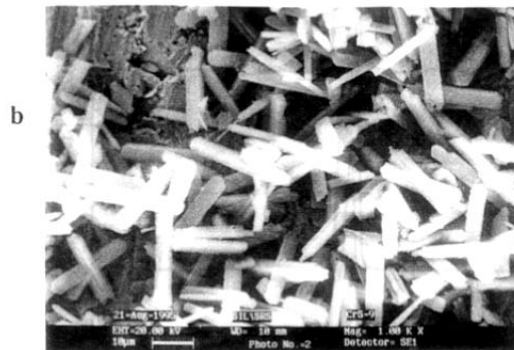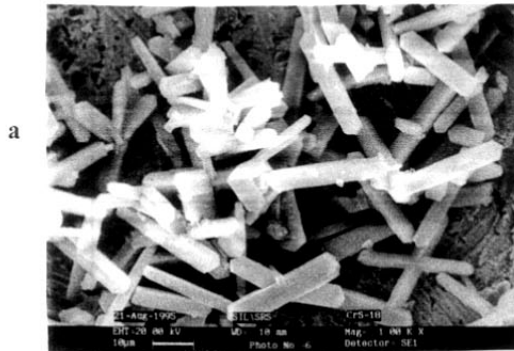
41

Fig. 2.8   Scanning electron photomicrographs of CrS-1 synthesized under static (a) and stirred (b) conditions.
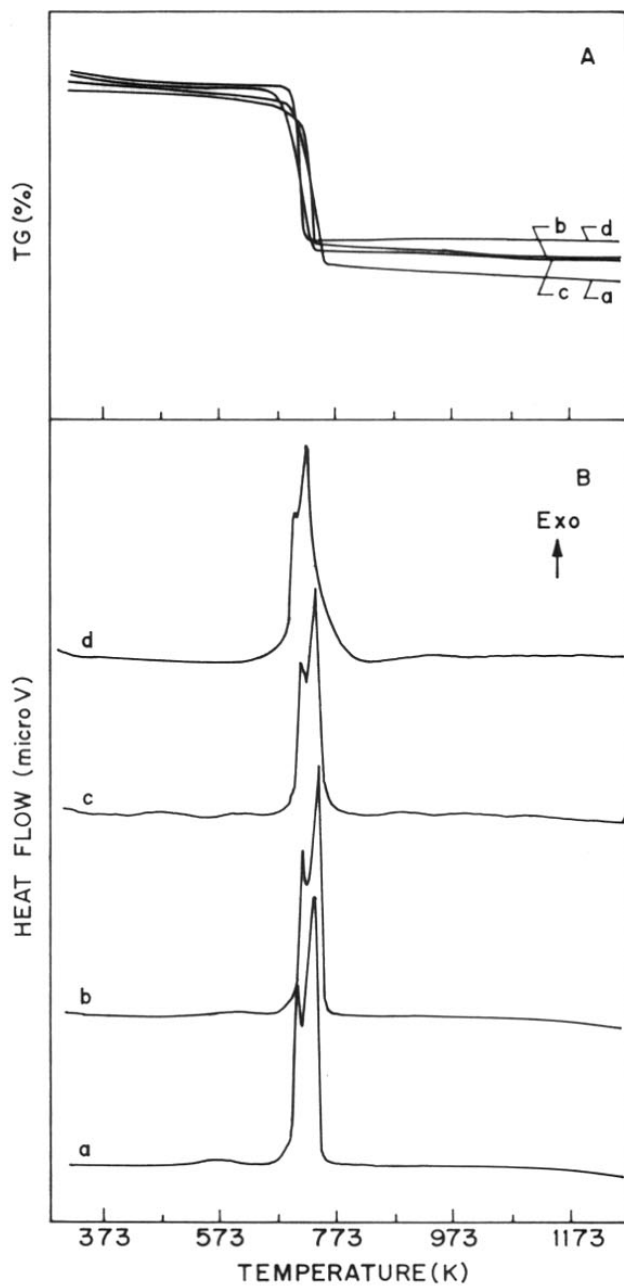
Fig. 2.9   TG (A) and DTA (B) curves for as-synthesized   samples   (a) CrS-1
            (Si/Cr = 43), (b) CrS-1 (Si/Cr = 68), (c) CrS-1 (Si/Cr = 94) and (d)
            Silicalite-1 (chromium-free).

sieves. The total weight loss due to the decomposition of the occluded organic template is found to be 10-11 % for all these samples.

In this hydrothermal synthesis of CrS-1, the role of organic template (TPA$^+$ ion) is not only as a structure-directing agent which influences the formation of chromium silicalite-1 (MFI) but also to stabilize the structure (as observed from the first thermal peak located at 693-703 K).

2.3.5 N$_2$ ADSORPTION ISOTHERM

The most fundamental characteristic of molecular sieves is the low pressure (p/p$_o$ = 0.01) N$_2$ adsorption isotherm at low temperature. The adsorption isotherms of N$_2$ on CrS-1 with different chromium contents are shown in Fig. 2.10. The surface area and micropore volume of the samples are in the range of 335 to 225 m^{2}g^{-1} and 0.16 to 0.13 mlg^{-1}, respectively. The surface area is substantially high in the chromium containing samples as against silicalite-1 (chromium-free). The adsorption measurements reveal a hysteresis loop for all the samples. This is not unexpected and is a reflection of the generation of hydroxylated internal "nests" by framework removal around the growing metal crystals[29]. The generation of such type of "nests" are well known[30] and discerned by transmission electron microscopy (TEM)[31]. It is generally noticed that the development of the hysteresis is only on the samples prepared via fluoride medium[32] whereas no such hysteresis is observed on the samples prepared via alkaline medium. Most probably, this must be due to the presence of hydroxylated internal "nests" generated by missing (SiO$_4$) tetrahedra[33].
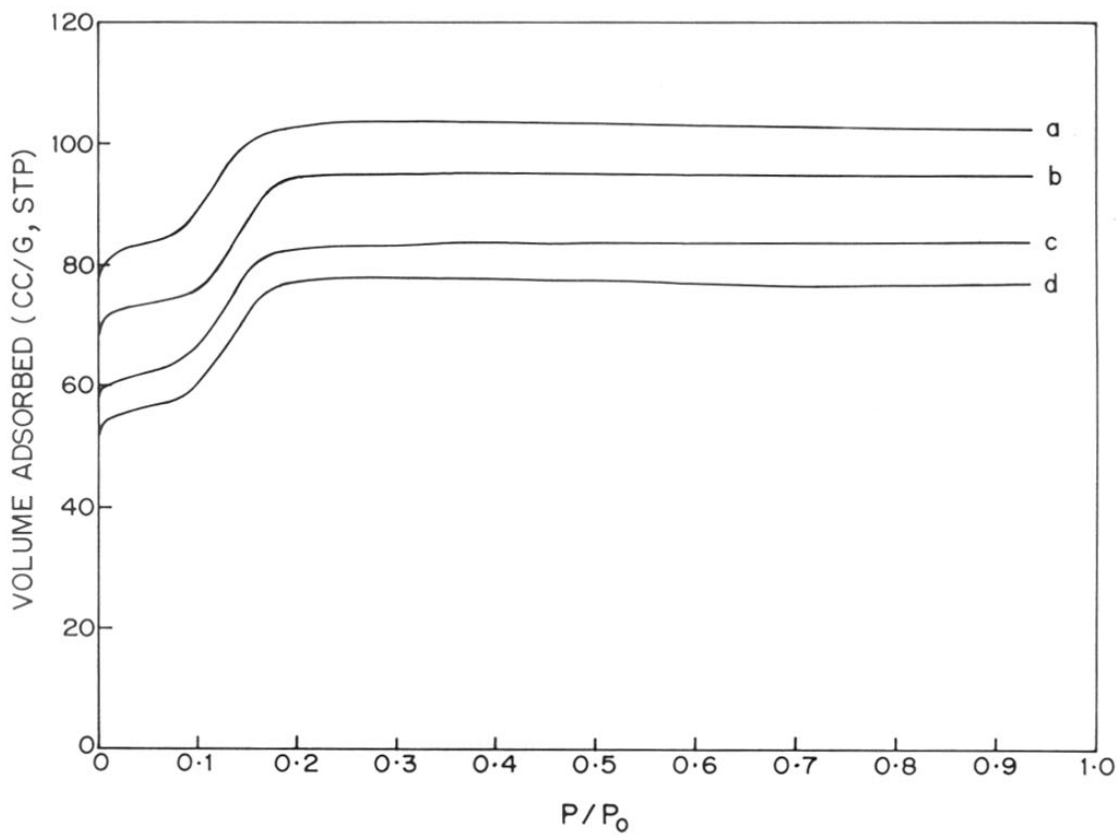
Fig. 2.10 Adsorption isotherms of N_2 at 77 K (a) CrS-1 (Si/Cr = 58), (b) CrS-1 (Si/Cr = 85), (c) CrS-1 (Si/Cr = 122) and (d) Silicalite-1 (chromium-free).

2.4 CONCLUSIONS

1. Crystalline, thermally stable chromium silicate molecular sieves with MFI structure, CrS-1, can be synthesized at 443 K in the presence of fluoride ions using tetrapropylammonium hydroxide (TPAOH) as organic template and tetraethyl orthosilicate as silica source.

2. Among the chromium source tested, $Cr(NO_3)_3 .9H_2O$ is found to be an effective source for the synthesis of CrS-1 compared to other sources such as $CrCl_3 .6H_2O$, $Cr_2(SO_4)_3$ and CrO_3.

3. The synthesis of CrS-1 has some features in common with the synthesis of metallosilicates with MFI structures: (i) increasing the Si/Cr molar ratio in the gel enhances the rate of crystallization and (ii) increasing the H_2O/Si molar ratio in the gel decreases the rate of crystallization.

4. SEM reveals that the crystals are uniform, lath shaped and free from amorphous materials.

5. TG-DTA studies reveal that the role of organic template (TPA^+ ion) is not only as a structure-directing agent which influences the formation of CrS-1, but also to stabilize the structure.

6. N_2 adsorption isotherm studies reveal a hysteresis loop which is attributed to the formation of defect sites (hydroxylated internal "nests"), generally noticed in the molecular sieves synthesized via fluoride medium.

2.5 REFERENCES

1. E. M. Flanigen, J. M. Bennett, R. W. Grose, J. P. Cohen, R. L. Patton, R. M. Kirchner and J. V. Smith, Nature, 271, 512 (1978).

2. G. Coudurier, A. Auroux, J. C. Vedrine, R. D. Farlee, L. Abrams and R. D. Shannon, J. Catal., 108, 1 (1987).

3. R. Szostak and T. L. Thomas, J. Catal., 100, 555 (1986).

4. T. Inui, Y. Makino, F. Okazumi and A. Miyamoto, J. Chem. Soc. Chem. Commun., 571 (1986).

5. R. Szostak, Molecular Sieves; Van Nostrand Reinhold: New York, 1989.

6. B. Notari, Stud. Surf. Sci. Catal., 60, 343 (1991).

7. M. S. Rigutto and H. van Bekkum, Appl. Catal., 68, L1 (1991).

8. N. K. Mal, V. Ramaswamy, S. Ganapathy and A. V. Ramaswamy, J. Chem. Soc. Chem. Commun., 1933 (1994).

9. P. B. Venuto and P. S. Landis, Adv. Catal., 18, 259 (1968).

10. W. F. Holderich, Stud. Surf. Sci. Catal., 49A, 69 (1989).

11. I. E. Maxwell, Adv. Catal., 31, 2 (1982).

12. P. Ratnasamy and R. Kumar, Stud. Surf. Sci. Catal., 97, 367 (1995).

13. J. C. Vedrine, Stud. Surf. Sci. Catal., 69, 25 (1991).

14. G. Bellussi and V. Fattore, Stud. Surf. Sci. Catal., 69, 79 (1991).

15. References 106 to 121, Chapter 1.

16. T. Selvam and M. P. Vinod, Appl. Catal., 134, L197 (1996).

17. A. J. H. P. van der Pol, A. J. Verduyn and J. H. C. van Hooff, Appl. Catal., 92, 113 (1992).

18. R. J. Argauer and G. R. Landolt, US. Pat., 3 702 886 (1972).

19. A. Miyamoto, D. Medhanavyn and T. Inui, Appl. Catal., 28, 89 (1986).

20. P. R. H. P. Rao, R. Kumar, A. V. Ramaswamy and P. Ratnasamy, Zeolites, 13, 663 (1993).

21. K-J. Chao, T. C. Tasi, M-S. Chen, and I. Wang, J. Chem. Soc. Faraday Trans. I, 77, 547 (1981).

22. J. S. Reddy and R. Kumar, Zeolites, 12, 95 (1992).

23. A. Thangaraj, Ph. D., Thesis, University of Pune (1991).

24. R. Mostowicz and L. B. Sand, Zeolites, 3, 219 (1983).

25. A. Erdem and L. B. Sand, J. Catal., 60, 241 (1979).

26. J. D. Lee, "A New Concise Inorganic Chemistry", 3 rd ed., p. 324 (1989).

27. F. Crea, A. Nastro, J. B. Nagy and R. Aiello, Zeolites, 8, 262 (1988)

28. J. El Hage-Al Asswad, N. Dewaele, J. B. Nagy, R. A. Hubert, Z. Gabelica, E. G. Derouane, F. Crea, R. Aiello and A. Nastro, Zeolites, 8, 221 (1988).

29. N. I. Jaeger, J. Rathousky, G. Schulz-Ekloff, A. Svensson and A. Zukal, Stud. Surf. Sci. Catal., 49B, 1005 (1989).

30. U. Lohse, G. Engelhardt and V. Patzelova, Zeolites, 4, 163 (1984).

31. V. Patzelova and N. I. Jaeger, Zeolites, 7, 240 (1987).

32. G. L. Marra, G. Tozzola, G. Leofanti, M. Padovan, G. Petrini, F. Genoni, B. Venturelli, A. Zecchina, S. Bordiga and G. Ricchiardi, Stud. Surf. Sci. Catal., 84, 559 (1994).

33. J. M. Chezeau, L. Delmotte, J. L. Guth and Z. Gabelica, Zeolites, 11, 598 (1991).

CHAPTER 3

PHYSICO-CHEMICAL CHARACTERIZATION OF CrS-1

3.1 INTRODUCTION

As perusal of the literature shows, great strides have been made in the synthesis of molecular sieves containing transition elements, especially chromium. However, the stability of chromium in the molecular sieves during the hydrothermal synthesis and after the thermal treatment has been found to be limited. Ammonium (acetate) exchange[1] and acetic acid treatments[2] have been shown to remove the incorporated chromium completely from the molecular sieves. In order to obviate the problem of chromium stability, chromium silicalite, CrS-1, has been synthesized in the presence of fluoride ions[3] (described in the previous chapter). Physico-chemical characterization of CrS-1 will provide answer to the question: Have we synthesized what we wanted to synthesize ? Since active sites of CrS-1, are so central to molecular sieve catalysis, special attention has been given in this chapter for their accurate characterization. Many techniques have been applied to quantitatively identify the changes brought about within the MFI structure upon the introduction of chromium ions. Among these techniques are: XRD, IR, UV, Raman spectroscopy, ESR, MAS NMR, CV (cyclic voltammetry) and XPS.

In addition to the conventional spectroscopic characterization, active sites of CrS-1 can also easily be specified or at least reasonably conjectured by indispensable catalytic reactions. The catalytic properties of CrS-1 in selective oxidation reactions will be discussed in the subsequent chapter.

3.2 EXPERIMENTAL

3.2.1 X-RAY DIFFRACTION

X-ray powder diffraction measurements were carried out on a Rigaku (model D-Max III VC, Japan) automated powder diffractometer with Ni-filtered Cu-Kα radiation. The range of

scanning was 5-50 degrees 2θ at a rate of 0.2° min^{-1}. Silicon was used as an internal standard for calibrating the 2θ values. The absence of chromium oxide species was checked by the library facility provided with the instrument.

3.2.2 INFRARED SPECTROSCOPY

Infrared spectra were obtained using the KBr pellet technique in a Perkin Elmer 221 infrared spectrophotometer in the range of 400-1400 cm^{-1}. A pellet of ~ 200 mg, with a diameter of 1 cm was obtained by pressing a mixture of 10 mg of CrS-1 and 200 mg of KBr at ~ 10,000 psi pressure.

3.2.3 UV-VISIBLE SPECTROSCOPY

Diffuse reflectance spectra (UV-Visible DRS) were done on a UV spectrometer (Shimadzu model UV/2101/PC) equipped with a diffuse reflectance attachment using barium sulfate (BaSO$_4$) as the reference. The spectra were recorded at room temperature in the range of 200-800 nm.

3.2.4 RAMAN SPECTROSCOPY

The Raman spectra were obtained with a Spex 1442 spectrometer controlled by a Spex Datamate computer. Excitation of all samples was done with the 514.5 -nm line of a Spectra Physics Ar-ion laser. The scattered light was detected with a RCA C31034 GaAs PM tube. The spectra were scanned in the region 800-1400 cm^{-1} with steps of 2 cm^{-1} and an integration time of 20 sec. The frequencies were measured with an accuracy of ± 2 cm^{-1}.

3.2.5 ELECTRON SPIN RESONANCE SPECTROSCOPY

Electron spin resonance spectra were performed at room temperature on a Bruker ER-200D X-band (9.7 GHz) first derivative e.s.r spectrometer equipped with a rectangular cavity ST 8424 and a 100 kHz magnetic field modulation unit. The spectra were systematically recorded with a constant weight (0.1 g) of the sample.

3.2.6 NUCLEAR MAGNETIC RESONANCE SPECTROSCOPY (NMR)

All solid-state NMR (^{29}Si-MAS and ^{13}C-CP/MAS) measurements were carried out on a Bruker MSL-300 spectrometer at a resonance frequency of 59.6 MHz (^{29}Si), and 75.8 MHz (^{13}C) in an external magnetic field of 7.0 Tesla. Samples were spun at the magic angle at 3.1 kHz (^{29}Si) and 2.9 kHz (^{13}C). Chemical shifts are given in ppm with respect to tetramethylsilane (TMS) as an external standard. The absence of aluminium in CrS-1 was also checked by ^{27}Al MAS NMR. All measurements were performed at room temperature.

3.2.7 CYCLIC VOLTAMMETRY

Cyclic voltammetric experiments were accomplished using Model 173 potentiostat coupled with a function generator (Princeton Applied Research, PAR 173). The resulting voltammograms were recorded using Model RE 0091 X-Y recorder. A conventional three-electrode single compartment cell was used. The reference electrode was a standard calomel electrode (SCE), the used counter electrode was a platinum foil and the working electrode was a graphite disc electrode (area, 0.063 cm^2) coated with molecular sieves. Molecular sieve modified electrodes were prepared by mixing 100 mg of pure graphite, 100 mg of molecular sieve and 10 mg of polystyrene (as binder) in 2 ml THF (Tetrahydrofuran) and the paste was coated on a graphite disc electrode. Cyclic voltammograms were taken in 0.1 M KCl solution in the potential range of 0 to + 1.0 V at a scan rate of 50 mV sec^{-1} . Before taking the cyclic voltammograms the electrolyte solutions were thoroughly degassed with argon.

3.2.8 X-RAY PHOTOELECTRON SPECTROSCOPY (XPS)

The XPS spectra were recorded on a VG Scientific (U. K) ESCA-3-MK-II electron spectrometer using Mg-Kα radiation (1253.6 eV). The anode was operated at 120 W (12 kV, 10 mA) and the analyzer was operated at a constant pass energy of 50 eV. The samples were

mounted on a stainless-steel holder with double side adhesive tape. The charging effect of the samples was corrected by using the carbon contamination as an internal standard.

3.3 RESULTS AND DISCUSSION

3.3.1 X-RAY DIFFRACTION (XRD)

XRD is one of the most frequently applied techniques for identification of a molecular sieve structure. The XRD patterns of chromium silicalite, CrS-1, with different Si/Cr ratio are given in Fig. 3.1. The XRD pattern of silicalite-1 shown here is in agreement with those published previously[4]. Since the XRD patterns of CrS-1 is nearly the same as that for silicalite-1, it is clear that CrS-1 possesses the same framework structure as silicalite-1 and did not reveal the presence of extra phases related to chromium oxide species. In the literature, it is reported that the ratio of the relative intensities of the (101) and (200) peaks (in the small 2θ region) decreases almost linearly with increasing Ga content[5]. Since the relative intensities changed from one sample to another, such a relation between the relative intensities and the chromium content was not observed in these XRD patterns of CrS-1.

Fig. 3.2 shows the XRD patterns of (a) as-synthesized and (b) calcined, exchanged and recalcined CrS-1. XRD reveals that the crystal symmetry of as-synthesized CrS-1 sample is always orthorhombic (Pnma)[6]. However, upon removal of the template molecules from the channels by calcination at 773 K, in air, the crystal symmetry of CrS-1 becomes monoclinic (P2₁/n). The XRD pattern shows the splitting of the diffraction peak near 24.4 (2θ) into two components. The monoclinic symmetry is characteristic of highly siliceous ZSM-5. This is in contrast with the XRD pattern of titanium substituted molecular sieves with MFI structure. The persistence of the orthorhombic symmetry even in the calcined state, is generally considered as a proof for the incorporation of Ti in the framework of the molecular sieves[7]. The orthorhombic –
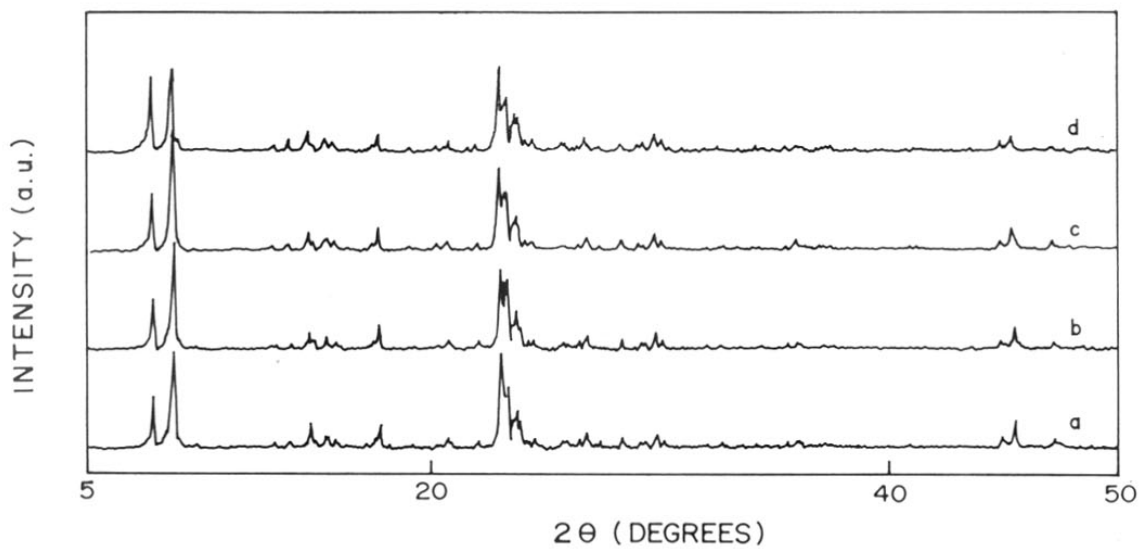
Fig. 3.1   X-ray diffraction patterns of samples (calcined, exchanged and recalcined):
(a) silicalite-1; (b) CrS-1 (Si/Cr = 58),   (c) CrS-1   (Si/Cr = 85)   and (d)
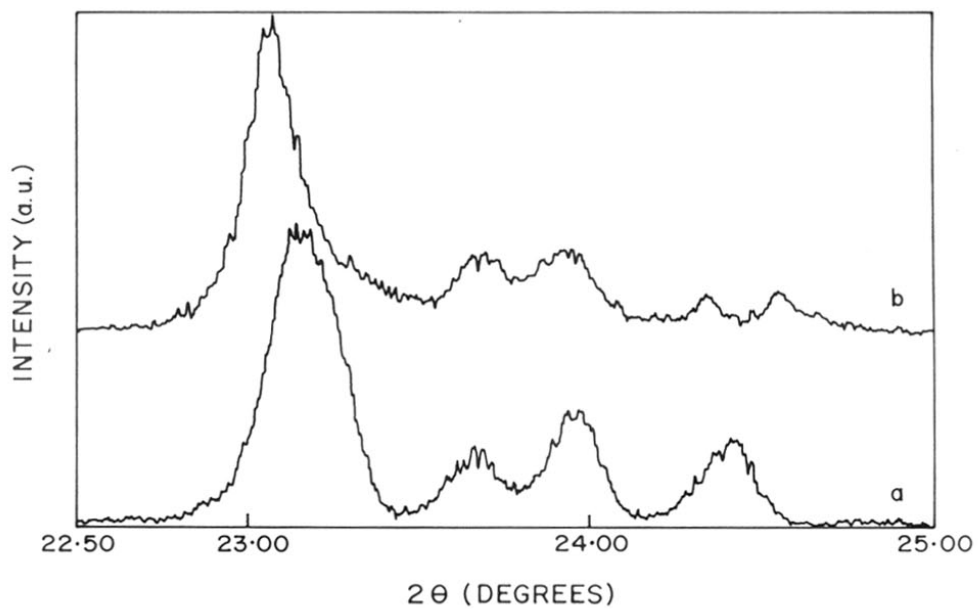CrS-1   (Si/Cr = 122).

Fig. 3.2   XRD powder patterns of CrS-1 sample: (a) as-synthesized; (b) calcined, exchanged and recalcined.

monoclinic transformations which is an unusual effect for the heteroatom substituted molecular sieves. However, Kraushaar[8] observed that the persistence of orthorhombic symmetry for only those samples which contain 1 titanium per unit cell and also the samples with less framework titanium content are all monoclinic. As suggested earlier by Chapus et al.[2], the persistence of orthorhombic symmetry cannot be considered as a determinant evidence for incorporation of heteroatom into the framework structure because silicalite-1 (heteroatom-free) can also exist either in the monoclinic or orthorhombic forms[9]. The changes of symmetry between monoclinic and orthorhombic are mainly dependent on the presence of sodium and aluminium as impurities. The symmetry change is further substantiated by loading/unloading H-ZSM-5 sample with various organic molecules[10,11]. The sorbate-loaded and un-loaded H-ZSM-5 show orthorhombic and monoclinic symmetry, respectively. It is worth noting that, the orthorhombic-monoclinic transition is also observed when titanium and germanium are incorporated into the MFI structure[12,13].

3.3.2 INFRARED SPECTROSCOPY (IR)

Fig. 3.3 shows the IR spectra of CrS-1 (calcined, exchanged and recalcined) samples and their silica analog in the region of 400–1400 cm^{-1}. In all four cases, the presence of a band at 550 cm^{-1} in addition to 460 cm^{-1} band confirms the presence of a five-membered ring of the pentasil (MFI) structures. The intensity ratios of the bands at 550 and 460 cm^{-1}, show that all samples are highly crystalline. The absence of a band at 889 cm^{-1} (which is present in the calcined sample, spectra not shown here) strongly suggests all the CrS-1 samples are free from extralattice chromate species[14]. The extralattice chromium species present in the calcined CrS-1 sample could easily be removed by ammonium (acetate) exchange treatment because of the freely soluble nature of the chromate species in the solution of ammonium acetate.
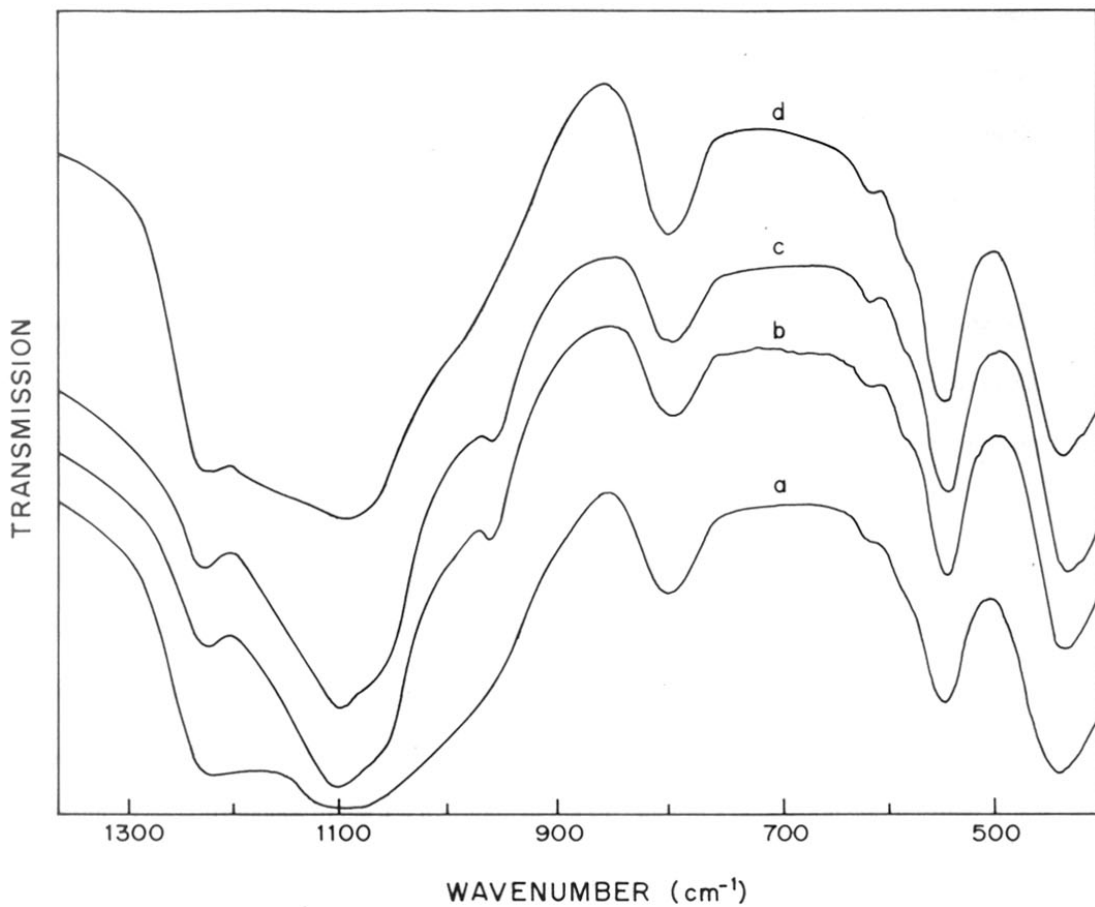
Fig. 3.3   IR spectra of: (a) silicalite-1; (b) CrS-1 (Si/Cr = 58); (c) CrS-1 (Si/Cr = 85) and (d) CrS-1 (Si/Cr = 122).

Although, IR spectra of CrS-1 is closely related to that of silicalite-1 (chromium-free), the most notable difference is a less intense band at 960 cm^{-1}, which is possibly due to Si-O-Cr linkages. As expected, no such band appeared in the IR spectrum of silicalite-1 (Fig. 3.3 curve 'a'). In the case of CrS-1 (Si/Cr = 122, Fig. 3.3 curve 'd'), no significant changes have been observed due to the incorporation of chromium. This is probably due to the low chromium content of the samples. A similar but somewhat intense absorption was already observed in the framework IR spectra of TS-1 and TS-2, which has been ascribed to vibrations of SiO$_4$ units bonded to titanium ions[7,15a]. However, Camblor et al.[15b] assigned this band to the Si-O$^-$...M$^+$ vibration (where M = Ti). Therfore, it is conceivable that chromium ions are part of the MFI structure. Moreover, in accordance with the literature, the chromium does not occupy a regular "T" site of the silicalite framework[16]. This may be one of the main reasons for the lower intensity of the band at 960 cm^{-1}.

3.3.3 UV-VISIBLE SPECTROSCOPY

UV-visible spectroscopy is a convenient tool to identify the oxidation state of chromium ions in chromium silicate samples. UV-visible spectra of chromium silicate samples are given in Fig. 3.4. The spectrum of as-synthesized sample (Fig. 3.4 curve 'a') contain two bands at 626 and 449 nm. This corresponds to the d-d transition of the Cr^{3+} ions in a octahedral coordination which gives a dark green colour to samples containing such species. Octahedral coordination for Cr^{3+} is also reported for as-synthesized CrAlPO$_4$-5[17,18]. Upon calcination, the colour of the as-synthesized sample which was dark green in colour turns into yellow. UV-visible spectrum of the calcined sample (Fig. 3.4 curve 'b') show absorptions at 252, 260, 367 and 613 nm. The bands at 367 and 252 nm (in the calcined sample) have previously been attributed to monochromate species[19,20]. UV-visible spectrum of CrS-1 (calcined, exchanged and recalcined, Fig. 3.4 curve 'c')
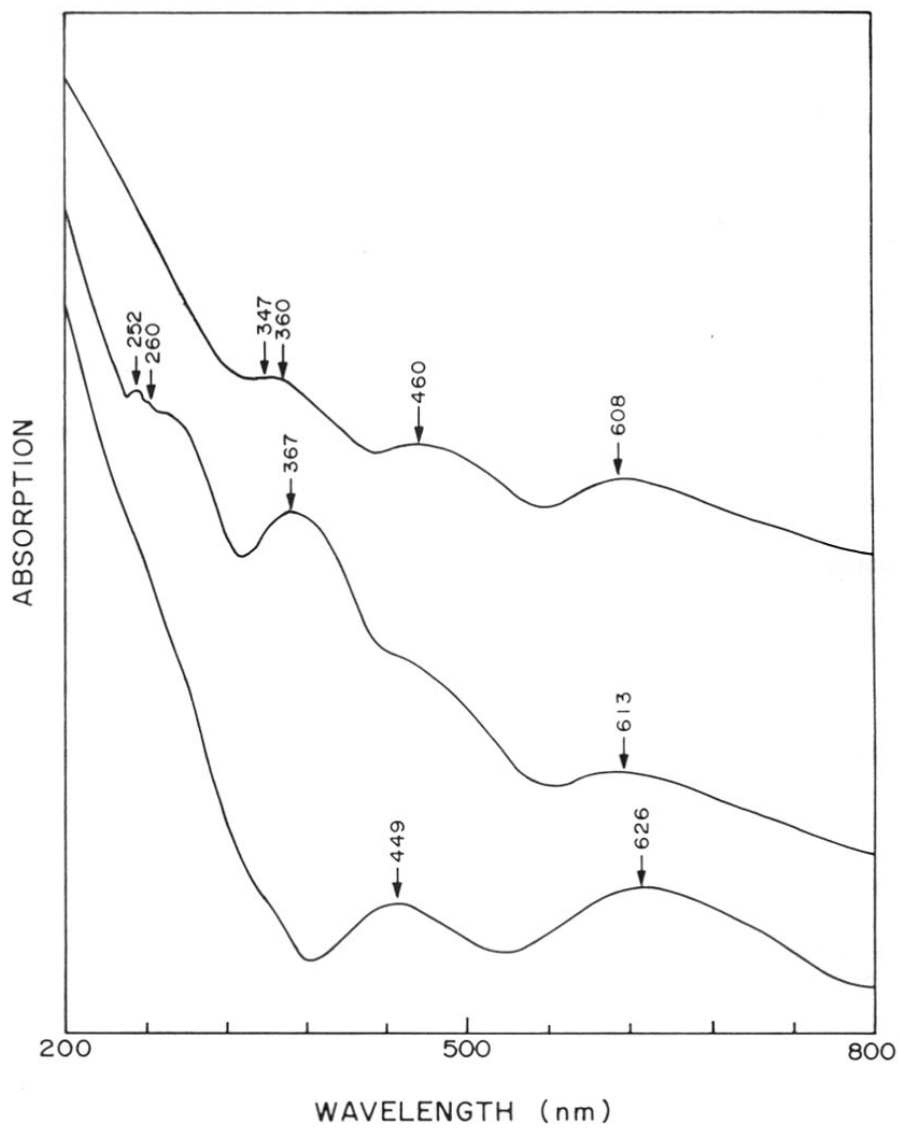
57

Fig. 3.4   UV-visible spectra of CrS-1: (a) as-synthesized; (b) calcined; (c) exchanged and recalcined.

shows major bands at 347, 360, 462 and 608 nm. The absence of two characteristic bands 252 and 367 nm confirms that the sample is free from extralattice chromate species. It should be noted that the final sample is green in colour. This suggests that the chromate species (yellow in colour) could be removed by ammonium acetate treatment. The bands at 347, 360, 462 and 608 nm are broad enough to be charge transfer bands (attributed to $O \rightarrow Cr^{5+}$).

3.3.4 RAMAN SPECTROSCOPY

Recently Raman spectroscopy has been considered as a valuable tool for the characterization of isomorphously substituted Si, Ge, Fe, Ti and V into the MFI structure[21-26]. In order to check whether the chromium silicate samples are free from extralattice chromate species, Raman spectra were recorded in the region of 800 - 1400 cm^{-1}. Fig. 3.5 shows the Raman spectra of chromium silicate samples with different chromium content.. The Raman spectra of silicalite-1 (chromium-free) is similar to those reported by Miecznikowski and Hanuza[21]. The Raman spectra of chromium silicate samples (Fig. 3.5 curve 'b', 'c' and 'd') are similar to the silicalite-1 (chromium-free, curve 'a') except for a less intense peak well evident at 960-970 cm^{-1}. It is generally known that this band is ascribed to the Si-O-Cr linkages. It is quite clear from the Fig 3.5 that the Raman spectra of all chromium silicate samples did not show the bands at 895 and 865 cm^{-1}, characteristic of dichromate and monochromate species[19]. This observation corroborates the absence of extralattice chromate species. A band at 834 cm^{-1} is also observed in the chromium silicate molecular sieves. Dutta and Puri[27] have assigned this band to the silanol ($Si-O^-$) groups in the chromium silicate molecular sieves. The bands at 1060 and 1220 cm^{-1} are due to the typical Si-O non symmetric stretching of SiO_4 tetrahedra.
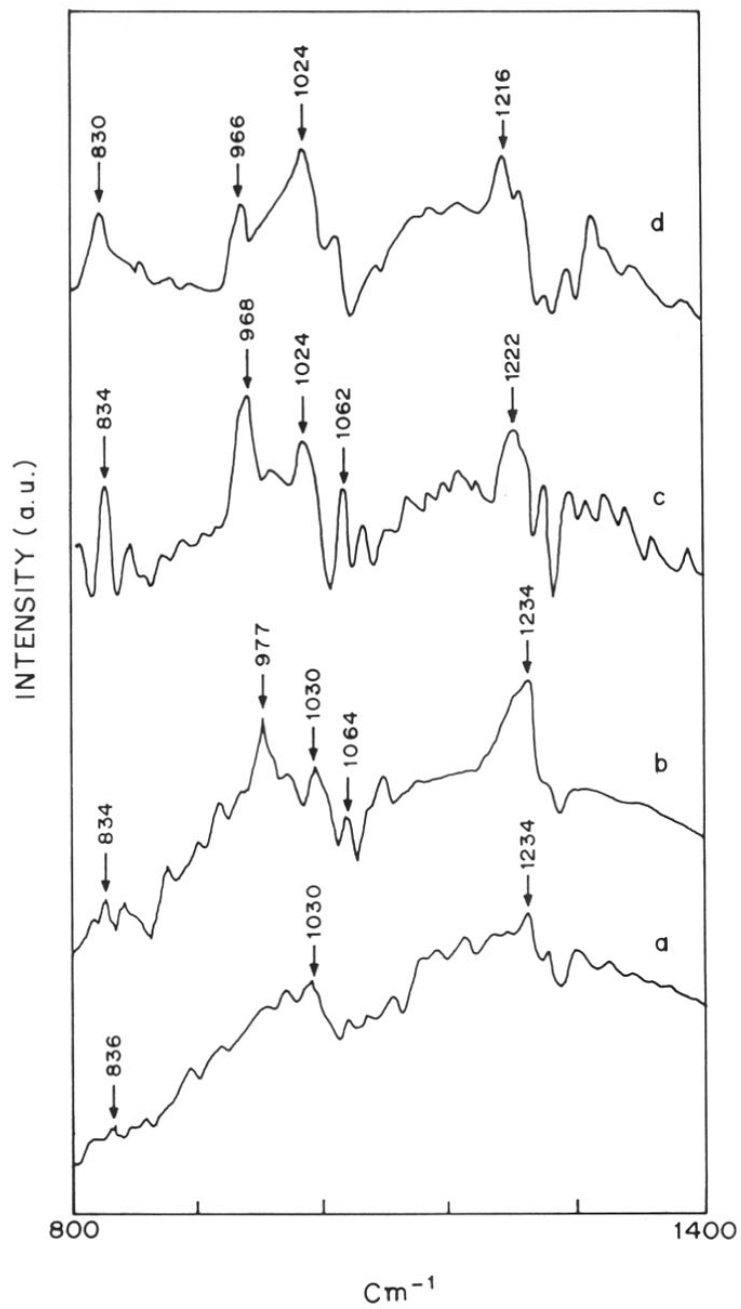
Fig. 3.5   Raman spectra of: (a) silicalite-1, (b) CrS-1 (Si/Cr = 58), (c) CrS-1 (Si/Cr = 85) (d) CrS-1 (Si/Cr = 122).

3.3.5 ELECTRON SPIN RESONANCE SPECTROSCOPY (ESR)

ESR studies yield valuable information about the paramagnetic species incorporated into the molecular sieves[28-31]. ESR spectroscopy is particularly useful in this regard because they allow the identification of both Cr^{3+} and Cr^{5+} ions. Earlier studies on ESR show that there are three different chromium species present in chromia-alumina catalysts: (i) Cr^{3+} on the surface or in the lattice (ii) clusters of Cr^{3+} (Cr_2O_3) and (iii) Cr^{5+} on the surface[32,33]. Kucherov and Slinkin employed the ESR spectra to observe the formation of isolated Cr^{5+} ions in Cr/H-ZSM-5 mixtures in the temperature range of 770- 1070 K. They assumed the transfer of chromium ions from the oxide to the zeolitic cationic sites[34]. In the chromium containing silicate synthesized by Ione et al[35], octahedral coordination for Cr^{3+} was reported on the basis of ESR studies.

Room temperature ESR spectra of chromium silicate molecular sieves: (a) as-synthesized (b) CrS-1 (Si/Cr = 58) (calcined, exchanged and recalcined) and (c) reduced in H_2 atmosphere are shown in Fig. 3.6. The ESR spectra of CrS-1 (as-synthesized) exhibit a broad singlet with a g value of 1.945, indicating the presence of Cr^{3+} ions with octahedral coordination[35]. Similar evidence of Cr^{3+} ions with octahedral coordination for CrAPO-5 molecular sieves is also reported[17,18]. Upon calcination of the as-synthesized CrS-1, the colour of the sample which was initially dark green turned to light yellow. The light yellow colour of the calcined sample can be logically assigned to the presence of Cr^{6+} ions in the form of CrO_4^{2-} or $Cr_2O_7^{2-}$ ions[36]. This clearly indicates that a part of Cr^{3+} ions are oxidized to Cr^{5+} and subsequently to Cr^{6+} ions. Furthermore, the presence of Cr^{6+} ions are also identified by the appearance of deep blue colour after the addition of hydrogen peroxide (Loba, 30%)[37]. These Cr^{6+} ions can easily be removed by ammonium (acetate) exchange treatment at 353 K because of the freely soluble nature of these chromate species. The ESR spectrum of CrS-1 (Si/Cr = 58) (calcined, exchanged and recalcined)
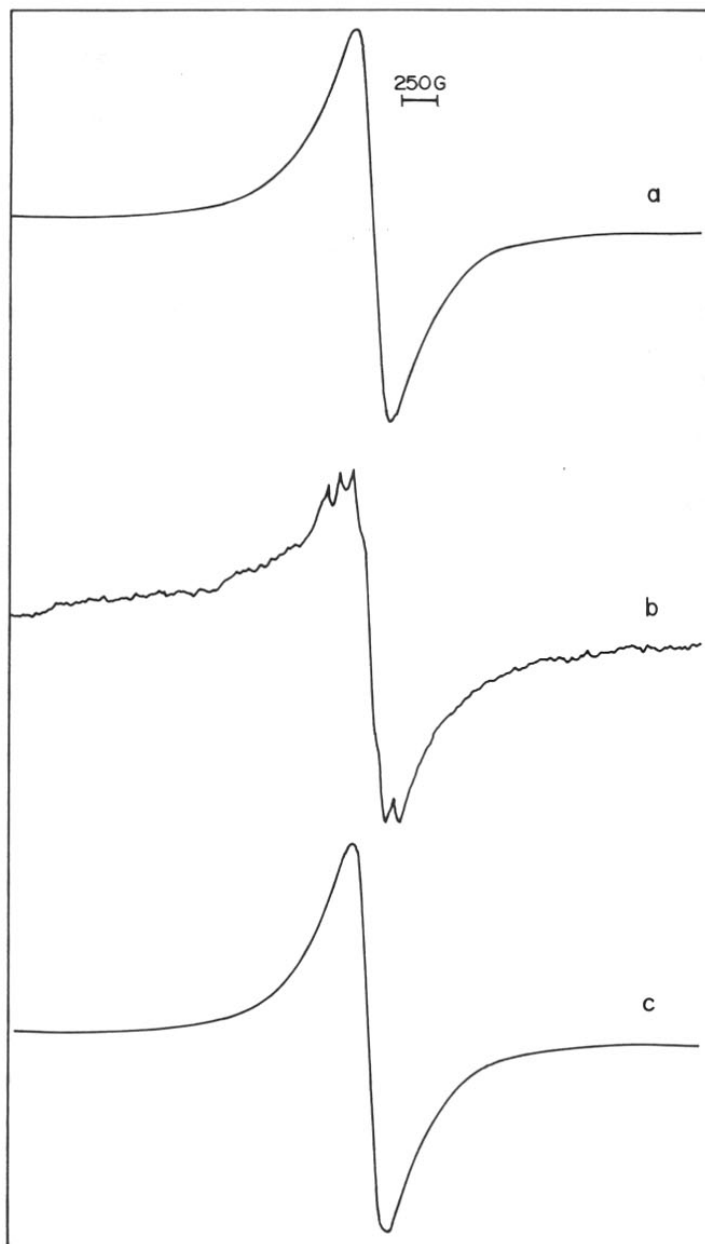
Fig. 3.6   Room temperature ESR spectra of CrS-1: (a) as-synthesized (b) calcined, exchanged and recalcined and (c) reduced sample (in H_2 flow at 723 K   for 6 h).

shows a new broad five line spectra with a g value of 1.951. This typical five line spectra is originating from the exchange interaction between Cr^{3+} and Cr^{5+} ions[3, 38]. It was recently shown that both Cr^{3+} and Cr^{5+} ions can be incorporated in cationic positions of zeolite of the ZSM-5 type[34]. Very recently, based on the ESR results (g = 1.98) Chapus et al. assigned the presence of chromium in the substitutional site[2]. Furthermore, the presence of Cr^{5+} ions in a distorted tetrahedral coordination with a g value of 1.986 has also been demonstrated by Kucherov and Slinkin[31]. In order to characterize further the nature of the chromium ions in CrS-1, the sample was reduced in H_2 flow at 723 K for 6 h. The ESR spectrum of CrS-1 after reduction at 723 K gives rise to a broad signal centered at g = 1.945, which is a characteristic ESR spectrum of Cr^{3+} in an octahedral coordination. Recalcination of the reduced sample at 773 K for 12 h, restores the five line ESR spectrum (in both intensity and shape) demonstrates thermally stable fixation of chromium within the structure.

ESR spectra of CrS-1 with different Si/Cr ratio are shown in Fig 3.7. As the Si/Cr ratio increases from 58 to 122 the integrated ESR intensity decreases linearly. Sample CrS-1 (Si/Cr = 122) exhibits only a broad singlet with a g value of 1.944. This observation clearly suggests the possibility of exchange interaction between Cr^{3+} and highly diluted Cr^{5+} ions[38]. Moreover, Cr^{3+} and Cr^{5+} ions are not in the framework positions but definitely as a part of the structure, in locations where they assume octahedral coordination due to their large size. Indeed, tetrahedral coordination is a must for the framework substitution in the transition metallosilicate molecular sieves. Since Cr^{3+} ions are not stable in framework tetrahedral coordination, they have a strong preference for the octahedral coordination [CFSE (Crystal Field Stabilization Energy) for octahedral = 224.5 kJmol^{-1}, tetrahedral = 66.9 kJmol^{-1})][39]. ESR analysis of CrS-1 thus suggests
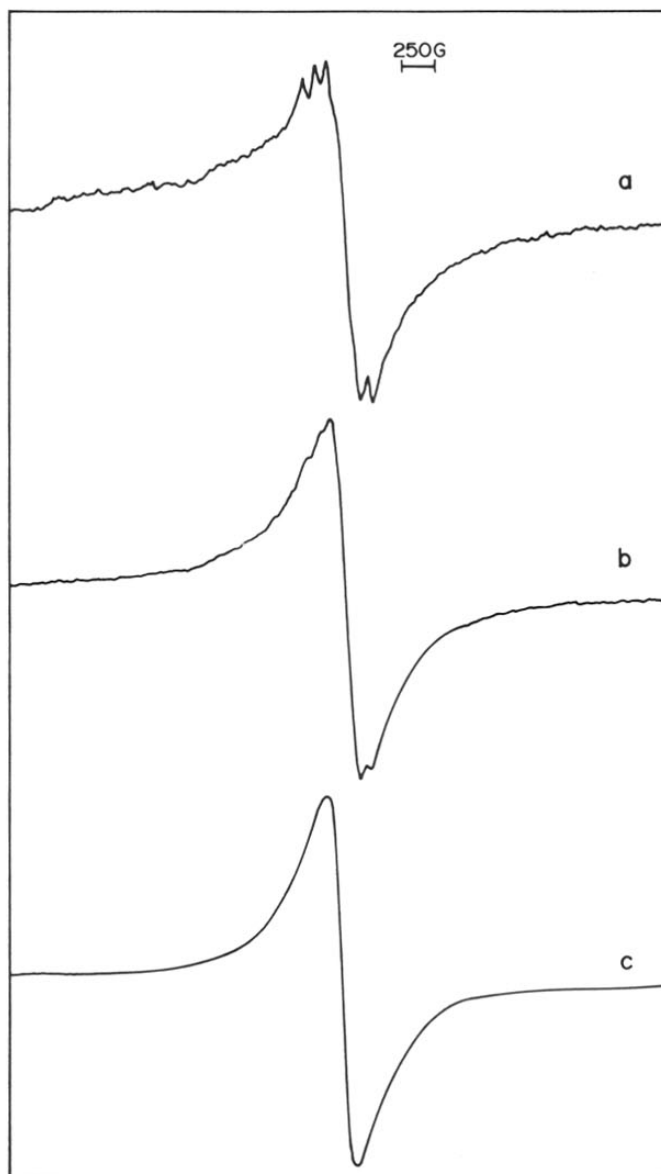
Fig. 3.7   Room temperature ESR spectra of CrS-1: (a) Si/Cr = 58 (b) Si/Cr = 85 and
(c) Si/Cr = 122.

the presence of chromium in different valence states such as Cr^{3+} and Cr^{5+} which have been stabilized within the structure.

3.3.6 NUCLEAR MAGNETIC RESONANCE SPECTROSCOPY (NMR)

3.3.6.1 ^{13}C CP/MAS NMR

^{13}C CP/MAS NMR is one of the best tools to investigate the tetrapropylammonium ions occluded inside the pores of the molecular sieves. The spectra of (a) neat TPAOH solution (^{13}C NMR) and (b) as-synthesized CrS-1 (^{13}C CP/MAS NMR) are given in Fig. 3.8. The neat TPAOH spectrum consists of three lines (the four propyl groups of TPA$^+$ are equivalent) at about 59.7, 14.7 and 9.7 ppm/Dioxane. On the other hand, the spectrum of as-synthesized CrS-1 is composed of five lines at about 64.9, 62.0, 15.8, 10.8 and 9.6 ppm/TMS. The resonance of the carbon belonging to the terminal methyl group (C-3) is generally split into two lines with equal intensities. This has been ascribed to the two different environments experienced by the terminal methyl group (C-3) of the propyl chain within the channels (linear channel, 9.6 ppm; zig-zag channel, 10.8 ppm). Similar splitting have been observed for methyl groups of TPA$^+$ ions in the MFI structure[40]. Guth et al.[41] observed three splitting of C-2 carbon of TPA$^+$ in silicalite-1, synthesized in the presence of fluoride ion and also F$^-$ ion was shown to be located next to three of the four methyl carbons (C-1) bonded to nitrogen atom. However, ^{13}C CP/MAS NMR spectrum of as-synthesized CrS-1 exhibits only one line (C-2) at 15.8 ppm. Similar results have already been reported for TS-1 (as-synthesized), synthesized in the presence of F$^-$ ions[42]. Two well-separated resonances at 64.9 and 62.0 ppm correspond to the methyl group (C-1) directly bonded to the nitrogen atom. They are presumably due to the presence of F$^-$ as counter ion for $(C_3H_7)_4N^+$. Assignment of these lines are also reported by Guth et al[41]. and Price et al[43].
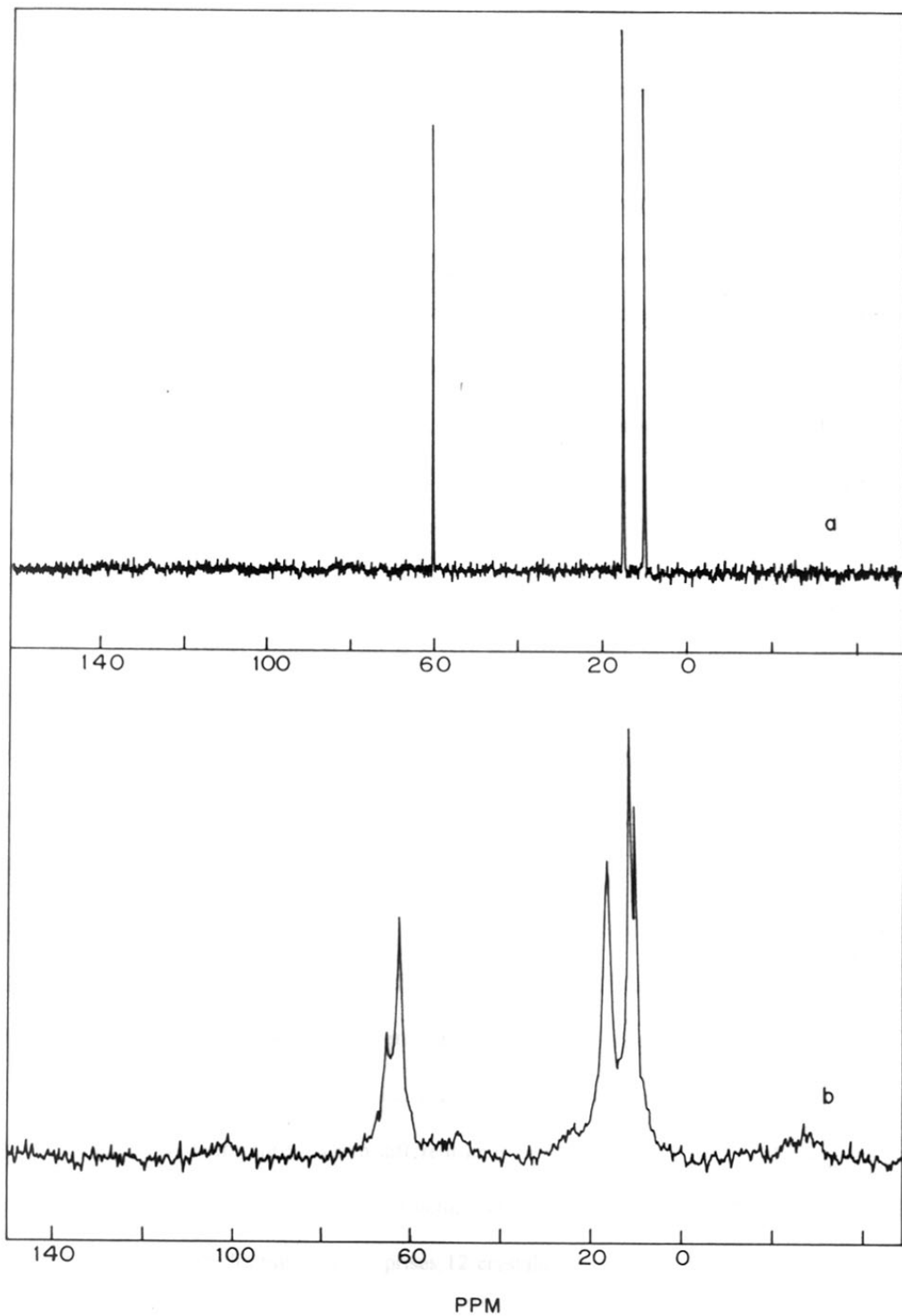
Fig. 3.8 ^{13}C CP/MAS NMR spectra of (a) TPAOH solution and (b) as-synthesized CrS-1.

^{13}C CP/MAS NMR results suggest that TPA cations are chemically intact in the channels of the molecular sieves (CrS-1) and are not decomposed during the synthesis process.

3.3.6.2 ^{27}Al MAS NMR

Although aluminium source was not added intentionally during the hydrothermal synthesis of CrS-1, it is important (by using ^{27}Al MAS NMR) to check the resultant chromium silicate, CrS-1, if it is completely free from residual aluminium content introduced during synthesis as an impurity in the starting materials. ^{27}Al MAS NMR spectrum of CrS-1 (calcined, exchanged and recalcined) is given in Fig. 3.9. As expected, ^{27}Al MAS NMR spectrum did not exhibit any characteristic signal between 100 to -100 ppm. So it is evident that the aluminium is absent in CrS-1 within the detectable limit of NMR instrument.

3.3.6.3 ^{29}Si MAS NMR

The ^{29}Si MAS NMR chemical shift is a very sensitive probe of the immediate structural surrounding of the SiO_4 tetrahedra in silicates and aluminosilicates[44]. In particular, numerous studies have been conducted on highly siliceous pentasil-type zeolites synthesized via alkaline medium[9, 45] as well as fluoride medium[41, 46]. The ^{29}Si MAS NMR spectra obtained on the as-synthesized CrS-1 and CrS-1 (Si/Cr = 58) (calcined, exchanged and recalcined) is given in Fig 3.10. Indeed, the ^{29}Si MAS NMR spectrum of as-synthesized CrS-1 exhibit, broad and strongly overlapping lines from which the assignment of peaks to distinct units is difficult or even impossible[47-49]. A signal at -103 ppm is attributed to the presence of silanol groups[48]. The ^{29}Si MAS NMR spectrum of CrS-1 (calcined, exchanged and recalcined) is remarkably different. It exhibits well resolved structure. Seven different lines belonging to the 12 crystallographically inequivalent Si sites of the orthorhombic structure are observed between -111.6 and -118.6 ppm/TMS. The 96 tetrahedra unit cell comprises 12 crystallographic sites for silicon that are not

67
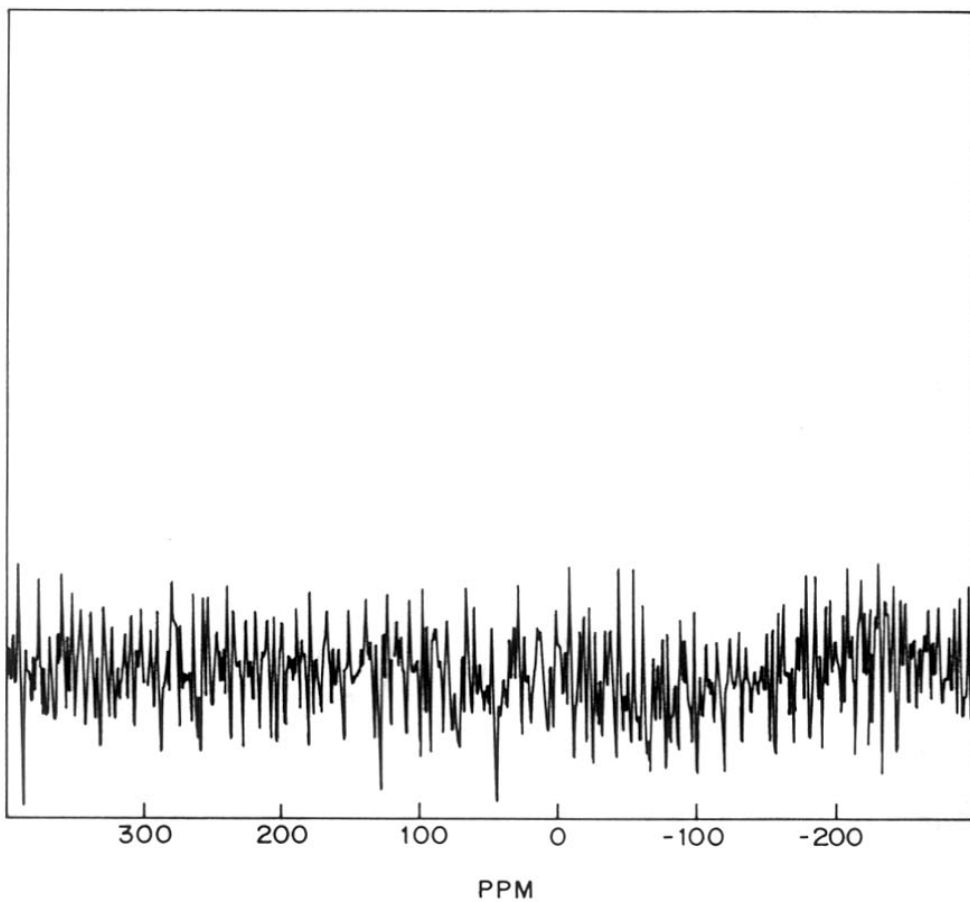
Fig. 3.9 ^{27}Al MAS NMR spectrum of CrS-1 (Si/Cr = 58).
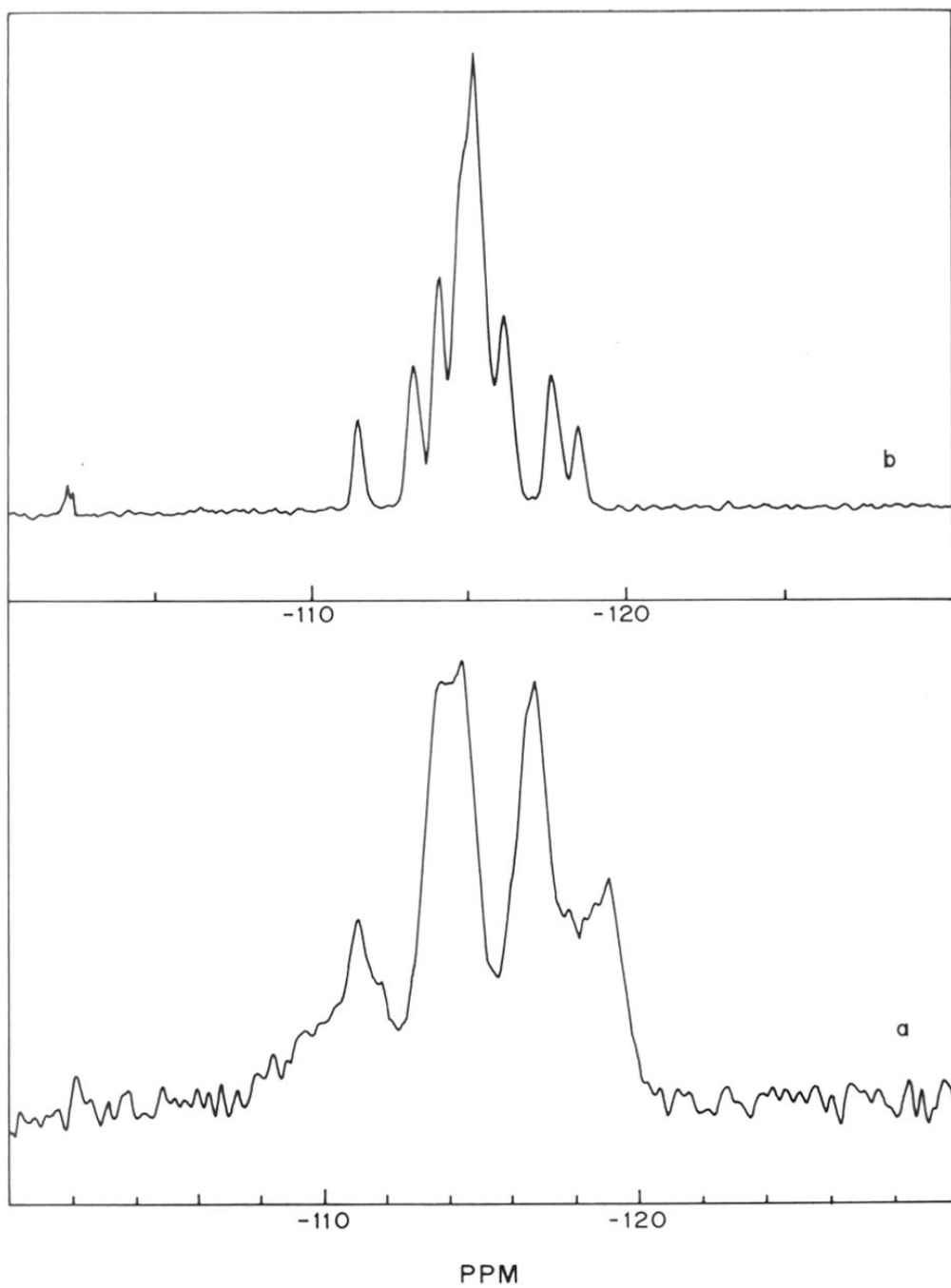
Fig. 3.10 ^{29}Si MAS NMR spectra of CrS-1: (a) as-synthesized and (b) calcined, exchanged and recalcined (Si/Cr = 58).

69
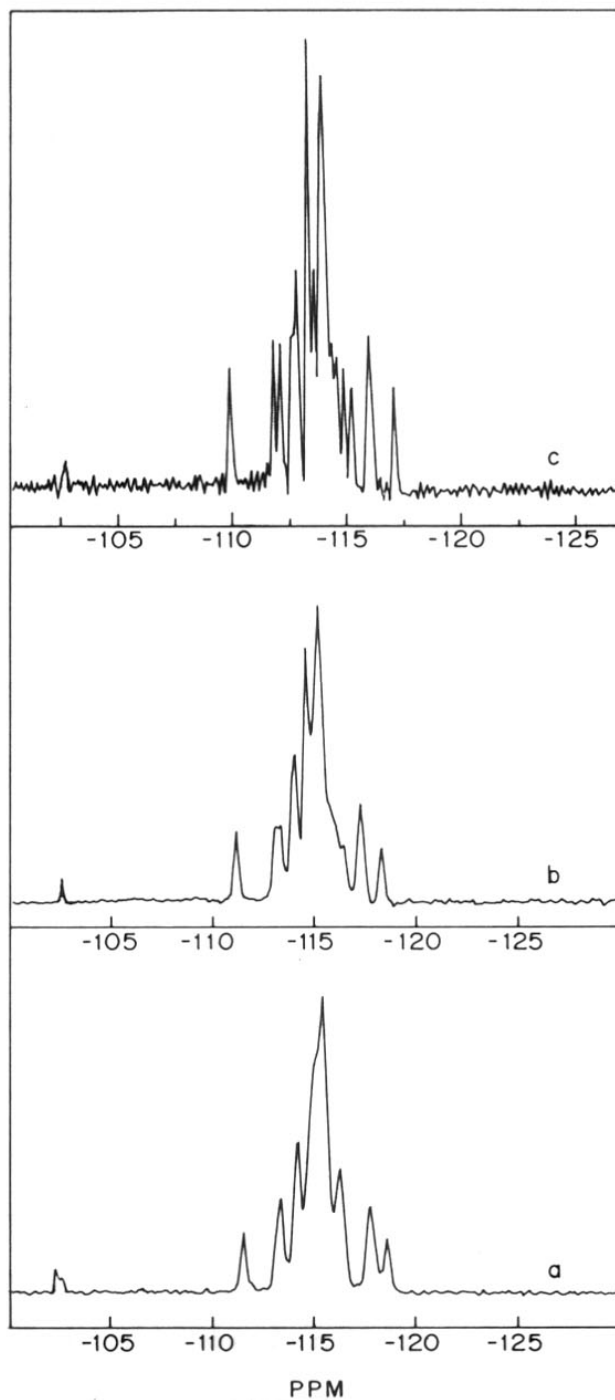
Fig. 3.11 ^{29}Si MAS NMR spectra of CrS-1: (a) Si/Cr = 58 (b) Si/Cr = 122 and (c) chromium-free silicalite-1.

completely resolved on the ^{29}Si MAS NMR spectrum. This spectrum is characteristic of a sample prepared by the fluoride route[46]. Similarly, Fyfe et al.[50] showed the existence of 12 inequivalent Si sites in the structural unit of silicalite-1 (orthorhombic). In contrast, XRD reveal that the crystal symmetry of CrS-1 (Si/Cr = 58, calcined, exchanged and recalcined) is monoclinic. It is well known that the ^{29}Si MAS NMR is very sensitive to the nature of the heteroatom in the coordination sphere surrounding the SiO$_4$ tetrahedron[9]. Therefore one can perceive that the incorporated chromium is having a stable fixation in the MFI structure.

This is further corroborated by the ^{29}Si MAS NMR spectra of a series of chromium silicate (Fig. 3.11), CrS-1 that differ by the content of chromium. Spectra are markedly different from each other. The ^{29}Si MAS NMR spectrum of CrS-1 (Si/Cr = 58) exhibit 7 lines (Fig. 3.11a) whereas the spectrum of CrS-1 (Si/Cr = 122) is quite well resolved with 9 lines (Fig. 3.11b) corresponding to the 12 crystallographically inequivalent Si sites. The resolution is lower for CrS-1 (Si/Cr = 58), the lines are relatively broad when compared to the spectrum of CrS-1 (Si/Cr = 122). As the Si/Cr increases, the line becomes more structured. This spectrum is identical to those of the results reported by Engelhardt and Koningsveld[45]. The spectrum of silicalite-1 (Fig. 3.11c) exhibits an extremely well resolved structure, fourteen lines (corresponding to the 24 crystallographically inequivalent Si sites) are seen between -109.9 and -117.0 ppm/TMS. It is characteristic of the monoclinic phase. These spectra are essentially similar to those already reported for highly siliceous ZSM-5[9].

3.3.7 CYCLIC VOLTAMMETRY

The art of obtaining information about the nature of transition metal ions residing in the molecular sieves is becoming increasingly sophisticated. Apart from conventional spectroscopic techniques, in particular, cyclic voltammetry is proved to be a unique tool for the characterization of redox sites in the zeolite lattice such as the titanium[51,52] and the vanadium[53,54] silicalites. Hence
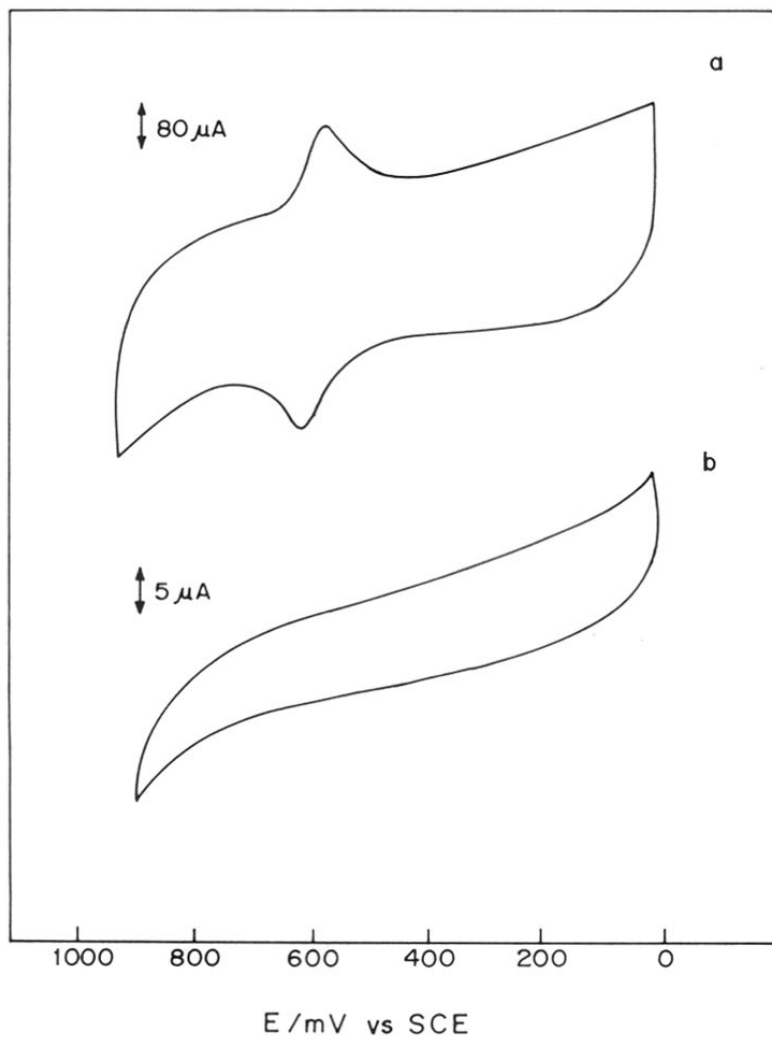
Fig. 3.12 Cyclic voltammograms of : (a) chromium silicate (Si/Cr = 58) and (b) silicalite-1 modified graphite electrode. The scan rate was 50 mV sec⁻¹

72

voltammetric measurements were carried out on these chromium silicate molecular sieves to unravel their oxidation states and their kinetic stability. For comparison silicalite-1 (chromium-free) was also subjected to cyclic voltammetric studies. Fig. 3.12 shows the cyclic voltammograms obtained with chromium silicate (Si/Cr = 58) and silicalite-1 (chromium-free) modified graphite electrodes. The cyclic voltammogram of CrS-1 (Si/Cr = 58) reveals a reversible system ($I_{p,a}$ / $I_{p,c}$ = 1, ΔE_p = 40 mV) with $E_{1/2}$ = + 588 mV vs standard calomel electrode (SCE). The ratio of the anodic to the cathodic peak current is approximately one. The $E_{1/2}$ value is calculated from cyclic voltammetric wave forms as the half-sum of anodic and cathodic peak potentials. ΔE_p values indicate a two electron transfer[55]. This response can be attributed to the Cr^{5+}/Cr^{3+} couple.

$$Cr^{3+} \quad \text{--------------->} \quad Cr^{5+} + 2\,e^- \quad (E_{1/2} = +\ 588\ mV)$$
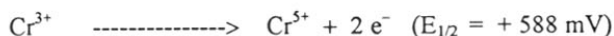
As expected cyclic voltammograms of silicalite-1 modified electrodes show no discernible redox peaks. It confirms the absence of electroactive species in the working potential range. Additionally, no peaks were observed with Cr/Silicalite-1 (chromium impregnated silicalite-1) modified graphite electrode. The characteristics mentioned above demonstrate that a reversible electrochemical reaction occurs only at the chromium silicate modified electrode. Similar observations have already been reported for Ti and V impregnated silicalite-1[52,53]. Moreover, the invariance of the CV pattern with cycling confirms the presence of chromium (both Cr^{3+} and Cr^{5+}) ions which are stabilized in the structure. Furthermore, Cr^{5+} ion is not undergoing further oxidation to Cr^{6+} in the working potential range (0 to + 1.0 V). The exact nature of the active site could only be elucidated by carrying out the cyclic voltammetric measurements for known chromium standards. Reference complexes with octahedral Cr^{5+} are difficult to find.

3.3.8 X-RAY PHOTOELECTRON SPECTROSCOPY

X-ray photoelectron spectroscopy (XPS) was also used to characterize all the chromium silicate, CrS-1 samples. XPS, being a surface analysis technique, is extremely sensitive towards surface contamination. Therefore, all the samples were treated with ammonium acetate solution twice (to remove extralattice chromium oxide species). In order to identify the species present in the CrS-1 samples, XPS of silicalite-1/Cr_2O_3 and silicalite-1/CrO_3 were also recorded. The binding energy (B.E) values of the Cr $2p_{3/2}$ level are 576.8 and 581.2, respectively. Since we had no Cr^{5+} standards, we used literature comparisons of B.E and peak shape. The XPS patterns of CrS-1 are given in Fig. 3.13 'A'. The Si/Cr ratios calculated from the intensities of XPS peaks are higher than that obtained from the elemental (ICP) analysis. The Si/Cr ratios of CrS-1 from XPS & ICP analyses are 58 & 138; 85 & 189 and 122 & 204; respectively, indicating that the surface is chromium-deficient. In other words chromium does not exist in the CrS-1 as extra-framework chromium oxide. The B.E of the Cr 2p level for Cr (III) (577.8 eV) in all the samples are higher (1.0 eV) than that for silicalite-1/Cr_2O_3 (576.8 eV). Generally metal substituted molecular sieves tend to show higher B.E values as compared to that obtained for pure metal oxides.

In order to get additional information on the oxidation states of chromium ions present in the CrS-1 sample, the XPS spectrum of CrS-1 (Si/Cr = 58) was deconvoluted using a commercially available software. An interesting feature which can be seen from the deconvoluted Cr 2p spectrum of CrS-1 (Si/Cr = 58, Fig. 3.13 'B') is the presence of chromium both as Cr^{3+} and Cr^{5+} ions in CrS-1. The first peak is assigned to Cr(III) (577.8 eV)[57, 58] and by comparison with available literature data the second peak (580.4 eV) is assigned to Cr(V). The percentage of Cr(III) and Cr(V) present in CrS-1 (Si/Cr = 58) are 49.6 and 50.4 %, respectively.
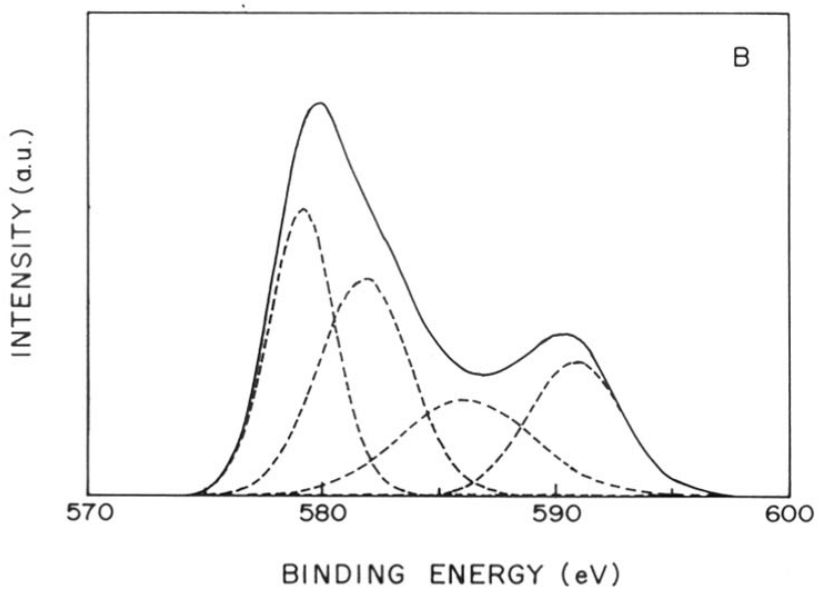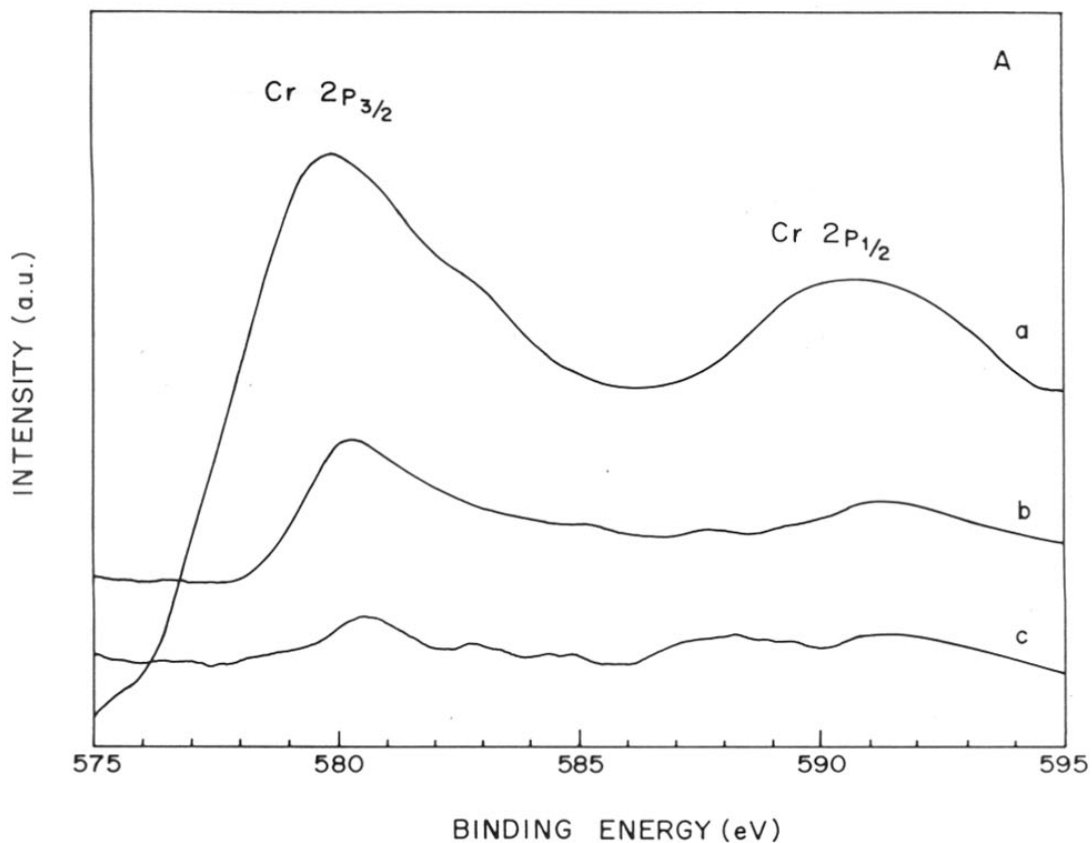
Fig. 3.13   XPS spectra of CrS-1 [A]: (a) Si/Cr = 58, (b) Si/Cr = 85 and (c) Si/Cr = 122;
[B]: Deconvoluted XPS spectrum of CrS-1 (Si/Cr = 58).

	Binding Energy (B. E) eV		
	Cr 2p$_{3/2}$	Cr 2p$_{1/2}$	ΔE
Cr (III)	$579.1 - 1.3 = 577.8^a$	$586.1 - 1.3 = 584.8^a$	7.0
Cr (V)	$581.7 - 1.3 = 580.4^a$	$590.8 - 1.3 = 589.5^a$	9.1

[a]After carbon correction

Our ΔE value (9.1 eV) agree closely with those reported by Jagannathan et al.[59] and Okamoto et al.[60] XPS, thus, confirms the presence of chromium in CrS-1 as Cr^{3+} and Cr^{5+} ions and the absence of Cr^{6+} ions.

3.4 CONCLUSIONS

1. It is possible to synthesize aluminium-free crystalline chromium silicalite-1 (MFI) by hydrothermal synthesis. XRD reveals the absence of extra phases related to chromium oxide species. Moreover, as-synthesized CrS-1 is always orthorhombic, upon calcination the crystal symmetry becomes monoclinic.

2. Evidence for Si-O-Cr linkages is suggested by the presence of a less intense IR band at 960 cm^{-1}; such a band is not observed in chromium-free silicalite-1

3. UV-visible spectroscopy shows that in the as-synthesized CrS-1 sample, Cr^{3+} is present in octahedral coordination. The formation of chromate species is also identified upon calcination. However, these species could be removed by ammonium acetate treatment. Ammonium acetate treated samples are free from chromate species as evidenced by UV-visible spectroscopy. In the UV spectrum of CrS-1 (calcined, exchanged and recalcined), the bands at 347, 360, 462 and 608 nm are broad enough to be charge transfer bands (attributed to O---> Cr^{5+}).

4. The Raman spectra of all samples did not show the bands at 895 and 865 cm^{-1} characteristic of dichromate and monochromate species. So it is evident that CrS-1 samples are free from chromate species.

5. The most reliable evidence for the presence of Cr^{5+} is provided by ESR and CV (cyclic voltammetry) studies. ESR studies reveal that both Cr^{3+} and Cr^{5+} ions are in octahedral coordination. This CrS-1 sample can readily change its oxidation state between Cr^{3+} and Cr^{5+} and it is reversible. The invariance of the CV pattern with continuous cycling as well as change of initial scan direction confirms the presence of chromium ions (both Cr^{3+} and Cr^{5+}) and also shows that chromium ions which have been stabilized in the structure are

sufficiently stable for such redox transformation.

6. In the ^{29}Si MAS NMR spectra of CrS-1 samples, a relatively weak resonance occurs at -103 ppm, indicating the presence of hydroxyl nests. In contrast to XRD; ^{29}Si MAS NMR reveals that the chromium incorporated samples are probably orthorhombic

7. XPS data yielded values for the surface Si/Cr ratios in the CrS-1 samples and also provided confirmation of the oxidation state of chromium to be III & V.

POSSIBLE MODEL OF Cr^{5+} IONS IN THE SILICALITE STRUCTURE

It is well known that for isomorphous substitution of any heteroatom into the zeolite lattice, tetrahedral coordination is necessary. This criteria can only be fulfilled by the heteroatom whose ionic radius is not be greater than that of Si^{4+} (0.26 Å). The replacement of Si^{4+} (0.26 Å) by chromium [Cr^{3+} (0.61 Å) and Cr^{5+} (0.49 Å)] causes the appearance of lattice defects which have been observed by ^{29}Si MAS NMR, Raman spectroscopic techniques and also from the N_2 adsorption isotherms.

As evidenced by UV and ESR spectral data, Cr^{3+} is present in octahedral coordination in the as-synthesized CrS-1 sample. So chromium in octahedral symmetry could not occupy framework sites with tetrahedral symmetry. The evidence for the octahedral Cr^{3+} (0.61 Å) sites in the framework is not known in detail. However, IR and Raman spectroscopic techniques have shown the existence of Si-O-Cr linkages. Furthermore, ammonium acetate treatment does not leach out the incorporated chromium ions (both Cr^{3+} and Cr^{5+}) suggesting that these chromium ions are held rigidly in the MFI structure. This argument is supported by the cyclic voltammetric studies as well. It should be noted that these samples are very sensitive to moisture. Upon exposure to open air, these samples (calcined, exchanged and recalcined) were found to change from green to dark green in colour. A possible structure of Cr^{5+} ions that reside in the silicalite

structure that is consistent with the information obtained from various physico-chemical characterization techniques is presented.
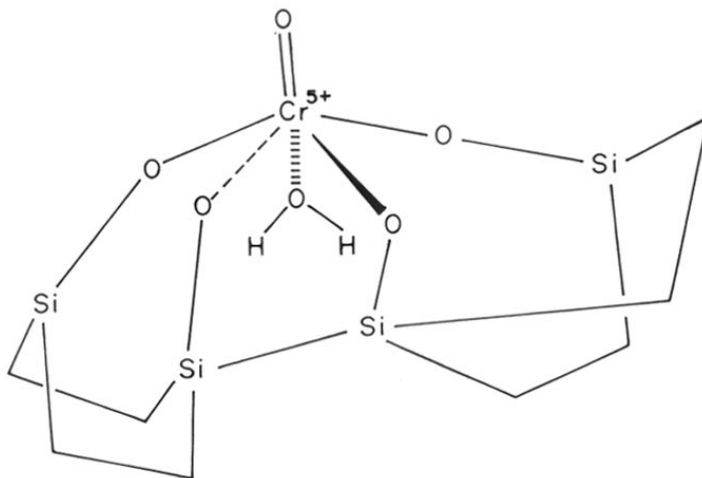
A similar model was proposed for the octahedral vanadium in silicalite-1 by Kornatowski et al[26].

3.5 REFERENCES

1.	U. Cornaro, P. Jiru, Z. Tvaruzkova and K. Habersberger, Stud. Surf. Sci. Catal., 69, 165 (1991).

2.	T. Chapus, A. Tuel, Y. Ben Taarit and C. Naccache, Zeolites, 14, 349 (1994).

3.	T. Selvam and M. P. Vinod, Appl. Catal., 134, L197 (1996).

4.	R. J. Argauer and G. R. Landolt, US. Pat., 3 702 886 (1972).

5.	X. Liu and J. Klinowski, J. Phys. Chem., 96, 3403 (1992).

6.	H. van Koningsveld, H. van Beckkum and J. C. Jansen, Acta Cryst., B34, 127 (1987).

7.	A. Thangaraj and S. Sivasanker, J. Chem. Soc. Chem. Commun., 123 (1992).

8.	B. Kraushaar, Ph. D. Thesis, The Technical University of Eindhoven, Eindhoven, The Netherlands, (1989).

9.	J. Klinowski, T. A. Carpenter and L. F. Gladden, Zeolites, 7, 73 (1987).

10.	C. A. Fyfe, G. J. Kennedy, C. T. De Schutter and G. T. Kokotailo, J. Chem. Soc. Chem. Commun., 541 (1984).

11.	G. T. Kokotailo, C. A. Fyfe, G. J. Kennedy, G. C. Gobbi, H. Strobl, C. T. Pasztor, G. E. Barlow and S. Bradley, Pure & Appl. Chem., 58, 1367 (1986).

12.	M. Taramasso, G. Perego and B. Notari, US. Pat. 4 410 501 (1983).

13.	Z. Gabelica and J. L. Guth, Stud. Surf. Sci. Catal., 49A, 421 (1989).

14.	K. Nakamoto, "Infrared and Raman Spectra of Inorganic and Coordination Compounds", Wiley, New York, 1986.

15a.	J. S. Reddy, R. Kumar and P. Ratnasamy, Appl. Catal., 58, L1 (1990).

15b.	M. A. Camblor, A. Corma and J. Perez-Pariente, J. Chem. Soc. Chem. Commun., 557 (1993).

16.	K. G. Ione, L. A. Vostrikova and V. M. Mastikhin, J. Mol. Catal., 31, 355 (1985).

17.	B. M. Weckhuysen and R. A. Schoonheydt, Zeolites, 14, 360 (1994).

18.	B. M. Weckhuysen , H. J. Spooren and R. A. Schoonheydt, Zeolites, 14, 450 (1994).

19.	B. M. Weckhuysen, R. A. Schoonheydt, J-M. Jehng, I. E. Wachs, S. J. Cho, R. Ryoo, S. Kijlstra and E. Poels, J. Chem. Soc. Faraday Trans., 91, 3245 (1995)

20.	B. M. Weckhuysen and R. A. Schoonheydt, Stud. Surf. Sci. Catal., 84, 965 (1994).

21.	A. Miecznikowski and J. Hanuza, Zeolites, 7, 249 (1987).

22. H. Kosslick, V. A. Tuan, R. Fricke, Ch. Peuker, W. Pilz and W. Storek, J. Phys. Chem., 97, 5678 (1993).

23. D. Scarano, A. Zecchina, S. Bordiga, F. Geobaldo, G. Spoto, G. Petrini, G. Leofanti, M. Padovan and G. Tozzola, J. Chem. Soc. Faraday Trans., 89, 4123 (1993).

24. G. Deo, A. M. Turek, I. E. Wachs, D. R. C. Huybrechts and P. A. Jacobs, Zeolites, 13, 365 (1993).

25. E. Astorino, J. B. Peri, R. J. Willey and G. Busca, J. Catal., 157, 482 (1995).

26. J. Kornatowski, B. Wichterlova, J. Jirkovsky, E. Löffler and W. Pilz, J. Chem. Soc. Faraday Trans., 92, 1067 (1996).

27. P. K. Dutta and M. Puri, J. Phys. Chem., 91, 4329 (1987).

28. J. H. Lunsford, Adv. Catal., 22, 265 (1972).

29. A. Tuel, J. Diab, P. Gelin, M. Dufaux, J-F. Dutel and Y. Ben Taarit, J. Mol. Catal., 63, 95 (1990).

30. A. Tuel, and Y. Ben Taarit, Zeolites, 14, 18 (1994).

31. A. V. Kucherov, A. A. Slinkin, G. K. Beyer and G. Borbely, Zeolites, 15, 431 (1995).

32. D. E. O'Reilly and D. S. Maciver, J. Phys. Chem., 66, 276 (1962).

33. C. P. Poole, W. L. Kehl and D. S. Maclver, J. Catal., 1, 407 (1962).

34. A. V. Kucherov and A. A. Slinkin, Zeolites, 7, 38 (1987).

35. K. G. Ione, L. A. Vostrikova, A. V. Ptrova and V. M. Mastikhin, in Proceedings 8 th Int. Cong. on Catal., Berlin, vol. 4. P. 519 (1984); verlag chemie, Weinheim.

36. J. S. T. Mambrim, E. J. S. Vichi, H. O. Pastore, C. U. Davanzo, H. Vargas, E. Silva and O. Nakamura, J. Chem. Soc. Chem. Commun., 922 (1991).

37. F. A. Cotton and G. Wilkinson, "Advanced Inorganic Chemistry", 3 rd ed., Wiley Eastern Ltd, p. 843 (1984).

38. M. Sugimoto, H. Katsuno, K. Takatsu and N. Kawata, Appl. Catal., 80, 13 (1992).

39. A. R. West, Basic Solid State Chemistry, Wiley, Chicester, 105 (1988).

40. G. Boxhoorn, R. A. van Santen, W. A. van Erp, G. R. Hays, R. Huis and D. Clague, J. Chem. Soc. Chem. Commun., 264 (1982).

41. J. M. Chezeau, L. Delmotte, J. L. Guth and M. Soulard, Zeolites, 9, 78 (1989).

42. Q. Shilun, P. Wenqin and Y. Shangqing, Stud. Surf. Sci. Catal., 49A, 133 (1989).

43. G. D. Price, J. J. Pluth, J. V. Smith, J. M. Bennett and R. L. Patton, J. Am. Chem. Soc., 104, 5971 (1982).

44. J. M. Thomas and J. Klinowski, Adv. Catal., 33, 199 (1985)

45. G. Engelhardt and H. van Koningsveld, Zeolites, 10, 650 (1990).

46. J. M. Chezeau, L. Delmotte, J. L. Guth and Z. Gabelica, Zeolites, 11, 598 (1991).

47. J. B. Nagy, Z. Gabelica and E. G. Derouane, Chem. Lett., 1105 (1982).

48. G. Boxhoorn, A. G. T. G. Kortbeek, G. R. Hays and N. C. M. Alma, Zeolites, 4, 15 (1984).

49. H. Hamdan and J. Klinowski, J. Chem. Phys. Lett., 139, 576 (1987).

50. C. A. Fyfe, J. H. O'Brien and H. Strobl, Nature, 326, 281 (1987).

51. S. de Castro-Martins, S. Khouzami, A. Tuel, Y. Ben Taarit, N. El Murr and A. Sellami, J. Electroanal. Chem., 350, 15 (1993).

52. S. de Castro-Martins, A. Tuel and Y. Ben Taarit, Zeolites, 14, 130 (1994).

53. N. Venkatathri, M. P. Vinod, K. Vijayamohanan and S. Sivasanker, J. Chem. Soc. Faraday Trans., 92, 473 (1996).

54. M. Chatterjee, D. Bhattacharya, N. Venkatathri and S. Sivasanker, Catal. Lett., 35, 313 (1995).

55. A. J. Bard and L. R. Faulkner, "Electrochemical Methods", John Wiley & Sons, Chapter 6 (1996).

56. R. D. Shannon, Acta Cryst., 32A, 751 (1976).

57. B. Wichterlova, L. Krajcikova, Z. Tvaruzkova and S. Beran, J. Chem. Soc. Faraday Trans. 1., 80, 2639 (1984).

58. B. Wichterlova, Z. Tvaruzkova, L. Krajcikova and J. Novakova, Stud. Surf. Sci. Catal., 18, 249 (1984).

59. K. Jagannathan, A. Srinivasan and C. N. R. Rao, J. Catal., 69, 418 (1981).

60. Y. Okamoto, M. Fujii, T. Imanaka and S. Teranishi, Bull. Chem. Soc. Japan, 49, 859 (1976).

CHAPTER 4

CATALYTIC OXIDATION REACTIONS OVER CrS-1

4.1 INTRODUCTION

The main agenda of this thesis was to make aluminium-free, thermally stable chromium silicate molecular sieves with MFI structure (CrS-1). Chapter 3 discussed the physico-chemical techniques used to (i) establish the structural integrity of CrS-1 and (ii) assess the substitution of chromium into the MFI structure. This chapter presents our efforts to examine the catalytic activity of CrS-1 in oxidation reactions using t-butyl hydroperoxide (TBHP) as the oxidant.

The discovery of transition metal substituted molecular sieves has opened up new area in the selective oxidation of organic compounds especially in the synthesis of organic fine chemicals[1-8]. Among the transition metallosilicate molecular sieves, titanium[1-5] and vanadium[6-8] silicates which are non-acidic zeolites are currently the object of much attention owing to their interesting properties in heterogeneous oxidation catalysis. Traditionally, non-regenerable homogeneous catalysts such as acetates of transition metal ions, potassium dichromate and potassium permanganate have been used in oxidation reactions[9-12]. Substitution of these catalysts by transition metallosilicates would result in simplified product recovery and reduction of undesirable waste streams.

Titanium silicalite, TS-1, has received considerable attention owing to its good activity and selectivity in the hydroxylation of aromatics[1], oxidation of alkanes[2], epoxidation of alkenes[3], sulphoxidation of thio ethers[4], and oxidation of aromatic and aliphatic amines[5]. It is widely believed that the remarkable catalytic behavior of TS-1 is due to isolated, tetrahedrally coordinated Ti^{4+} ions. Vanadium silicate molecular sieves, like their titanium analogs, are also a new class of catalysts with remarkable catalytic properties in the selective oxidation of various organic molecules using H_2O_2[6-8]. It has been demonstrated that VS-1 is able to activate the primary carbon for various hydrocarbons, for example, in the oxidation of n-alkanes and p-chlorotoluene[13-14]. Reports concerning chromium silicate molecular sieves so far have dealt

mainly with the synthesis and the physico-chemical characterization[15,16] but they were not found to be active in the oxidation reactions due to the instability of the chromium ions within the structure. Recently Sheldon et al.[17] and Chen et al.[18] have reported the synthesis and the use of chromium aluminophosphate molecular sieves (Cr-AlPO$_4$-5) in the oxidation reactions. The papers dealing with the catalytic properties of chromium silicate molecular sieves , CrS-1, are scarce. However, a recent report by Chen et al.[19] demonstrated that CrS-1 itself can be used as an effective catalyst for the oxidation of benzyl alcohol and ethyl benzene using TBHP as the oxidant. The claimed catalyst is reported to be active in the temperature range of 333-353 K. Moreover, the stability of chromium in these molecular sieves during the oxidation reaction and whether the reaction proceeds through heterogeneous or homogeneous catalysis are not given in detail. Very recently, the use of chromium silicate molecular sieves with MEL structure, CrS-2, as a catalyst in the epoxidation of alkenes and oxidation of aromatic primary amine to their corresponding nitro derivatives has been reported by Jayachandran et al.[20,21].

The following reactions were chosen in order to study the intrinsic catalytic activity of the CrS-1.

      1. Oxidation of toluene

      2. Oxidation of n-hexane

      3. Oxidation of n-heptane

      4. Oxidation of n-octane

      5. Oxidation of cyclohexane

4.2 EXPERIMENTAL

4.2.1 CATALYTIC MATERIALS AND CHARACTERIZATION

Synthesis of CrS-1 with different Si/Cr ratios and their characterization are described in detail in chapters 2 and 3. The samples were calcined at 773 K for 12 hours, in order to remove the trapped organic cations. Mild treatments with aqueous 1 M ammonium acetate at

353 K were performed in order to wash away unstable chromium species and recalcination was done at 773 K for 6 h. Before reaction all the catalysts were dried overnight at 373 K and stored in a desiccator. For comparison, VS-1[22] , Si-1[23] (silica polymorph of MFI structure) and Cr/Si-1 (chromium impregnated silicalite-1) were synthesized following the previously published procedures. The Cr/Si-1 was prepared by impregnating silicalite-1 with $Cr(NO_3)_3$.$9H_2O$ solutions by maintaining the concentration of chromium similar to CrS-1 (Si/Cr = 52).

4.2.2 OXIDATION OF TOLUENE

Catalytic reactions were performed in a two-necked glass reactor (50 ml capacity) equipped with a reflux condenser and a magnetic stirrer. Typically, 0.5 g of catalyst, 5 g of toluene and 20 ml of acetonitrile were introduced in to the reactor and heated at the reaction temperature 353 K under stirring for 24 h. Subsequently, appropriate amount of t-butyl hydroperoxide (TBHP) was added in one lot using a 10 ml graduated syringe as soon as the reaction temperature was attained. The toluene/TBHP molar ratio was taken to be 1. The reaction was monitored by taking small aliquots (0.4 ml) of samples from the reaction mixture at different times and analyzed using gas chromatography.

4.2.3 OXIDATION OF ALKANES

In the case of cyclohexane, n-hexane, n-heptane and n-octane , the reactions were carried out in a stirred autoclave (Parr Instruments Company, Illinois, USA) of 300 ml capacity at a temperature of 353-373 K for 12 h under autogeneous pressure. Typically, 0.5 g of catalyst, 5 g of alkane were mixed with 25 ml of acetonitrile. An appropriate amount of TBHP (alkane/TBHP = 3 molar ratio) was added to the reaction mixture.

4.2.4 PRODUCT ANALYSIS

Product samples were analyzed by gas chromatograph (HP model 5880 series II) equipped with a flame ionization detector (FID) and a capillary column (50 m x 0.2 mm) of methyl silicone gum. Since, the GC response of different compounds vary, the composition of

the reaction products was determined by comparing their gas-chromatograms with those of authentic samples. The product analyses were normalized using these GC response factors. The identity of the products were established by GC-MS (Shimadzu, QP 2000 A).

4.3 RESULTS AND DISCUSSION

4.3.1 OXIDATION OF TOLUENE

Methyl groups on an aromatic ring can be oxidized to aldehyde by several homogeneous oxidizing agents. Among other oxidizing agents that have been used to accomplish the conversion of toluene to benzaldehyde are ceric ammonium nitrate[24] and ceric trifluroacetate[25]. Schmidt and Schmidbaur have reported that trimethylsilyl chromate oxidizes toluene to benzyl alcohol[26]. It has been reported that benzaldehyde can be obtained in the oxidation of toluene using a $Co(OOCH_3)_2$ catalyst and NaBr or paraldehyde promotor[27]. The Cr-PILC (Pillared Clay) catalyst has also been shown to mediate selective benzylic oxidation of alkyl substituted aromatic hydrocarbons with TBHP as an oxidant[28]. Catalysts consisting of vanadium oxide monolayers on silica coated with various amounts of titania have also been shown to catalyze the oxidation of toluene[29].

Liquid phase oxidation of toluene using metallosilicate molecular sieves has been studied by several researchers[30-32]. Rao et al.[30] reported that vanadium silicates catalyze the oxidation of toluene into a mixture of benzaldehyde and cresols. Similarly, the use of V-ZSM-48 has also been demonstrated in the oxidation of toluene[31]. In contrast to vanadium silicates, titanium silicates[32] show a different catalytic behavior i.e. the hydroxylation occurred only at the aromatic ring. More recently, Marchal et al.[33] have pointed out that the nature of the products formed strongly depends on the type of oxidant used. They have shown that H_2O_2 leads preferentially to the hydroxylation of the aromatic ring whereas TBHP oxidized the side chain of the aromatic hydrocarbons.

4.3.1.1 INFLUENCE OF CATALYST

The oxidation of toluene under mild reaction conditions with TBHP over CrS-1, VS-1 and Cr/S-1 yields benzaldehyde (BZD), benzyl alcohol (BZAlC), benzoic acid (BZAC), dibenzyl (DBZ) and trace amounts of o-cresol (o-CRS) and p-cresol (p-CRS). A blank run was also carried out for comparison. The products are found to be similar to those reported earlier in the oxidation of toluene using VAPO-5 as the catalyst and TBHP as the oxidizing agent[33]. Table 4.1 compares the activities of different catalysts under identical reaction conditions. It is seen that CrS-1 show higher activity than VS-1 and Cr/S-1. In the absence of a catalyst only a very low conversion of toluene (2.1 wt.%) is observed. The variation of the selectivity towards products is found to be different on the three catalysts (Table 4.1). CrS-1 yields higher amount of DBZ (45.1 wt.%) whereas catalyst VS-1 gave only 9.2 wt.% of DBZ and no DBZ formation is observed over Cr/S-1. The conversion of toluene over CrS-1, VS-1 and Cr/S-1 is found to be 18.4, 8.3 and 3.3 wt.%., respectively. The corresponding rate of toluene conversions are 0.83, 0.38 and 0.15 mmolg^{-1}h^{-1}, respectively. The conversion of toluene over VS-1 is lower than over CrS-1; however, this is mainly due to the lower vanadium content in VS-1 (Si/V = 118) as compared to the chromium content in CrS-1 (Si/Cr = 52).

4.3.1.2 EFFECT OF REACTION TIME

The influence of reaction time is also examined on the conversion of toluene using CrS-1. Fig. 4.1 shows the conversion of toluene, ratio of BZAC/BZD and product yields at 353 K using CrS-1 as a function of reaction time. It can be seen from the Fig. 4.1 that the conversion of toluene as well as the product yields increase gradually with the progress of the reaction and level off after 24 h of reaction time. The ratio of BZAC/BZD increases linearly from 0.13 to 1.1 when the reaction time was increased from 7 to 24 h, respectively. Benzoic acid is formed only after a few hours and its yield reaches maximum after a period of time.

Table 4.1

Oxidation of toluene[a].

Catalyst	Conversion (wt.%)	Rate of toluene conversion $(\text{mmolg}^{-1}\text{h}^{-1})$[b]	Product distribution (wt.%)[c]					
			BZD	BZAlC	BZAC	o-CRS	p-CRS	DBZ
CrS-1	18.4	0.83	23.3	5.2	25.7	0.4	0.3	45.1
VS-1	8.3	0.38	42.9	15.1	24.8	-	8.0	9.2
Cr/S-1[d]	3.3	0.15	47.7	9.7	37.0	1.7	3.9	-
Blank[e]	2.1	0.10	72.0	28.0	-	-	-	-

[a]Reaction conditions: catalyst = 0.5 g (Si/Cr = 52; Si/V = 118), toluene = 5 g, reaction temperature = 353 K, solvent (acetonitrile) = 20 ml, TBHP/toluene (molar ratio) = 1, reaction time = 24 h.

[b]mmoles of toluene converted per gram of catalyst in an hour.

[c]BZD = benzaldehyde, BZAlC = benzylalcohol, BZAC = benzoic acid, o-CRS = ortho-Cresol, p-CRS = para-Cresol, DBZ = dibenzyl.

[d]Chromium impregnated silicalite-1.

[e]No catalyst was used.

Benzoic acid is formed by the subsequent oxidation of benzaldehyde (which is formed from benzyl alcohol). In addition, dibenzyl formation takes place probably via a radical mechanism[33].

4.3.1.3 EFFECT OF MOLAR RATIOS OF REACTANTS

Another aspect studied was the influence of the ratio of reactants on the conversion of toluene. The conversion of toluene is strongly influenced by the amount of TBHP. The ratios were changed by keeping the amount of toluene constant. As can be observed from Table 4.2, measurements carried out at 353 K in the presence of CrS-1 show that the conversion of toluene is favored by an excess of TBHP. The conversion rises from 6.8 to 18.4 wt.% as the TBHP/toluene molar ratio is increased from 0.33 to 1.0. The selectivity to the product is also influenced by the increase in TBHP/toluene molar ratio.

4.3.1.4 EFFECT OF CATALYST REMOVAL

The results of this part of work are much more significant and show whether the toluene conversion proceeds through heterogeneous or homogeneous catalysis using CrS-1 as catalyst and TBHP as the oxidant at 353 K. **Fig.** 4.2 illustrates the effect of the catalyst removal on the conversion of toluene during the reaction. The CrS-1 was removed by filtration from the reaction solution after 7 h, the reaction was further carried out using the filtered reaction solution in the absence of CrS-1 and compared with a reaction solution containing the CrS-1 catalyst. The results of the catalyst removal experiment indicate that the conversion levels off (Fig. 4.2) and that no furhter conversion of toluene is seen when catalyst is removed from the reaction solution (after 7 h). Further, the final reaction mixture was analyzed for chromium using Atomic Absorption Spectroscopy (AAS). From AAS experiment it appears that indeed some chromium is extracted during the reaction from CrS-1. Presumably, a small amount of chromium is leached out from the CrS-1 during 7 h of reaction time but that amount is insufficient to catalyze the reaction. The results confirm that CrS-1 acts as a heterogeneous catalyst in the system.
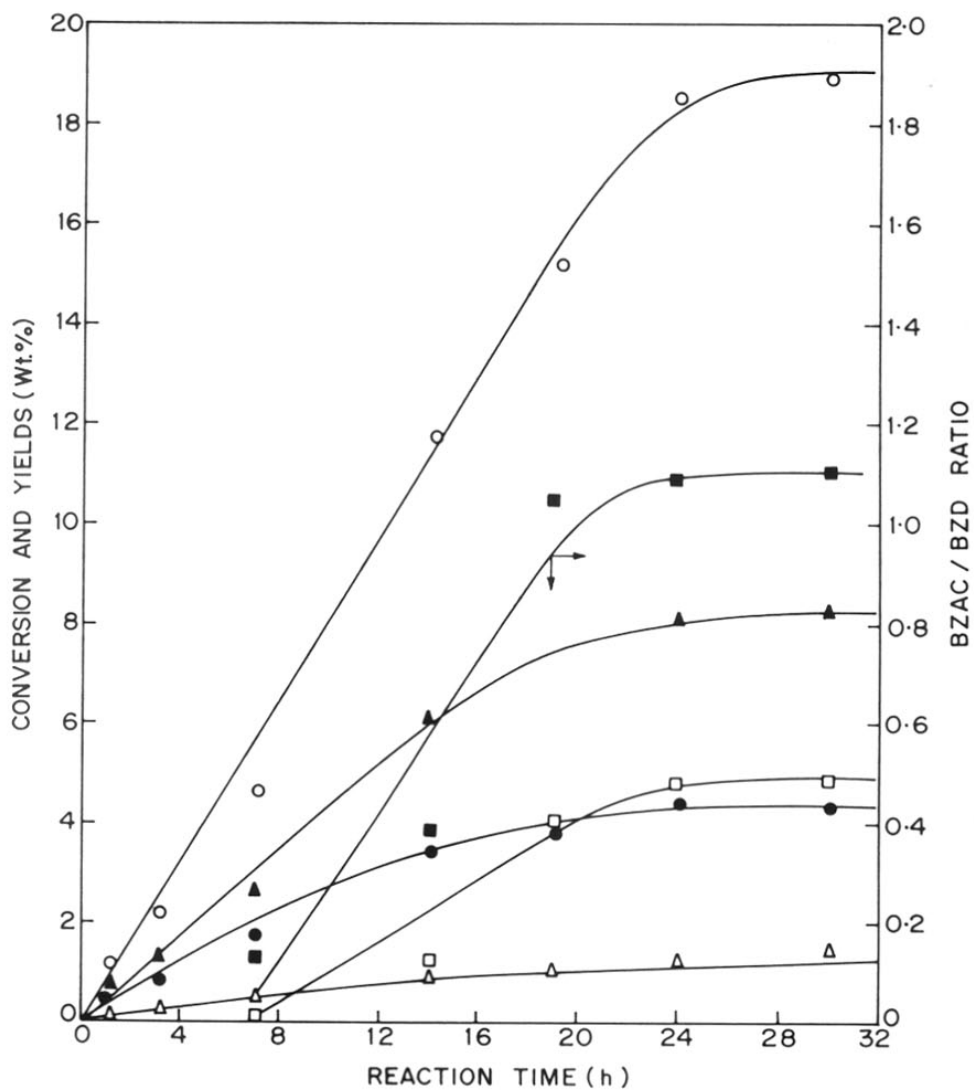
Fig. 4.1 Effect of reaction time on the conversion of   toluene (o), BZAC/BZD ratio (■) and product yields, BZAlC (△), BZD (●), BZAC (□) and DBZ (▲).

Table 4.2

Influence of TBHP/toluene molar ratio[a].

TBHP/ toluene (molar ratio)	Conver- sion (wt.%)	Rate of toluene conversion $(mmolg^{-1}h^{-1})$[b]	Product distribution (wt.%)[c]					
			BZD	BZAlC	BZAC	o-CRS	p-CRS	DBZ
0.3	6.8	0.31	72.6	13.3	14.1	-	-	-
0.5	11.2	0.51	58.7	9.1	17.4	0.4	0.2	14.2
1.0	18.4	0.83	23.3	5.2	25.7	0.4	0.3	45.1

[a]Reaction conditions: catalyst = 0.5 g (Si/Cr = 52), toluene = 5 g, reaction temperature = 353 K, solvent (acetonitrile) = 20 ml, reaction time = 24 h.

[b]mmoles of toluene converted per gram of catalyst in an hour.

[c]BZD = benzaldehyde, BZAlC = benzylalcohol, BZAC = benzoic acid, o-CRS = ortho-Cresol, p-CRS = para-Cresol, DBZ = dibenzyl.
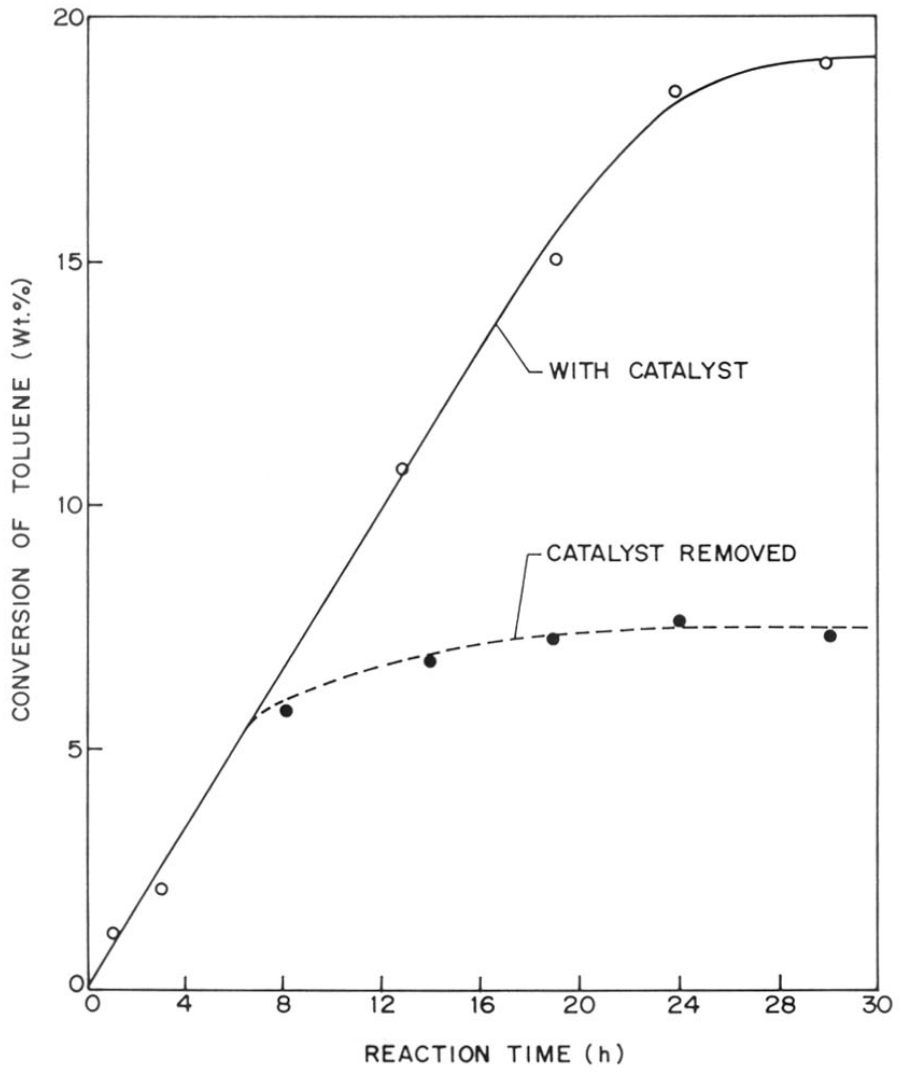
Fig. 4.2 Effect of catalyst (CrS-1) separation on the conversion of toluene.

4.3.1.5 RECYCLING OF THE CATALYST

In order to check the stability of chromium in the catalyst (CrS-1), four reaction cycles were carried out using the same catalyst in the oxidation of toluene. The results are presented in Table 4.3. After completion of the reaction, the catalyst was removed by filtration from the reaction mixture and washed thoroughly with acetonitrile. The reaction mixture and washings were combined and analyzed for chromium. Prior to use in the next cycle, the catalyst was calcined at 773 K for 16 h in the presence of air. AAS revealed that only a small amount of chromium was leached out in the reaction mixture after one reaction cycle and Si/Cr ratio was changed from 52 to 54. The amount of chromium leached out decreased with the increase in number of cycles and Si/Cr ratio remained constant (Si/Cr = 55) after second recycle. These results demonstrate that CrS-1 is an active and stable catalyst and conversion of toluene decreases marginally from 18.4 to 17.4 wt.% after the first reaction cycle. However, nearly similar conversions are obtained over CrS-1 in the third (15.3 wt.%) and fourth (15.0 wt.%) recycles. The observed decrease in the catalytic activity of CrS-1 seems to be related to the leaching of a small amount of chromium from the catalyst. The product distribution remained nearly similar in all recycle experiments. In order to check the structure and crystallinity of the catalyst after reaction, X-ray powder diffraction (XRD) patterns were recorded. XRD measurements (Fig. 4.3) indicated that the catalyst retains the CrS-1 structure and the crystallinity was found to be 95% (after fourth cycle) when compared to the fresh catalyst (100% crystallinity).

4.3.2 OXIDATION OF n-ALKANES

Oxygenation of alkanes with a variety of catalysts and reagents (both in homogeneous and heterogeneous media) is well documented in the literature. The selective oxidation of unactivated alkanes has been demonstrated by using metalloporphyrin based catalyst[34,35]. Heteropolyanions are also able to catalyze the oxidation of alkanes with various primary

Table 4.3

Catalyst recycling[a].

Run	Conversion (wt.%)	Si/Cr ratio	Rate of toluene conversion $(\text{mmol g}^{-1}\text{h}^{-1})$[b]	Product distribution (wt.%)[c]					
				BZD	BZAlC	BZAC	o-CRS	p-CRS	DBZ
1	18.4	52	0.83	23.3	5.2	25.7	0.4	0.3	45.1
2	17.5	54	0.79	26.9	9.5	26.5	0.5	0.4	35.9
3	15.3	55	0.69	22.6	5.8	33.9	0.3	0.2	36.9
4	15.0	55	0.68	28.0	10.1	27.0	0.5	0.3	34.1

[a]Reaction conditions: catalyst = 0.5 g, toluene = 5 g, reaction temperature = 353 K, solvent (acetonitrile) = 20 ml, TBHP/toluene (molar ratio) = 1, reaction time = 24 h.

[b]mmoles of toluene converted per gram of catalyst in an hour.

[c]BZD = benzaldehyde, BZAlC = benzylalcohol, BZAC = benzoic acid, o-CRS = ortho-Cresol, p-CRS = para-Cresol, DBZ = dibenzyl.
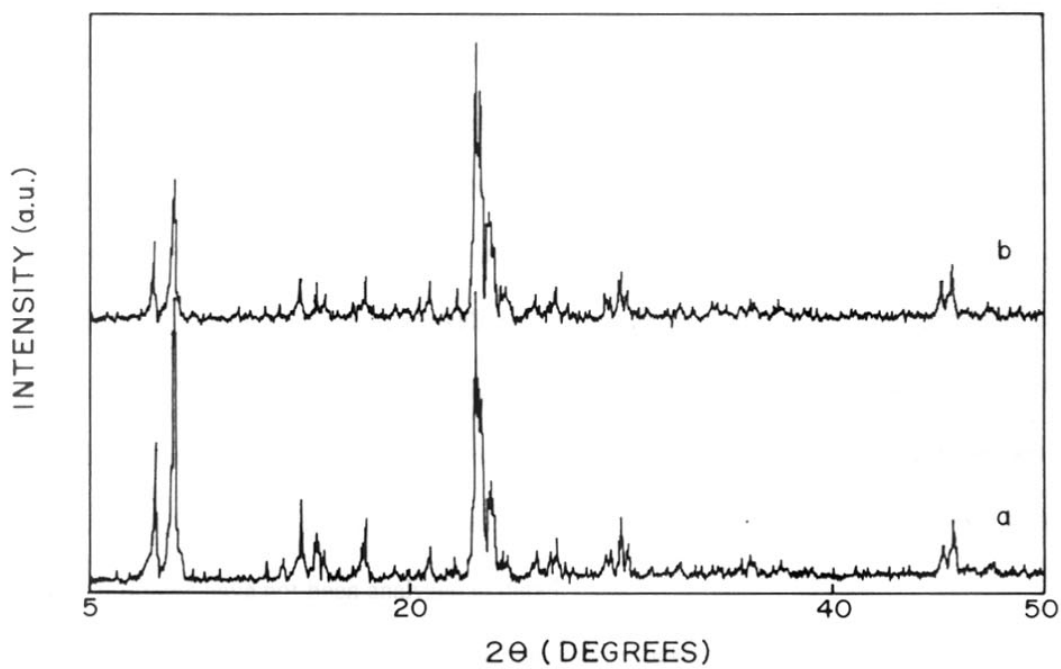
Fig. 4.3. X-ray powder patterns of: (a) fresh CrS-1 and (b) after fourth recycling.

oxidants including TBHP[36,37]. Oxygenation of alkanes using a Pd-Fe zeolite in an O_2/H_2 atmosphere has been reported in the literature[38]. Fe-Phthalocyanin (FePc) encapsulated in zeolite Y and VPI-5 were also used as catalysts for the oxidation of alkanes to alcohols and ketones with TBHP[39]. Titanium silicate molecular sieves, TS-1[2,40] and TS-2[41] have recently been found to catalyze the oxygenation of alkanes most preferentially at the C-2 position using aqueous H_2O_2.

Analogous to titanium silicates, vanadium silicate molecular sieves, VS-2 (with MEL structure)[13,30] are also able to give alcohols and ketones in this oxygenation reaction. Interestingly, apart from alcohols and ketones; primary carbon activated products such as primary alcohols and aldehydes were also observed in the final reaction mixture.

Like vanadium silicate molecular sieves, chromium silicates, CrS-1 (MFI), are also able to oxygenate primary carbon of the unactivated alkanes in the presence of TBHP as the oxidant. The results obtained for each alkane over CrS-1 is compared with VS-1 catalyst. The results of the oxidation of n-hexane, n-heptane and n-octane over CrS-1 and VS-1 are listed in Table 4.4. Between the two catalysts studied CrS-1 and VS-1 show approximately the same trends for substrate conversion as well as product distribution. The major products of the reaction are corresponding alcohols, aldehydes and ketones. Unidentified products designated as others with more than one functional group viz. dihydroxyalkanes and lactones are also detected. Since there was no authentic samples for those dihydroxy alkanes and lactones, these products have not been analyzed in detail.

The conversion of n-hexane, n-heptane and n-octane over CrS-1 are 11.3, 9.8 and 7.7 wt.% respectively. The rate of substrate conversion decreased in the order n-hexane > n-heptane > n-octane. This marked difference in the activity of alkane oxygenation between n-hexane, n-heptane and n-octane can be related to the decrease in diffusivity of these alkanes in molecular sieves with increase in chain length and molecular size[42].

96

Table 4.4

Oxidation of n-alkanes[a].

Alkane	Catalyst	Conversion (wt.%)	Rate of n-alkane conversion (mmol g^{-1}h^{-1})[b]	Product distribution (wt.%)[c]								
				4-one	3-one	2-one	4-ol	1-al	3-ol	2-ol	1-ol	Others[d]
Hexane	CrS-1	11.3	1.10	-	28.2	30.9	-	4.1	4.3	6.1	0.2	26.2
Hexane	VS-1	11.6	1.12	-	28.7	31.3	-	4.0	4.7	6.6	0.1	24.6
Heptane	CrS-1	9.8	0.82	6.9	16.0	20.9	10.3	14.3	5.2	7.0	2.3	17.1
Heptane	VS-1	10.9	0.91	8.0	17.2	20.3	10.9	16.2	5.1	7.2	3.6	11.5
Octane	CrS-1	7.7	0.56	11.6	6.6	11.9	7.9	8.4	18.3	11.8	1.0	22.5
Octane	VS-1	8.7	0.64	5.7	13.7	22.5	6.1	6.8	12.6	7.3	0.2	25.1

[a]Reaction conditions: catalyst = 0.5 g (Si/Cr = 52, Si/V = 118), alkane = 5 g, alkane/TBHP = 3 (mole ratio),   solvent = acetonitrile (25 ml), reaction temperature = 373 K, reaction time = 12 h.
[b]mmoles of alkane converted per gram of catalyst in an hour.
[c]1-ol = alcoh-1-ol, 2-ol = alcoh-2-ol, 3-ol = alcoh-3-ol, 4-ol = alcoh-4-ol, 1-al = 1-aldehyde, 2-one = ket-2-one, 3-one = ket-3-one and 4-one = ket-4-one of corresponding alkanes.
[d]Mostly oxygenates with more than one functional group and lactones.

The position of oxygenation of alkanes (excluding others) such as n-hexane, n-heptane and n-octane are given in Fig. 4.4. It can be seen from the Fig. 4.4. that in the product distribution of n-hexane reaction, the oxygenation of the second carbon is the most favoured position. The trend in the position of oxygenation is as follows C-2 > C-3 > C-1. A closer look at the position of oxygenation between n-heptane and n-octane would indicate that in the case of n-octane there is a slight increase in the percentage of oxygenation at C-3 (24.9%) and C-4 (19.5%) when compared to n-heptane oxygenates (C-3, 21.2% and C-4, 17.2%) and also the position of oxygenation at C-2 (23.7%) in n-octane is lower than n-heptane C-2 (27.9%) position.

4.3.3 OXIDATION OF CYCLOHEXANE

Apart from these n-alkane oxygenation, the oxidation of cyclohexane to cyclohexanol and cyclohexanone is an industrially important reaction because of the commercial utility of cyclohexanone in the manufacture of nylon 6,6[43]. Cyclohexanone and cyclohexanol are mainly produced by direct cyclohexane oxidation with air in the presence of soluble cobalt catalysts or boric acid[44]. In addition to homogeneous catalysts, Mn^{2+}-exchanged clay-catalyzed oxidation of cyclohexane with TBHP at reflux temperatures has also been communicated by Tateiwa et al.[45]. Recently, the use of titanium silicate molecular sieves, TS-1 (MFI)[46] and TS-2 (MEL)[47] in the oxidation of cyclohexane to cyclohexanol and cyclohexanone is reported. Furthermore, chromium substituted aluminophosphate molecular sieves (Cr-AlPO$_4$-5) have been found to catalyze the oxidation of cyclohexane by air in the presence of TBHP as an initiator[48].

Table 4.5 summarizes the catalytic activities of CrS-1 and VS-1 in the oxidation of cyclohexane. To avoid unnecessary side products (designated as others) a lower reaction temperature (353 K) and a cyclohexane/TBHP molar ratio 3 were chosen for the cyclohexane oxidation reaction. A blank run was also carried out for comparison. The major products of the reaction are cyclohexanone and cyclohexanol. It is seen that CrS-1
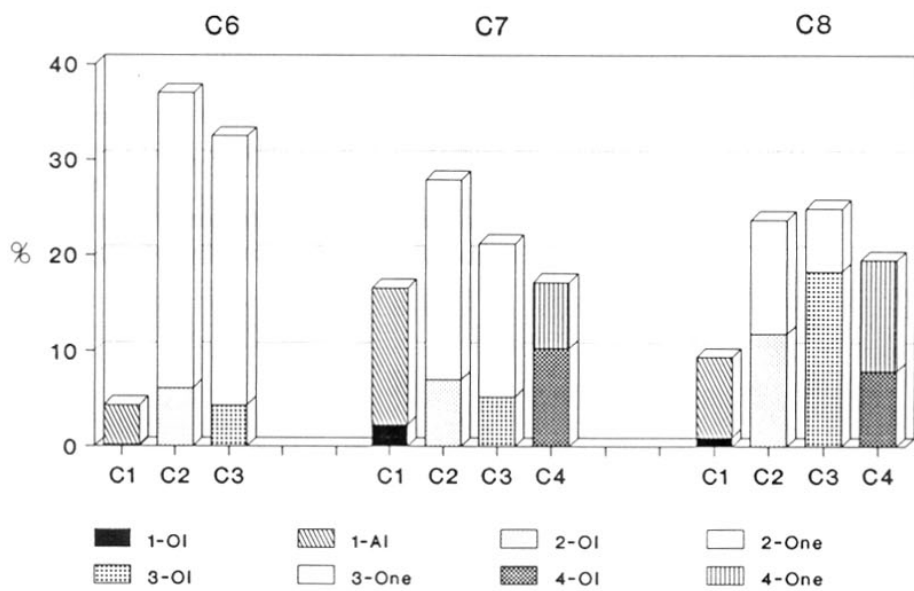
Fig. 4.4 Position of oxygenation in the alkane chain by TBHP over CrS-1.

Table 4.5

Oxidation of cyclohexane[a]

Catalyst	Conversion (wt.%)	Rate of cyclohexane conversion $(\text{mmolg}^{-1}\text{h}^{-1})$[b]	Product distribution (wt. %)		
			Cyclohexanone	Cyclohexanol	Others[c]
CrS-1	8.5	0.84	49.1	50.2	0.7
VS-1	5.6	0.55	47.6	51.9	0.5

[a]Reaction conditions: Catalyst = 0.5 g (Si/Cr = 52, Si/V = 118), cyclohexane = 5 g, reaction temperature = 373 K, solvent (acetonitrile) = 25 ml, cyclohexane/TBHP (molar ratio) = 3, reaction time = 12 h.
[b]mmoles of cyclohexane converted per gram of catalyst in an hour.
[c]Mostly oxygenates with more than one functional group.

sample is found to be more active than VS-1. A blank run failed to give any conversion of cyclohexane. The conversion of cyclohexane over CrS-1 and VS-1 is found to be 8.5 and 5.6, wt.% respectively. The corresponding rates of cyclohexane conversion are 0.84 and 0.55 mmolg^{-1}h^{-1}, respectively. The ratio of cyclohexanone to cyclohexanol is 0.97. These results are in good agreement with the results reported by Reddy and Sivasanker[47].

4.3.4 MECHANISM

The oxidation of toluene may proceed via the reduction of Cr^{5+} to Cr^{3+} by toluene followed by the formation of chain complex reaction of TBHP with chromium sites (Cr^{5+}). It is well known that vanadium (V^{5+}) in the calcined form of VAPO-5 could be reduced easily to V^{4+} with toluene at 373 K[49]. This is possible because the initial attac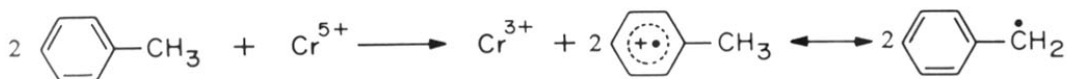k on the aromatic substrate may occur through an electron-transfer mechanism rather than through direct hydrogen abstraction by a radical. Benzyl radical is formed from the cation-radical intermediate followed by the loss of a proton. In the process of oxidation Cr^{5+} is reduced to Cr^{3+}.

The involvement of the redox system Cr^{5+}/Cr^{3+} present in chromium silicate molecular sieves is substantiated by the ESR studies of the catalysts obtained before and after the toluene oxidation. ESR spectra were recorded for CrS-1 before and after it was used for the catalytic reaction of toluene. The reaction used a mixture of toluene (5 g), TBHP (6.9 g), acetonitrile (20 ml) and catalyst (0.5 g) at 353 K. For ESR studies, the catalyst (after 24 h of reaction time) was recovered by filtration from the reaction mixture and washed several times with acetonitrile followed by drying at 353 K for 12 h. The ESR spectra of these catalysts before
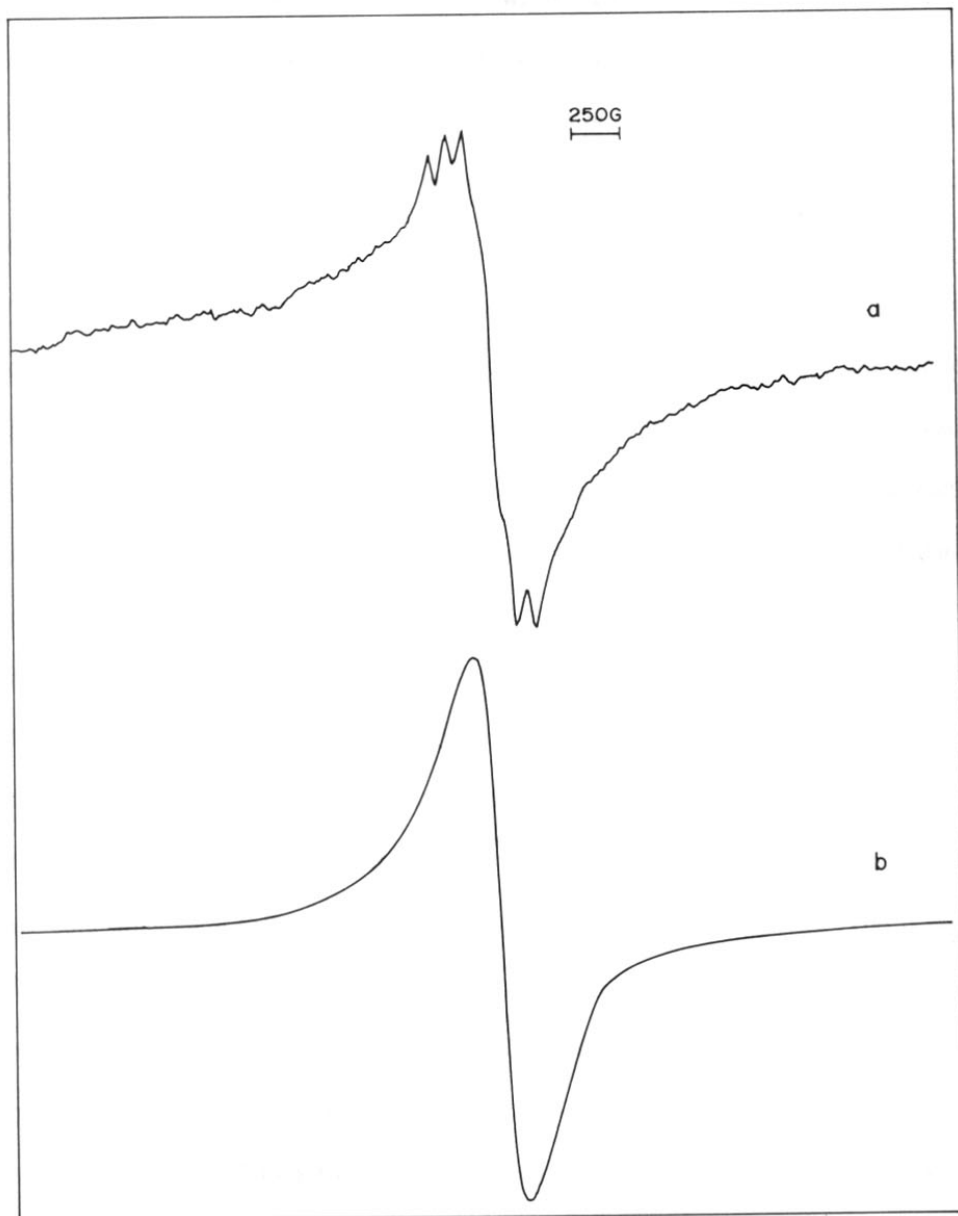
250G

a

b

Fig. 4.5 ESR spectra of : (a) fresh CrS-1 and (b) after reaction.

and after reaction are given in Fig. 4.5. The fresh catalyst shows a five line spectrum (g = 1.951) indicating the presence of Cr^{3+} and Cr^{5+} whereas the ESR spectrum of the catalyst after the reaction shows a broad singlet (g = 1.946); the characteristic spectrum of Cr^{3+} reappears indicating the reversibility of Cr^{5+}/Cr^{3+}. On the basis of ESR results, it is believed that the catalytic behavior of CrS-1 is due to the reversible transformation of Cr^{5+}/Cr^{3+} within the structure.

Furthermore, to find more about the location of the active sites in VAPO-11, peroxides of different sizes were employed (t-butyl hydroperoxide, α, α-dimethylbenzyl hydroperoxide and triphenylmethyl hydroperoxide)[50]. Likewise, in order to find out whether the reaction occurs inside the channels or at the outer surface of the CrS-1 particles, the catalytic reactions were carried out with hydrocarbons having different molecular dimensions using TBHP as the oxidant. Molecular dimensions of toluene, and 1-methyl naphthalene are 4.78 x 1.78 Å and 6.7 x 2.0 Å, respectively. The molecular dimensions were calculated using Silicon Graphics Indigo workstation supplied by Biosym Technology, Inc. The micropore dimensions of ZSM-5 (5.4 x 5.6 Å) are sufficient enough for TBHP (4.06 x 4.11 Å) to diffuse into the pores of CrS-1. The activity trend based on the conversion is, toluene > 1-methyl naphthalene. Thus the pore structure of CrS-1 plays a significant role in the oxidation reactions. This is evident from the results obtained on the conversion of toluene (18.4 wt.%) over CrS-1. Since the molecular dimensions of toluene is 4.78 x 1.78 Å, the accessibility of toluene into the molecular sieves is not difficult when compared to 1-methyl naphthalene (6.70 x 2.00 Å). As expected CrS-1 failed to activate the bulkier 1-methyl naphthalene. These findings were further substantiated by the results reported by Chen et al[19]. They revealed that the oxidation reaction occurred inside the pores of CrS-1. When triphenyl methyl hydroperoxide was used as an oxidant in place of TBHP, the reaction hardly took place, since the oxidant is too bulky to enter into the micropores.

The above results are further corroborated by the negligible catalytic activity of as-synthesized CrS-1, where the organic template used in the synthesis remained intact in the channels of the molecular sieves. These observations strongly suggest that the outer surface of the CrS-1 has only a small contribution to the catalytic activity and that the reaction takes place inside the pores of the molecular sieves.

4.4 CONCLUSIONS

1. Chromium silicate molecular sieves, CrS-1 is an active, recyclable catalyst for the liquid phase oxidation of toluene, cyclohexane, n-hexane, n-heptane and n-octane with TBHP.

2. CrS-1 exhibits higher activity than VS-1 in the oxidation of toluene whereas CrS-1 and VS-1 are found to be comparable in the oxidation of n-alkanes.

3. A higher yield of the products can be achieved by changing the reaction parameters such as the reaction time and the TBHP/toluene molar ratios.

4. CrS-1 is quite stable even after four recycling experiments in the oxidation of toluene.

5. The reactions proceeds through a heterogeneous catalytic route and no conversion of toluene is observed when CrS-1 was removed by filtration from the reaction solution after 7 h of reaction time.

6. The reactivity of the n-alkanes over CrS-1 in the presence of TBHP is greatly influenced by the chain length of the alkane. CrS-1 is also active in the oxidation of cyclohexane to cyclohexanol and cyclohexnone.

4.5 REFERENCES

1. B. Notari, Stud. Surf. Sci. Catal., 60, 413 (1989).

2. T. Tatsumi, M. Nakamura, S. Negishi and H. Tominaga, J. Chem. Soc. Chem. Commun., 476 (1990).

3. J. S. Reddy, U. R. Khire, P. Ratnasamy and R. B. Mitra, J. Chem. Soc. Chem. Commun., 1234 (1992).

4. R. S. Reddy, J. S. Reddy, R. Kumar and P. Kumar, J. Chem. Soc. Chem. Commun., 84 (1992).

5. J. S. Reddy and P. A. Jacobs, J. Chem. Soc. Perkin Trans. I. 2665 (1993).

6. P. R. H. P. Rao, K. R. Reddy, A. V. Ramaswamy and P. Ratnasamy, Stud. Surf. Sci. Catal., 76, 385 (1993).

7. K. R. Reddy, A. V. Ramaswamy and P. Ratnasamy, J. Chem. Soc. Chem. Commun., 1613 (1992).

8. K. R. Reddy, A. V. Ramaswamy and P. Ratnasamy, J. Catal., 143, 275 (1993).

9. C. Walling, C. Zhao and G. M. El-Taliawi, J. Org. Chem., 48, 4910 (1993).

10. J. Muzart, Chem. Rev., 92, 113 (1992).

11. H. V. Borgaonkar and S. B. Chandalia, J. Chem. Tech. Biotechnol., 34A, 107 (1984).

12. D. E. 3, 308, 448 to F. Marcel.

13. P. R. H. P. Rao and A. V. Ramaswamy, J. Chem. Soc. Chem. Commun., 1245 (1992).

14. T. Selvam and A. P. Singh, J. Chem. Soc. Chem. Commun., 883 (1995).

15. U. Cornaro, P. Jiru, Z. Tvaruzkova and K. Habersberger, Stud. Surf. Sci. Catal., 69, 165 (1991).

16. G. W. Skeels and E. M. Flanigen, Stud. Surf. Sci. Catal., 49A, 331 (1989).

17. R. A. Sheldon, J. D. Chen, J. Dakka and E. Neeleman, Stud. Surf. Sci. Catal., 83, 407 (1994).

18. J. D. Chen, M. J. Haanepen, J. H. C. van Hooff and R. A. Sheldon, Stud. Surf. Sci. Catal., 84, 973 (1994).

19. J. D. Chen, H. E. B. Lempers and R. A. Sheldon, Stud. Surf. Sci. Catal., 92, 75 (1995).

20.   R. Joseph, M. Sasidharan, R. Kumar, A. Sudalai and T. Ravindranathan, J. Chem. Soc. Chem. Commun., 1341 (1995).

21.   B. Jayachandran, M. Sasidharan, A. Sudalai and T. Ravindranathan, J. Chem. Soc. Chem. Commun., 1523 (1995).

22.   G. Centi, S. Perathoner, F. Trifiro, A. Aboukais, C. F. Aissi and M. Guelton, J. Phys. Chem., 96, 2617 (1992).

23.   R. J. Argauer and G. R. Landolt, U. S. Pat., 3 702 886 (1972).

24.   W. S. Trahanovsky and L. B. Young, J. Org. Chem., 31, 2033 (1966).

25.   M. Marrocco and G. Brilmyer, J. Org. Chem., 48, 1487 (1983).

26.   M. Schmidt and M. Schmidbaur, Angew. Chem., 70, 704 (1958).

27.   H. V. Borgaonkar, S. R. Raverkar and S. B. Chandalia, Ind. Eng. Chem. Prod. Res. Dev., 23, 455 (1984).

28.   B. M. Choudary, A. D. Prasad, V. Bhuma and V. Swapna, J. Org. Chem., 57, 5841 (1992).

29.   A. A. Elgwezabal, N. E. Quaranba, J. L. G. Fierro and V. C. Corberan, Proc. of the DGMK Conference "Selective Oxidations in Petrochemistry" September 16-18, p. 267 (1992).

30.   P. R. H. P. Rao, A. V. Ramaswamy and P. Ratnasamy, J. Catal., 141, 604 (1993).

31.   A. Tuel and Y. Ben Taarit, Appl. Catal., 102, 201 (1993).

32.   G. Perego, G. Bellussi, C. Corno, M. Taramasso, F. Buonomo and A. Esposito, Proc. of 7 th IZC, Tokyo, p. 129 (1986).

33.   C. Marchal, A. Tuel and Y. Ben Taarit, Stud. Surf. Sci. Catal., 78, 447 (1993).

34.   P. Bationi, J. Renaud, J. F. Bartoli and D. Mansuy, J. Chem. Soc. Chem. Commun., 341 (1986).

35.   B. Meunier, Bull. Soc. Chim. Fr., 578 (1986).

36.   R. Newmann and C. Abu-Gnim, J. Chem. Soc. Chem. Commun., 1324 (1989).

37.   W. Herron, C. A. Tolman, J. Am. Chem. Soc., 109, 2837 (1987).

38.   A. E. Shilov, "Activation of Saturated Hydrocarbons by Transition Metal Complexes", Reidel, Dordrecht, p. 88 (1984).

39.   R. F. Parton, L. Uytterhoeven and P. A. Jacobs, Stud. Surf. Sci. Catal., 59, 395 (1991).

40.   D. R. Huybrechts, L. De Bruycker and P. A. Jacobs, Nature 345, 240 (1990).

41.   J. S. Reddy, S. Sivasanker and P. Ratnasamy, J. Mol. Catal., 70, 335 (1991).

42. P. B. Weisz, in T. Seiyama and K. Tanabe (Eds), Proc. of 7 th Int. Cong. on Catalysis, Elsevier, Amsterdam, Tokyo, p. 3 (1980).

43. "Ulmann's Encyclopedia of Industrial Chemistry", 5 th ed., vol A18, p. 264 (1991).

44. Kirk-Othmer, "Encyclopedia of Chemical Technology", 4 th ed., vol 13, p. 830 (1995).

45. J. Tateiwa, H. Horiuchi and S. Uemura, J. Chem. Soc. Chem. Commun., 2567 (1994).

46. U. Schuchardt, H. O. Pastore and E. V. Spinace, Stud. Surf. Sci. Catal., 84C, 1877 (1994).

47. J. S. Reddy and S. Sivasanker, Catal. Lett., 11, 241 (1990).

48. J. D. Chen and R. A. Sheldon, J. Catal., 153, 1 (1995).

49. S. H. Jhung, Y. Sunuh and H. Chou, Appl. Catal., 62, 61 (1990).

50. M. J. Haanepen and J. H. C. van Hooff, Proc. of the DGMK Conference "Selective Oxidations in Petrochemistry" September 16-18, p. 227 (1992).

CHAPTER 5

OXIDATION OF ANILINE TO AZOXYBENZENE OVER METALLOSILICATE   (Ti, V
and Cr) MOLECULAR SIEVES WITH MFI STRUCTURE

5.1 INTRODUCTION

This chapter is part of a continuous research effort to explore alternative routes for azoxybenzene synthesis. More specifically, we have studied the oxidation of aniline to azoxybenzene using catalytic amount of titanium silicate, TS-1, in the presence of H_2O_2 as the oxidant. The performance of TS-1 was also compared to other metallosilicates with MFI structure, including VS-1 and CrS-1.

Oxidation of aniline and substituted anilines with a variety of reagents and catalysts (both in homogeneous and heterogeneous media) is well documented[1-6]. Depending on the type of catalyst and/or the oxidant used, the product spectrum can be varied. Azobenzene is obtained using MnO_2 as stoichiometric oxidant[1]. Aqueous peracids oxidize aniline to azo- and azoxybenzenes[2], while anhydric peracids oxidize aniline to nitrobenzene[3]. Homogeneous catalytic oxidation of aniline has also been carried out using transition metal complexes such as titanium[4], vanadium[5], iron[6] and molybdenum complexes[7]. Titanium complexes[4] catalyze the oxidation of aniline to azoxybenzene, whereas with vanadium oxyacetylacetonate[5] only nitrobenzene is obtained in the presence of t-butyl hydroperoxide (TBHP). With molybdenum complex, $[Mo(O)(O_2)_2(H_2O)(hmpa)]$ in the presence of hydrogen peroxide, nitrosobenzene is obtained selectively[7]. Tungsten oxide in the presence of H_2O_2 oxidizes aniline to nitroso- and azoxybenzenes[8]. $FeCl_3$[9] and $Pb(OAc)_4$[10] also catalyze the oxidation of aniline to nitrosobenzene. The oxidation of aniline to either azoxybenzene or to nitrobenzene using $RuCl_3$ or quarternary ammonium chloride in the presence of hydrogen peroxide has been reported [11].

The transition metallosilicate molecular sieves, TS-1, VS-1 and CrS-1 (with MFI structure) exhibit unique catalytic properties in a number of reactions such as the hydroxylation of phenol[12] and benzene[13], the epoxidation of olefines[14], the ammoximation of carbonyl compounds[15]

and the oxyfunctionalization of alkanes[16,17], using aqueous H_2O_2 as oxidant. These are the first set of metallosilicate molecular sieves having shape-selective oxidation capability, which can be exploited in many organic chemical transformations.

Heterogeneous catalytic oxidation of aniline involving transition metallosilicate molecular sieves such as TS-1/H_2O_2[18-22] and VS-1/H_2O_2[23] is reported to produce azoxybenzene in high selectivity. Indeed, oxidation of alkylamines to give the corresponding oximes[24,25] and secondary amines to nitrones[26] have also been reported. Patent literature also claims that TS-1 catalyzes the oxidation of secondary amines to the corresponding hydroxylamines[27]. Recently Sudalai et al. have reported that the oxidation of primary amine to their corresponding nitro compounds using chromium silicate molecular sieves with MEL structure[28] and TBHP as the oxidant.

5.2 EXPERIMENTAL

5.2.1 CATALYTIC MATERIALS AND CHARACTERIZATION

Previously published methods were used for the preparation of Ti, V and Cr containing molecular sieves with MFI structure[29-31]. The characterization techniques such as XRD, IR, UV, SEM, ESR, MAS-NMR and catalytic tests were used to characterize these metallosilicate molecular sieves. The samples were calcined at 773 K in air for 12 hours, in order to remove the trapped organic cations. Mild treatments with aqueous 1 M ammonium acetate at 353 K were performed in order to wash away unstable vanadium and chromium species. The physico-chemical properties of these molecular sieves are given in Table 5.1.

5.2.2. CATALYTIC REACTIONS

The oxidation of aniline was carried out batchwise in a 100 ml round bottomed flask fitted with a condenser and with continuous stirring using TS-1, VS-1 or CrS-1 as the catalyst. In a typical run, 0.25 g of the catalyst was dispersed in a solution containing 5 g of aniline (54 mmol) and 10 ml of a solvent. The mixture was vigorously stirred and 1.7 ml of H_2O_2 (30% aqueous

solution) (18 mmol) was then added in one lot using a 5 ml graduated syringe as soon as the reaction temperature (333-353 K) was attained. After the completion of the reaction, the products were analyzed in a capillary gas chromatograph (HP 5880), fitted with a 50 m long cross linked methyl silicone gum capillary column. The identity of the products was established by GC-MS (Shimadzu, QP 2000 A).

5.2.3 CYCLIC VOLTAMMETRY

Cyclic voltammetric (CV) studies were carried out in a three compartment, single electrode cell with molecular sieves modified electrode as the working electrode. 100 mg of molecular sieves (TS-1, VS-1 and CrS-1), 100 mg graphite and 10 mg polystyrene were mixed in 2 ml of THF and the paste was coated on a platinum ultra microelectrode (Platinum UME, radius 10 μm); a platinum foil and silver wire were used as counter electrode and quasi reference electrode (AgQRE) respectively. Cyclic voltammograms were carried out in 0.1 M TBATFB (Tetrabutylammonium tetrafluoborate) in acetonitrile as the electrolyte added separately with 0.1 M aniline and 0.1 M H_2O_2.

5.2.4 COULOMETRY

Controlled potential electrolysis (CPE) experiments were carried out at various potentials determined from CV, using a graphite disc electrode (area 0.0625 cm^2) modified with molecular sieves, in acetonitrile.

5.3 RESULTS AND DISCUSSION

5.3.1 MODE OF ADDITION OF H_2O_2

The mode of addition of H_2O_2 is an important factor determining the selectivity towards azoxybenzene and nitrosobenzene, since oxygen is consumed in two different stages of the overall oxidation reaction. Three different modes of H_2O_2 addition have been adopted: (i) addition of all the H_2O_2 in one lot in the beginning of the reaction (Fig. 5.1); (ii) addition of H_2O_2 over a period

Table 5.1

Physico-chemical properties of metallosilicate molecular sieves.

Sample	Si/M ratio[a]		Yield (wt.%)	Particle size (μm)	Surface area (m^2g^{-1})	Cyclohexane adsorption (wt.%)[b]
	Gel	Product				
TS-1	100	80	70-75	0.3	389	6.0
VS-1	50	118	85-90	0.2	475	7.2
CrS-1	20	52	90-95	5 x 25	336	5.2

[a]M = Ti, V and Cr
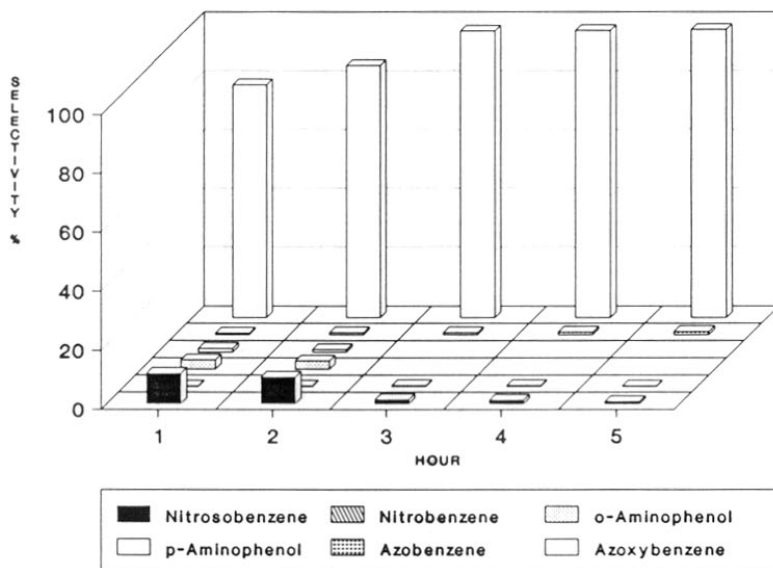[b]Gravimetric (Cahn balance), temperature = 298 K, $P/P_0 = 0.5$
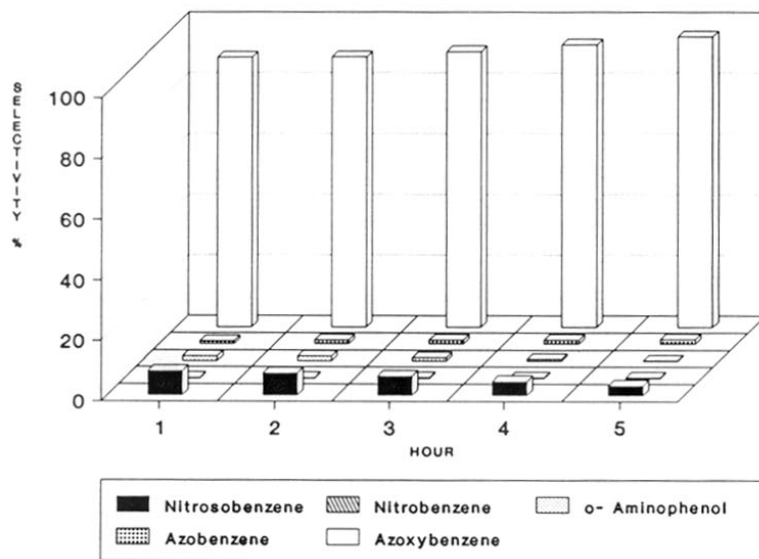
Fig. 5.1 Addition of H_2O_2 in one lot.

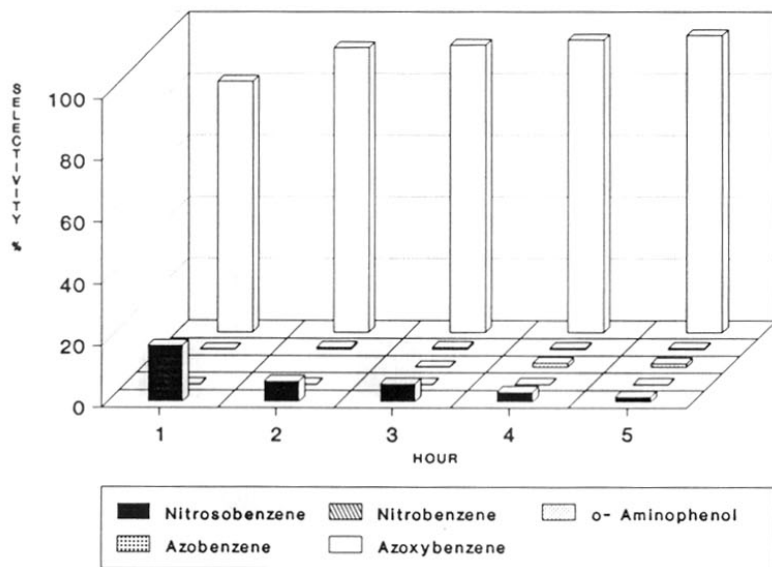Fig. 5.2 Addition of H_2O_2 over a period of 1 h.
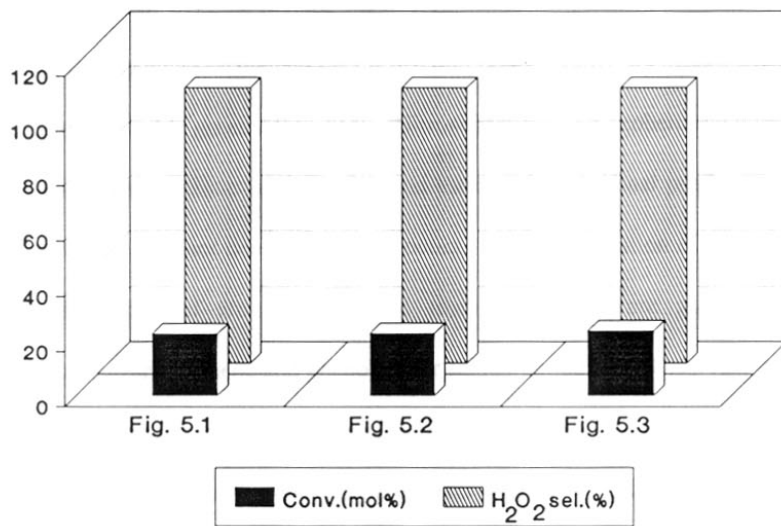
Fig. 5.3 Addition of H_2O_2 over a period of 5 h.

Fig. 5.4   Aniline conversion and H_2O_2 selectivity for each mode of addition of H_2O_2 corresponding to Figures 5.1, 5.2 and 5.3 respectively.

of 1 h (Fig. 5.2); and (iii) addition of H_2O_2 slowly over a period of 5 h   (Fig. 5.3).   The conversions obtained in the three cases are shown in Fig. 5.4.

In the initial stages of the reaction mixture, the concentration of nitrosobenzene was found to be quite high when compared to other products such as nitrobenzene, azobenzene, o- and p-aminophenols. Initially formed nitrosobenzene from phenyl hydroxylamine is more reactive and is immediately consumed in the formation of azobenzene by condensation with unreacted aniline and then converted into azoxybenzene.   Azoxybenzene could also be formed by the direct condensation of the two intermediates phenyl hydroxylamine and nitrosobenzene. Depending upon the initial concentration of H_2O_2, nitrobenzene could also be a major product, but within the aniline/H_2O_2 mole ratios of 1-10 studied here, only traces of nitrobenzene are observed in the product. The major product at the end of 5 h reaction period is azoxybenzene, which is obtained with a selectivity invariably greater than 85%. Nitrosobenzene and azobenzene intermediates and small quantities of nitrobenzene are identified and estimated in the final product of the reaction. Phenyl hydroxylamine was not detected in the product. The hydroxylation of the aromatic nucleus leads to the formation of aminophenols and titanium silicates are good catalysts in the hydroxylation of benzene, toluene and phenol under similar conditions. Only very small quantities of both o-aminophenol and p-aminophenol were found in the early stages of the reaction. However, in the final reaction/product mixture (after 5 h of run), the aminophenols were not detected. Presumably, the initially formed aminophenols were converted into high molecular weight tars, which are not detected in the GC analysis.

5.3.2 INFLUENCE OF DIFFERENT SOLVENTS

In many oxidation and hydroxylation reactions involving titanium silicate as catalyst, the solvent used in the batch reaction is known to influence the activity and the selectivity to the

desired products[32,33]. The results on the use of five different solvents of different polarities and dielectric constants in the oxidation of aniline are given in Table 5.2. The reactions were carried out at 353 K, keeping aniline to H_2O_2 mole ratio of 3 in the reaction mixture. The extent of conversion of aniline (upto 5 h of reaction duration) in different solvents is found to be in the order acetone > acetonitrile > methanol > t-butanol > water. However, the selectivity towards azoxybenzene in the product is found to be in the order t-butanol > water > acetonitrile > methanol > acetone . Methanol and t-butanol are reported to be suitable solvents in the synthesis of oximes from primary aliphatic amines on TS-1[24]. In presence of acetone, primary amines and anilines are known to condense strongly forming corresponding imines (Ph-N=CMe$_2$ from aniline)[34]. The formation of imine and their hydroxylated products accounts for about 40% of the total products (Table 5.2) when acetone is used as solvent and hence the selectivity to azoxybenzene is considerably lower in acetone than in other solvents. This condensation reaction also occurs in the absence of a catalyst.

In methanol and in acetonitrile , the H_2O_2 selectivity is found to be in the order of 94-100%, whereas in t-butanol and water, it is at least about 25% lower. One notable feature is that the concentration of nitrosobenzene, is considerably higher (13.4 %) in the product when methanol is used as solvent. The condensation reaction between nitrosobenzene and aniline leading to the formation of azobenzene is probably inhibited in methanol solvent. This is one of the reasons for the lower selectivity to azoxybenzene in this case. On the other hand, a selectivity of the order of 97% to azoxybenzene in both t-butanol and water is due to negligible by-product formation at an aniline conversion level of about 15 mol%. The amount of nitrobenzene, however, is found to be slightly higher in these two solvents.

Table 5.2

Effect of solvent, temperature and H_2O_2 concentration on the oxidation of aniline over TS-1[a]

Aniline/H_2O_2 mole ratio	Temp. (K)	Solvent	Conv. (mol%)	H_2O_2 sel.[b] (%)	Product distribution (%)				
					NSOB	NB	AB	AXYB	Others[c]
3	353	CH_3OH	20.6	93.3	13.4	0.3	2.8	80.6	1.9
3	353	t-BuOH	15.2	69.6	0.2	1.8	0.6	97.3	0.1
3	353	H_2O[d]	14.3	65.7	0.5	2.3	0.4	96.7	0.1
3	353	CH_3COCH_3	24.8	66.7	5.7	0.2	0.9	51.2	39.6[e]
3	353	CH_3CN	23.7	100.0	1.6	0.2	2.2	91.8	4.2
3	353[f]	CH_3CN	19.1	82.4	4.8	-	1.3	88.1	5.8
3	343[f]	CH_3CN	13.4	63.3	20.7	-	0.8	77.9	0.6
3	333[f]	CH_3CN	9.8	50.8	21.8	-	0.3	75.7	2.2
1	333[f]	CH_3CN	14.7	21.7	3.1	1.9	6.3	86.4	2.3
5	333[f]	CH_3CN	7.3	57.8	24.6	-	4.3	71.1	-
10	333[f]	CH_3CN	5.7	90.6	27.1	-	2.0	70.1	0.8

[a]Reaction conditions: aniline = 54 mmol, catalyst = 0.25 g (TS-1 (Si/Ti = 80)), reaction time = 5 h.
[b]H_2O_2 utilized in the formation of nitroso- (NSOB), nitro- (NB), azo- (AB) and azoxybenzenes (AXYB).
[c]Mostly oxygenated with more than one functional group.
[d]Products were extracted with benzene.
[e]Condensation (imine) and their hydroxylated products.
[f]Catalyst amount used in this study was 0.05 g.

5.3.3 INFLUENCE OF H$_2$O$_2$ CONCENTRATION

The results on the variation of aniline to H$_2$O$_2$ ratio in the reaction mixture are included in Table 5.2. The data at 333 K show that as the concentration of H$_2$O$_2$ in the reaction mixture is increased, both conversion and selectivity to azoxybenzene increase. For maximum conversion and azoxybenzene formation, the aniline to H$_2$O$_2$ (mole) ratio must be kept as low as possible. The azoxybenzene to nitrosobenzene ratio is also higher when the H$_2$O$_2$ concentration is more, the ratios being 27.8, 3.4, 2.8 and 2.5 at aniline to H$_2$O$_2$ ratio of 1, 3, 5 and 10, respectively (Table 5.2). This indicates that the oxidation of azo- to azoxybenzene becomes more prominent than nitroso- to nitrobenzene as the H$_2$O$_2$ concentration in the reaction mixture is increased. In fact, at high concentration of H$_2$O$_2$ and in presence of phase-transfer catalysts, selective formation of nitrobenzene has been reported[11].

5.3.4 INFLUENCE OF TEMPERATURE

Acetonitrile was chosen as the solvent for studying the influence of temperature between 333 and 353 K on the conversion and selectivity in this reaction, while keeping the aniline to H$_2$O$_2$ mole ratio at 3 and the catalyst amount (gram per moles of aniline) at 0.93 (0.05 g of catalyst). The results are included in Table 5.2. The reaction temperature has a positive influence on aniline conversion, which increases from 9.8 to 19.1 mol% between 333 and 353 K, respectively. The reaction rate increases from 2.9 to 5.8 x 10-7 mol cm^{-3} s^{-1} between these two temperatures. From the product distribution, it is seen that the azoxybenzene to nitrosobenzene ratio is dependent on the reaction temperature, the ratio being 3.4 at 333 K, 3.7 at 343 K and 18.3 at 353 K. At temperatures above 343 K, the condensation of nitrosobenzene with aniline is probably faster. Further oxidation of azobenzene to azoxybenzene is relatively less influenced by an increase in the reaction temperature. The selectivity to azoxybenzene, therefore, increases from 75.7% at 333 K to 88.1% at 353 K.

5.3.5 INFLUENCE OF TITANIUM CONTENT AND CATALYST CONCENTRATION

Table 5.3 reports the catalytic activity of TS-1 samples with two different Si/Ti ratios in the oxidation reaction, using acetonitrile as solvent, Both aniline conversion and H_2O_2 selectivity are marginally higher with high Ti-catalyst (Si/Ti = 35) but these are significantly higher than when the reaction was carried out with Ti-free silicalite-1 as catalyst. That TS-1 is active in this reaction is also clear from the blank experimental results given in Table 5.3. It may be noted that in the blank experiments (one without catalyst and one with Ti-free silicalite-1) the selectivity to azoxybenzene is still the maximum. Presence of titanium and its content in the reaction mixture enhances the rate of oxidation of aniline to phenyl hydroxylamine and then to nitrosobenzene. When the amount of catalyst is increased from 0.93 to 4.65 g per mole of aniline in the reaction mixture, both conversion and efficiency in the utilization of H_2O_2 increase from 9.8 to 21.8 mol% and 50.8 to 100%, respectively.

5.3.6 COMPARISON WITH VS-1 AND CrS-1

A comparison of the activities of TS-1, VS-1 and CrS-1 in the oxidation of aniline using H_2O_2 as oxidant is given in Table 5.4. The extent of conversion of aniline and the H_2O_2 selectivity in different catalyst is found to be in the order TS-1 > VS-1 > CrS-1. Between TS-1 and VS-1, the conversion and H_2O_2 selectivity are higher with TS-1 as catalyst. VS-1 also catalyzes the oxidation of aniline to azoxybenzene at a conversion of 35.0 % with a selectivity of about 95.2 %. As seen in Table 5.4, the conversion of aniline over VS-1 is lower than over TS-1; however, this is mainly due to the lower vanadium content in VS-1 as compared to the titanium content in TS-1. The selectivity to azoxybenzene, is also higher on TS-1 under similar conditions. It may be noted that the conversion of aniline over CrS-1 (32.3 %) is comparable with VS-1 (35.0 %).

Table 5.3

Influence of titanium content and catalyst concentration on aniline oxidation[a]

Si/Ti ratio	Catalyst amount (gram per mole of aniline)	Conv. (mol%)	H_2O_2 sel. (%)[b]	Product distribution (%)				
				NSOB	NB	AB	AXYB	Others[c]
35	0.93	16.1	79.4	8.4	-	0.4	87.0	4.2
80	0.93	9.8	50.8	21.8	-	0.3	75.7	2.2
S-1[d]	0.93	4.1	20.1	23.2	-	2.1	67.3	7.4
80	2.79	14.9	73.8	12.7	-	1.7	81.2	4.4
80	4.65	21.8	100.0	8.2	0.2	0.8	84.7	6.1
Blank[e]	Nil	2.8	14.4	26.1	-	9.8	63.0	1.1

[a]Reaction conditions: aniline = 54 mmol, aniline/H_2O_2 (mole ratio) = 3, reaction time = 5 h, solvent = acetonitrile (10 ml), temperature = 333 K.
[b]H_2O_2 utilized in the formation of nitroso- (NSOB), nitro- (NB), azo- (AB) and azoxybenzenes (AXYB).
[c]Mostly oxygenated with more than one functional group.
[d]Titanium-free silicalite-1 sample, for comparison.
[e]No catalyst was used.

Table 5.4

Oxidation of aniline over VS-1 and CrS-1[a]

Catalyst	Conv. (mol%)	H₂O₂ sel. (%)[b]	Product distribution (%)				
			NSOB	NB	AB	AXYB	Others[c]
TS-1	66.7	100.0	-	0.5	0.3	97.9	1.1
VS-1	35.0	51.7	0.6	-	2.2	95.2	2.0
CrS-1	32.3	48.6	0.5	4.1	5.7	88.0	1.7
Blank[d]	26.1	37.6	1.3	1.1	7.7	86.3	3.6

[a]Reaction conditions: aniline = 54 mmoles, reaction time = 5 h, temperature = 353 K, catalyst = 0.25 g [Si/Ti = 80, Si/V = 118 and Si/Cr = 52), aniline/peroxide (mole) = 1, solvent = acetonitrile (10 ml).
[b]H₂O₂ utilized in the formation of nitroso- (NSOB), nitro- (NB), azo- (AB) and azoxybenzenes (AXYB).
[c]Mostly oxygenated with more than one functional group.
[d]No catalyst was used.

The observed difference between TS-1 and CrS-1 could be due to the larger particle size of the CrS-1. Differences in particle size or the morphology are known to influence the activity of TS-1 in phenol hydroxylation reaction.

5.3.7 MECHANISTIC STUDIES

In order to understand the mechanism of conversion of aniline to azoxybenzene, cyclic voltammetric studies (CV) were carried out using Ti, V and Cr- silicate molecular sieves modified electrodes as the working electrode in the presence of H_2O_2. Zeolite Modified Electrodes (ZME) are one new class of rapidly developing electrodes with their unique size and shape selective properties leading to unusual product selectivity[35]. The CV profiles of aniline with H_2O_2 in Platinum UME modified with Ti, V and Cr-silicate molecular sieves are shown in Fig. 5.5 . It can be seen from the Fig. 5.5 that all the CV profiles (TS-1/H_2O_2, VS-1/H_2O_2 and CrS-1/H_2O_2) consists of two irreversible oxidation peaks at -250 mV and $+1100$ mV vs AgQRE. These correspond to the respective formation of phenyl hydroxylamine and nitrosobenzene[36]. Nitrosobenzene was identified by controlled potential analysis using molecular sieves modified electrodes at selected potentials obtained from the CV followed by GC analysis. Since there was no authentic sample of phenyl hydroxylamine, this phenyl hydroxylamine was identified by comparison of $E_{1/2}$ values available in the literature and also to the magnitude of potential observed by CV corresponding to phenyl hydroxylamine.

CV studies confirm that the formation of phenyl hydroxylamine and nitrosobenzene (from subsequent oxidation of phenyl hydroxylamine) occurs presumably within the channels of the molecular sieves when we use H_2O_2 as oxidant . The bulkier azoxybenzene could be formed in the solution phase either by condensation of nitrosobenzene with unreacted aniline to azobenzene[37] and then subsequently to azoxybenzene[38] or by direct condensation of the two intermediates
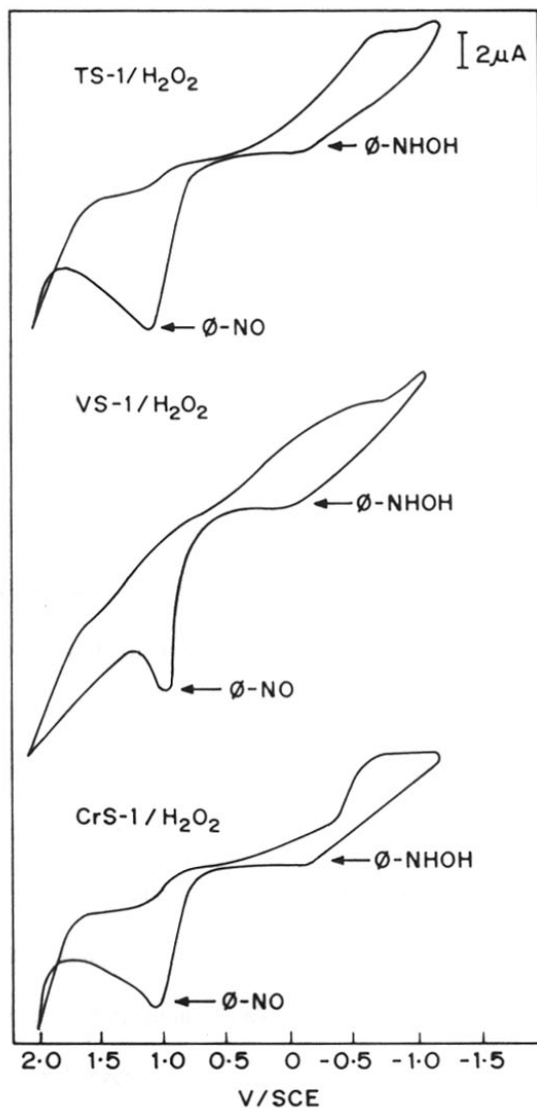
Fig. 5.5 CV profiles for the oxidation of aniline in H_2O_2 (a) TS-1 (b) VS-1 and (c) CrS-1: these voltammograms were taken on a molecular sieves modified platinum UME as a working electrode in 0.1 M of TBATFB in acetonitrile.

phenyl hydroxyalmine and nitrosobenzene[39]. In general , the oxidation of aniline over titanium silicate molecular sieves takes place according to the following stoichiometric equations.

$$PhNH_2 \quad + \quad H_2O_2 \quad \text{--------------------->} \quad PhNHOH \quad + \quad H_2O$$

$$PhNH_2 \quad + \quad 2H_2O_2 \quad \text{-------------------->} \quad PhNO \quad + \quad 3H_2O$$

$$PhNH_2 \quad + \quad 3H_2O_2 \quad \text{--------------------->} \quad PhNO_2 \quad + \quad 4H_2O$$

$$2PhNH_2 \quad + \quad 3H_2O_2 \quad \text{--------------------->} \quad PhN(O)=NPh \quad + \quad 5H_2O$$

$$2PhNH_2 \quad + \quad 2H_2O_2 \quad \text{--------------------->} \quad PhN=NPh \quad + \quad 4H_2O$$

5.4 CONCLUSIONS

1. The titanium silicate molecular sieve TS-1 catalyzes the oxidation of aniline selectively to azoxybenzene with aqueous hydrogen peroxide at relatively low temperatures.

2. Lower aniline to H_2O_2 (mole) ratios, and higher catalyst concentrations in the reaction mixture are favorable for higher conversion of aniline.

3. Titanium silicate, TS-1, exhibit better activity and selectivity as compared to VS-1 and CrS-1 in the oxidation of aniline.

4. The catalytic activity of titanium silicates in the oxidation of aniline with H_2O_2 strongly depends on the solvent used. Acetonitrile is found to be a good solvent in this reaction. In presence of acetone, formation of imine and their hydroxylated products results in poor selectivity to azoxybenzene.

5. The oxidation path of this reaction of aniline to azoxybenzene is followed by cyclic voltammetric techniques. The CV of aniline with H_2O_2 in metallosilicate modified electrode in acetonitrile with TBATFB consists of two irreversible oxidation peaks at -250 mV and $+1100$ mV vs AgQRE. These two peaks are attributed to the respective formation of

125

6.   The formation of phenyl hydroxylamine and nitrosobenzene occurs presumably within the channels of the metallosilicate molecular sieves; whereas bulkier azoxybenzene could be formed in the solution phase either by condensation of nitrosobenzene with unreacted aniline to azobenzene which is then oxidized to azoxybenzene or by direct condensation of the two intermediates, viz; phenyl hydroxylamine and nitrosobenzene.

5.5 REFERENCES

1.   O. D. Wheeler and D. Gonzales, Tetrahedron, 20, 189 (1964).

2.   H. R. Gutman, Experentia, 20, 128 (1964).

3.   W. D. Emmons, J. Am. Chem. Soc., 79, 5528 (1957).

4.   K. Kosswig, Justus Liebigs Ann. Chem., 749, 206 (1971).

5.   G. R. Howe and R. R. Hiatt, J. Org. Chem., 35, 4007 (1970).

6.   S. Tollari, D. Vergani, S. Banfi and F. Porta, J. Chem. Soc. Chem. Commun., 442 (1993).

7.   S. Tollari, M. Cuscela and F. Porta, J. Chem. Soc. Chem. Commun., 1510 (1993).

8.   P. Burchard, J. P. Fleury and F. Weiss, Bull. Soc. Chem. France, 2730 (1965).

9.   I. D. Entwistle, T. Gilkerson, R. A. W. Johnstone and R. P. Telford, Tetrahedron, 34, 213 (1978).

10.   H. E. Baumgarten, A. Staklis and E. M. Miller, J. Org. Chem., 30, 1203 (1965).

11.   G. Barak and Y. Sasson, J. Org. Chem., 54, 3484 (1989).

12.   M. Taramasso, G. Perego and B. Notari, US. Pat. 4,410,510 (1983).

13.   A. Thangaraj, R. Kumar and P. Ratnasamy, Appl. Catal. 57, L1 (1990).

14.   M. G. Clerici, G. Bellussi and U. Romano, J. Catal. 129, 159 (1991).

15.   P. Roffia, M. Padovan, E. Moretti and G. De Alberti, EP 208 (1987, 311 (1987); CA 106: 155944 S.

16.   T. Tatsumi, M. Nakamura, S. Negishi and H. Tominaga, J. Chem. Soc. Chem. Commun., 476 (1990)

17.   D. R. C. Huybrechts, L. D. Bruycker and P. A. Jacobs, Nature, 345, 240 (1990).

18.   H. R. Sonawane, A. V. Pol, P. P. Moghe, S. S. Biswas and A. Sudalai, J. Chem. Soc. Chem. Commun., 1215 (1994).

19.   S. Gontier and A. Tuel, Stud. Surf. Sci. Catal., 94, 689 (1995).

20.   S. Gontier and A. Tuel, J. Catal., 157, 124 (1995).

21.   S. Gontier and A. Tuel, Appl. Catal., 118, 173 (1994).

22.   T. Selvam and A. V. Ramaswamy, Catal. Lett., 31, 103 (1995).

23.   J. S. Reddy and A. Sayari, Catal. Lett., 28, 263 (1994).

24.   J. S. Reddy and P. A. Jacobs, J. Chem. Soc. Perkin Trans., I, 22, 2665 (1993).

25. J. S. Reddy and A. Sayari, Appl. Catal., 128, 231 (1995).

26. R. Joseph, A. Sudalai and T. Ravindranathan, Syn. Lett., 1177 (1995).

27. S. Tonti, P. Roffia, A. Cesana, M. A. Mantegazza and M. Padovan, EP 03141475 (1988).

28. B. Jayachandran, M. Sasidharan, A. Sudalai and T. Ravindranathan, J. Chem . Soc. Chem. Commun., 1523 (1995).

29. B. Notari, Stud. Surf. Sci. Catal., 60, 413 (1989).

30. G. Centi, S. Perathoner, F. Trifiro, A. Aboukais, C. F. Aissi and M. Guelton, J. Phys. Chem., 96, 2617 (1992).

31. T. Selvam and M. P. Vinod, Appl. Catal., 134, L 197 (1996).

32. A. Tuel, S. Moussa-Khouzami, Y. Ben Taarit and C. Naccache, J. Mol. Catal., 68, 45 (1991).

33. A. Thangaraj, R. Kumar and P. Ratnasamy, J. Catal., 131, 294 (1991).

34. W. P. Jencks, J. Am. Chem. Soc., 81, 475 (1959).

35. D. R. Rolison, Chem. Rev., 90, 867 (1990).

36. T. Selvam, M. P. Vinod and K. Vijayamohanan, React. Kinet. Catal. Lett., (in press).

37. R. W. Faessinger and E. V. Brown, J. Am. Chem. Soc., 73, 4606 (1950).

38. B. T. Newbold, J. Org. Chem., 27, 3919 (1962).

39. A. R. Becker and L. A. Sterson, J. Org. Chem., 45, 1708 (1980).

CHAPTER 6

SUMMARY AND CONCLUSIONS

Our results demonstrate that we have met the primary objective of this investigation to synthesize thermally-stable, chromium silicate, CrS-1.

It has been presented (chapter 2) that chromium can be incorporated by direct hydrothermal synthesis, into the MFI structure. The success of the synthesis is apparently due to the chemical composition of the synthesis gel and primarily the use of fluoride ions as solubilizing agent. This fluoride route is well suited to synthesize thermally stable chromium silicate molecular sieves because Cr^{3+} ions are not stable in conventional alkaline medium synthesis. The influence of various synthesis parameters such as : influence of chromium source, Si/Cr, Si/TPAOH and H_2O/Si molar ratios were investigated. $Cr(NO_3)_3 \cdot 9H_2O$ is found to be the best source for chromium to prepare highly crystalline CrS-1 with high BET surface area. The level of chromium in chromium silicalite-1 can be controlled by varying the amount of chromium in the gel, higher the chromium content in the gel, slower the rate of crystallization. The amount of TPAOH and dilution of the synthesis gel also significantly affect the amount of chromium incorporation into the MFI structure. SEM of these chromium silicates revealed that the crystals are uniform, lath shaped and free from amorphous materials.

A series of chromium silicate samples with different Si/Cr ratio have been synthesized by fluoride route and their detailed characterization (chapter 3) was done by using the standard techniques such as XRD, IR, UV, Laser Raman, ESR, ^{29}Si MAS NMR, CV and XPS.

XRD showed the presence of a typical MFI phase. As-synthesized CrS-1 sample is always orthorhombic, upon calcination the crystal symmetry becomes monoclinic. IR studies showed a less intense band around 960 cm^{-1}, attributed to Si-O-Cr linkages. UV-visible and Raman spectroscopy revealed that the resultant chromium silicate (calcined, exchanged and recalcined) is free from chromate species. Such chromate species as observed by UV-visible spectra in the calcined sample, could be removed during ammonium (acetate) exchange

because of the freely soluble nature of these chromate species in ammonium acetate solution. UV-visible spectra revealed that the Cr^{3+} ions are in octahedral coordination.

ESR studies revealed the presence of both Cr^{3+} and Cr^{5+} in octahedral coordination. ESR spectra of CrS-1 (calcined, exchanged and recalcined) exhibited a new five line spectra with a g value of 1.951, originated from the exchange interaction between Cr^{3+} and Cr^{5+} ions. Reduction in H_2 and recalcination of these chromium silicates have shown to possess Cr^{5+}/Cr^{3+} redox system. The presence of Cr^{5+}/Cr^{3+} redox couple in the chromium silicate is also substantiated by most reliable cyclic voltammetric technique. The invariance of the CV pattern with cycling confirmed the chromium ions in the MFI structure to be sufficiently stable for such a redox transformation. In contrast to the XRD results, ^{29}Si MAS NMR spectra of CrS-1 exhibited seven lines between -111.6 to -118.6 ppm/TMS attributed to the orthorhombic symmetry. ^{13}C CP/MAS NMR results suggested that TPA cations are chemically intact in the channels of the molecular sieves (as-synthesized CrS-1) and are not decomposed during the synthesis process. ^{27}Al MAS NMR spectra of CrS-1 did not exhibit any characteristic signal between 100 to -100 ppm suggesting that the sample is completely free from residual aluminium content. XPS data yielded values for the surface Si/Cr ratios in the CrS-1. Use of various physico-chemical characterization techniques has allowed us to predict a possible model for Cr^{5+} sites in the MFI structure.

Chromium silicate, CrS-1, has been found to catalyze the oxidation of many organic compounds in the presence of t-butyl hydroperoxide (TBHP). Five different substrates viz., toluene, n-hexane, n-heptane, n-octane and cyclohexane were chosen to study the intrinsic catalytic activity of CrS-1 in the presence of TBHP (chapter 4). The results obtained in the oxidation reactions over CrS-1 have been compared with those of vanadium silicate molecular sieves with MFI (VS-1) structure. In the liquid phase oxidation of toluene, CrS-1 has been shown to be more active than VS-1 using TBHP as the oxidant. CrS-1 showed resistance to

chromium leaching from the catalyst even after fourth recycling experiments. Separation of the catalyst, CrS-1, from the reaction mixture after 7 h of reaction time showed that the catalytic activity of the chromium which was leached into solution was also low. The higher yield of products can be achieved by changing the reaction parameters such as the reaction time and the TBHP-toluene molar ratios. The reactivity of the n-alkanes over CrS-1 in the presence of TBHP is greatly influenced by the particular structure of the alkane. Thus, increasing the chain length of alkanes from n-hexane to n-octane results in a decrease of the reactivity. Like vanadium silicates, VS-1, chromium silicates are also able to activate the primary carbon of the hydrocarbons. CrS-1 is also active in the oxidation of cyclohexane to cyclohexanol and cyclohexanone. The reversible transformation of Cr^{5+}/Cr^{3+} within the structure is primarily responsible for the catalytic behavior of these chromium silicates.

Catalytic conversion of aniline into azoxybenzene over metallosilicate molecular sieves with MFI structure (TS-1, VS-1 and CrS-1) using aqueous H_2O_2 as the oxidant is described (chapter 5). Among the catalysts (TS-1, VS-1 and CrS-1) tested, TS-1 is found to be more active in the selective oxidation of aniline to azoxybenzene. The effect of various reaction parameters such as the mode of addition of H_2O_2, Si/Ti ratios, temperature, solvent and catalyst concentration were investigated. Lower aniline to H_2O_2 ratios and higher catalyst concentrations in the reaction mixture are favourable for high conversion of aniline. The catalytic activity of titanium silicates in the oxidation of aniline strongly depends on the solvent used. Acetonitrile is found to be a good solvent in this reaction. In presence of acetone, formation of imine and their hydroxylated products results in poor selectivity to azoxybenzene. Mechanistic pathways of this conversion of aniline to azoxybenzene is also revealed by cyclic voltammetry. Azoxybenzene could be formed either by condensation of nitrosobenzene with unreacted aniline to azobenzene, which is then further oxidized to azoxybenzene or by the direct condensation of the two intermediates, viz; phenyl hydroxylamine and nitrosobenzene.

LIST OF PUBLICATIONS

1. **T. Selvam** and A. V. Ramaswamy
   Selective catalytic oxidation of aniline to azoxybenzene over titanium silicate molecular sieves.
   Catal. Lett., 31, 103 (1995).

2. **T. Selvam** and A. V. Ramaswamy
   A new catalytic method for the selective oxidation of aniline to nitrosobenzene over titanium silicate molecular sieve, TS-1, using H_2O_2 as oxidant.
   J. Chem. Soc. Chem. Commun., 1215 (1996).

3. **T. Selvam** and M. P. Vinod
   A novel efficient synthesis and characterization of crystalline chromium-silicate molecular sieves with MFI structure.
   Appl. Catal., 134, L197 (1996)

4. **T. Selvam** and A. P. Singh
   Single step selective oxidation of para-Chlorotoluene to para-Chlorobenzaldehyde over vanadium silicate molecular sieves.
   J. Chem. Soc. Chem. Commun., 883 (1995).

5. A. P. Singh and **T. Selvam**
   Liqid phase oxidation of para-chlorotoluene to para-chlorobenzaldehyde using vanadium silicate molecular sieves.
   Appl. Catal., 143, 111 (1996).

6. **T. Selvam**, A. V. Ramaswamy, M. P. Vinod and K. Vijayamohanan
   A mechanistic study of the oxidation of the aniline to nitrobenzene over vanadium silicate molecular sieves, VS-1, using t-butyl hydroperoxide (TBHP) as the oxidant.
   Paper presented at National Workshop on Catalysis, CSMCRI, Bhavnagar, December 20-22 (1995).

7. **T. Selvam**, M. P. Vinod and K. Vijayamohanan
   Catalytic and electrocatalytic oxidation of aniline to nitrobenzene over vanadium silicate molecular sieves, VS-1, using t-butyl hydroperoxide (TBHP) as the oxidant.
   React. Kinet. Catal. Lett. (accepted)

8. A. P. Singh and **T. Selvam**
   Liquid phase oxidation reactions over chromium silicalite-1 (CrS-1) molecular sieves
   J. Mol. Catal., (accepted).

PATENTS

1. **T. Selvam** and A. V. Ramaswamy
    A process for the preparation of crystalline microporous chromium silicate designated as CrS-1 (Indian Pat. filed).

2. **T. Selvam** and A. V. Ramaswamy
    A process for the preparation of crystalliine microporous chromium silicate composite material (Indian Pat. filed).

3. **T. Selvam** and A. V. Ramaswamy
    An improved process for the oxidation of organic compounds using chromium silicate composite material (Indian Pat. filed).

TH-1056